PhD thesis

Selim OMRANE

Further characterization of the *Lotus japonicus* ammonium transporters

Links to the nodulation pathway

PhD Supervisor: Dr Maurizio CHIURAZZI. Institute of Genetics & Biophysics CNR, Naples
PhD Tutor: Ch.mo Dr Salvatore COZZOLINO. Botanical Garden, Naples
Coordinator: Ch.ma Prof. Silvana FILOSA. FEDERICO II Univ, Naples

PhD thesis

In advanced Biology

Field: Molecular systematic

(XX cycle)

Further characterization of the *Lotus japonicus* ammonium transporters:
Links to the nodulation pathway

Candidate: Selim OMRANE

PhD Supervisor: Dr Maurizio CHIURAZZI. Institute of Genetics & Biophysics CNR, Naples

PhD Tutor: Ch.mo Dr Salvatore COZZOLINO. Botanical Garden, Naples

Coordinator: Ch.ma Prof. Silvana FILOSA. FEDERICO II Univ, Naples

Naples
Order N°

Federico II University of Naples
Institute of genetics and biophysics CNR-Naples

THESIS
submitted
to obtain

Degree in Doctor of philosophy
from the Federico II University

Laboratory of Symbiosis and Nitrogen fixation
Institute of Genetic and biophysics-CNR Naples; Italy

By
Selim OMRANE

Further characterization of the *Lotus japonicus*
ammonium transporters:
Links to the nodulation pathway

Defended on December the 24th

Chairman and examiners: **Prof. Fucci L. (Monte Sant'Angelo Univ., Naples, Italy),**
Prof. Galderisi U. (IInd University of Naples, Italy; Medicine
Department),
Prof. Luparello C. (Palermo Univ., Italy; Cellular and Development
Biology
Department),
Prof. Ligrone R. (IInd University of Naples, Italy; Environment and
Ecosystems Department).

Fall 2008

Acknowledgments

First of all I would thank a lot my direct supervisor Dr Maurizio Chiurazzi who hosted me during these three years in his team and defined the good development of the PhD work in Italy as well as during all my European meetings.

A special thank is addressed to our PhD coordinator, Prof. S. Filosa who provided the ideal support to their Doctorate students, being present till the end.

I am grateful to my Tutor Dr Salvatore Cozzolino for its availability and his good mood especially in treating the admin tasks during the few monthly meetings that we had together.

I would stress my gratitude to my devoted collaborators and their respective Team leaders who helped me and gave me the right support for the edification of the different sub-projects of this PhD thesis. In particular a big thank to:

- Dr Alberto Ferrarini and Dr Massimo Delledonne (Verona Univ.) for all their support in the combimatrix project;

- Dr Luigi Mandrich and Dr Giuseppe Manco (Instituto di biochimica e proteomica, Naples) for the *in vitro* protein-protein interaction investigation

- Michele Cermola and Salvatore Arbucci for the technical support in light microscopy and confocal microscopy.

This PhD was also undertaken in the framework of a European project termed "Integral network". Different trips gave me the opportunity to learn more about the research in labs of other EU countries. I would say my affection to all the students of the network and their respective staffs that I met. They shared the same objectives working in a symbiotic fashion to understand and solve the mystery of a symbiotic interaction.

Beyond the common team notion, I found in Alessandra Rogato (detta Limoncello girl), Enrica d'Apuzzo (detta the girl of Ipanema), Ani Barbulova (detta the fried Russian girl), Alessandra Ruggiero (detta Dalila) and Simone Cossu (detto l'uomo del cavo(lo ☺)) the refuge of a true protective family. To my special sisters, and brother, I would say: together, forever, in the best as in the worst…

I could not forget my Mum and Dad who gave me the right sustain in moments of doubt and difficulties. They are my north my south my east and west, my only guides. I Love you!

Finally, for all of them, form the IGB till the common mortals and even the camorra who rendered my staying in Naples a permanent discovery and gave me an exciting and extreme way of city life, I would embrace 'em all as a true Neapolitan. So a big hug, I will not forget you!

Dedication to Judith

(…) Flowers of ink dropping pollen like commas
Lull them asleep, in their rows of squat flower-cups
Like dragonflies threading their flight along the flags (…)

Rimbaud *in* **The seated**

I. INTRODUCTION

A. Brief description, framework and aim of the project

The mutualistic feeding exchange between leguminous plants and its respective symbionts Rhizobia and Mycorrhiza diminish the soil nutritional dependency, for the plant partner and limits the agrochemical adds enhancing agriculture sustainability in an ecological way. Furthermore, the leguminous themselves accounts for about one third of the world's primary crop production, human dietary protein, and represent a major source for livestock and raw material for industry.

It is well known that abiotic factors such as light, temperature and especially nutrient availability can affect the occurrence and the efficiency of beneficial plant-microbe interaction such as the Symbiotic Nitrogen Fixation (SNF). Sessile organisms such as plants must be able to perceive continuously the surrounding environment in order to respond efficiently to different correlated abiotic and biotic signals. The plant control over this plethora of biotic and abiotic factors, acting at the rhizosphera level, occurs through a complicated network of signaling pathways. For example, the competence of leguminous plants for the symbiotic interaction is determined by the presence of combined Nitrogen sources in the soil and in particular, the limitation of these N sources is a prerequisite that has to be satisfied.

The question of how legume plants sense the environmental N availability and how this signal can interfere with the Nod factor-dependent transduction pathway leading to nodule organogenesis is a central objective of my PhD thesis.

The present PhD program is undertaken in the frame of the European Network Project (INTEGRAL = Intensifying Training in Europe for Genomic Research Activity on Legumes) dedicated to the study of the molecular and genetic basis of mutualistic symbioses (interactions between plants and soil microbes) that provide legumes, such as *Lotus japonicus*, with nutrients for growth. In the last fifteen years *Lotus japonicus* became as well as *Medicago truncatula*, a very important model plant for the understanding of the symbiotic relationship between the legume plant family and their corresponding symbionts.

In our laboratory, we are focusing our attention on the pathway of transfer and assimilation of ammonium, which represents also the final product of the SNF. For many

high eukaryotes this transfer occurs through two main transport systems: the LATS (low affinity transport system) and the HATS (high affinity transport system) and the ammonium transporters play a crucial role in the latter by acting as gate regulators of the ammonium fluxes. We have already characterized 3 high affinity ammonium transporters in *Lotus* (D'Apuzzo *et al.,* 2004). This preliminary characterization was based essentially on the elucidation of the patterns of expression and biochemical characteristics of the three members of the *LjAMT1* family: *LjAMT1.1*, *LjAMT1.2* and *LjAMT1.3*. This first characterization will be mostly reminded in the introductive chapter.

During my PhD program I further characterized the *AMT1* gene family by focusing my attention on the effects of the environmental conditions on the gene expression trying to correlate these profiles with the *Lotus* growth phenotypes (2nd chapter). I thought opportune to figure out how the ammonium transporters could react to some parameters controlling plant growth that are implemented in each of our experiments.

In the chapter II-section D, I describe two strategies we chose for fishing AMT interactants. In section D.2, we use a variant of the yeast two-hybrid system (RRRs: Reverse RAS Recruitment system) that is suitable for hydrophobic protein embedded into the plasma membrane as it's the case of our full length AMT1 proteins. The second strategy is based on the use of the c-terminal part of the AMT transporters as bait to fish putative interactants directly from plant crude extracts. The dis/advantages of both techniques are discussed in the related section.

B. Legume Model Plant: *Lotus japonicus*

B.1. Generalities: Legumes and *Lotus*

With 650 genera and over 18000 species grain legumes are only second to grasses in economic importance in world agriculture right after cereal crops. In 2004, more than 300 million metric tones of grain legumes were produced on 190 million ha (FA0 stat (2007); http://www.faostat.fao.org). Three quarters of the world production of grain legumes is soybean with 186 million metric tones, increased by 215% over the last 30 years, while the others grain legumes yielded 57 million tones in 2007 (http://www.grainlegumes.com/). On December 2004 a scientific legume community represented by almost 50 legume researchers and Funding agency met in CATG conference (Cross-Legume Advanced through Genomics) in Santa Fe (Ca, USA) to figure out a consensus effort on legumes as model plant family (http://catg.ucdavis.Edu/). During, this conference many aspects of the application of the growing model plants with both cultivated *Medicago truncatula* (Alfalfa) and *Glycine max* (Soybean) as well as the uncultivated *Lotus japonicus* (birdfoot trefoil) were mentioned as potential references for the grain legume in agriculture (Gepts *et al.,* 2005). The same year, other scientific efforts were made by the publication of an organized LIS database (The Legume Information System) giving the state of the art on grain legume genomics cross comparison, in order to encourage the opportunity to enlarge the circle of the scientific community on applied legume research projects (Gonzales *et al., .*2005). The scientific progresses obtained over the last fifteen years in both model legumes: *M truncatula* and *L. japonicus* indicate a striking difference when compared to the results obtained in other grain legumes such as soybean or chickpea. In the legume world, *Lotus japonicus* is an excellent model plant that gave to the legume research community new tools, revealing new important genes involved in the symbiotic and development pathways (Nishimura R. *et al.* 2002; Sato and Tabata, 2006).

B.1.1. Domestication and geographic distribution

Before to reach the status of model plant, *Lotus* as *Medicago* are first of all plants that became nowadays very important in the agriculture fields. Both plants are considered as important source of forage for the cattle but the domestication of *Lotus* species is more recent compared to *Medicago* (Asuaga 1994). Different species are used to improve pastures in association with other grasses (Papadopoulos and Kelman, 1999). Among more than 180 inventoried *Lotus* species only 4 annual species were concerned by domestication: *L. corniculatus* (birds foot trefoil), *L. uliginosus Schkuhr* (greater *Lotus*), *L Glaber Mill.*

(narrow-leaf trefoil) and *L. subbiflorus* Lagasca (hairy birdsfoot trefoil). However, only *Lotus corniculatus* is widely spreaded for sowing but these last species are extensive sources of new diversity necessary in the different breeding programs (Diaz *et al.,* 2005).

Lotus japonicus (Regel) Larsen was discovered centuries ago at the ancient capital of Japan Kyoto. Its natural habitat is East and central Asia. However, the spreading of the genus occurred only through sowing its domesticated species and the principal area of cultivation of *Lotus* species is the Mediterranean basin (Europe and North Africa; Figure 1). In 1950, Professor Isao Hirayoshi (Kyoto Univ. *in* VandenBosh and Stacey (2003)) collected *Lotus* plants growing in Gifu on a riverbank. Then Prof. William F Grant collected its progeny. However, the first Researchers who established *Lotus japonicus* (Gifu progeny B-129) as model plant were Kurt Handberg and Jens Stougaard (1992, Aarhus Univ., Dk.). Since then, *Lotus* Gifu B-129 had a lab world wide distribution. Many other ecotype of *Lotus* can be found at: http://www.Shigen.nig.ac.jp/bean/*Lotusjaponicus*/top/top.js. The Ecotype Miyakojima (MG-20) found on the island of the same name is also an extensively used ecotype especially to get progeny after its crossing with Gifu ecotype (Kawagushi, 2000). The derived population is useful for the construction of genetic linkage map, map based cloning and QTL identification. Finally MG-20 is the ecotype serving for the *Lotus* sequencing genome program undertaken by the Kazusa DNA Research Institute (http://www. kazusa.or.jp/*Lotus*/index.html.; Udvardi *et al.,* 2005)
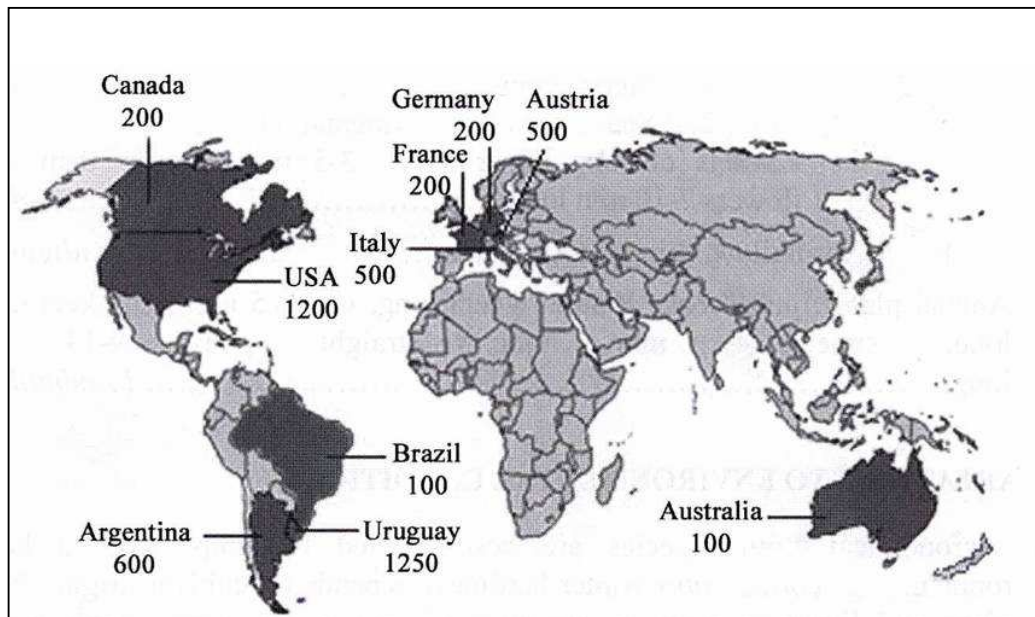

Figure 1. Countries with more than 100 thousands hectares sown with *Lotus* species. Under the country, the sowing area in thousands of hectares is indicated. (In *Lotus japonicus* handbook (2005); Marquez ed.)
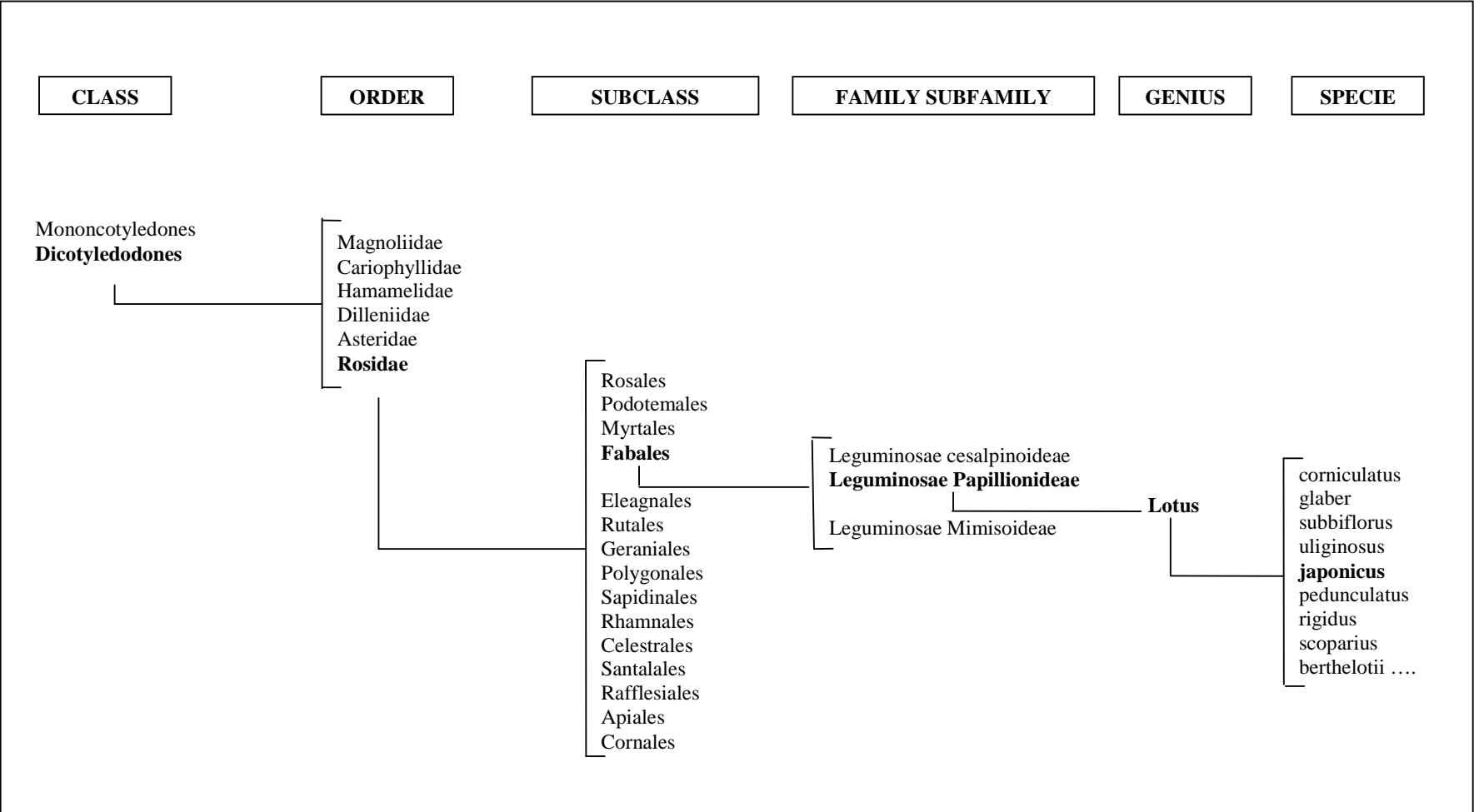
| CLASS | ORDER | SUBCLASS | FAMILY SUBFAMILY | GENIUS | SPECIE |

Mononcotyledones
Dicotyledodones

Magnoliidae
Cariophyllidae
Hamamelidae
Dilleniidae
Asteridae
Rosidae

Rosales
Podotemales
Myrtales
Fabales

Leguminosae cesalpinoideae
Leguminosae Papillionideae

Leguminosae Mimisoideae

Eleagnales
Rutales
Geraniales
Polygonales
Sapidinales
Rhamnales
Celestrales
Santalales
Rafflesiales
Apiales
Cornales

Lotus

corniculatus
glaber
subbiflorus
uliginosus
japonicus
pedunculatus
rigidus
scoparius
berthelotii ….

Figure 2. Taxonomic classification of *Lotus japonicus*

B.1.2.Taxonomy

The genus *Lotus* is an Angiosperm, true dicotyledonous plant belonging to the large family of Fabaceae also termed Leguminoseae or Papilioneae and the Subfamily of the Faboideae (figure2). It regroups both perennial and annual species. The specie *japonicus* as well as the agronomical ones are included in the subgenus *Edento Lotus*, characterized by its non dental style, section *XantoLotus* composed with legumes terete and laterally compressed yellow flowers (Arambariri, 1999). As shown in figure 3, the morphology of the *Lotus* plant is quite similar within the same genus. Plants have erected or decumbent stems and pentafoliate leaves with two of the leaflets at the petiole base resembling stipules. Leaves are green to grey-green. Inflorescences with eight flowers are umbel-like cymes at the end of long axillary's branches. However, it is possible to differentiate the species according to their belonging to both perennial and annual life cycles (Key words *in* Lotus japonicus handbook, (2005)).
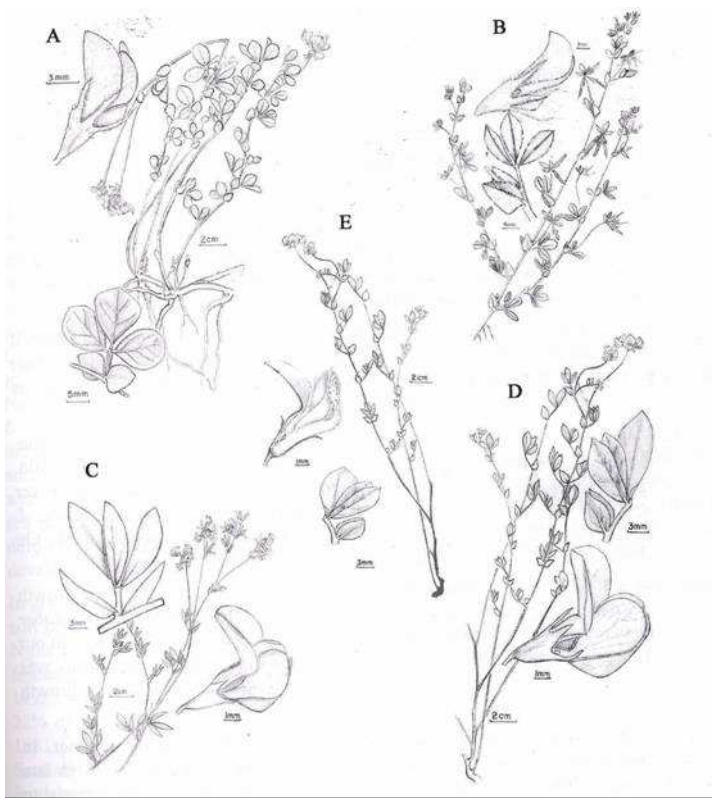

Figure 3. Botanical drawing of agriculturally important species and L. *japonicus*(A) L. uliginosus, (B) L. subbiflorus ; (C) L. glaber ; (D) L. corniculatus
In *Lotus japonicus* handbook (2005); Marquez ed.

B.1.3. Biology and life cycle

On the contrary of many legume plants, *Lotus japonicus* is a perennial, diploid, self-fertile plant, that develops straight seed pods with two halves and seeds are arranged along a simple linear axis. After germination *Lotus japonicus* observes a relatively slow growth. However, in growth chamber, the life cycle from young axenic plantlets (3 weeks) till the mature plants producing seeds, is about 3 months, sometimes less. One week post germination, the seedlings are less than 5 cm long (shoot and root). This fact makes easy its *in vitro* high density culturing (figure 4). Moreover, *Lotus* is quite amenable to *Agrobacterium* mediated transformation (Lombari *et al.,* 2003). The flow chart of the transformation procedure was recently shortened (Barbulova *et al.,* 2005). A program of DNA tagging of *Lotus japonicus* was established in different labs to obtain insertion mutant lines. The relative small genome (450 mb) is another positive point to dissect different pathways and to define a very short term sequencing program.

One important characteristic of *Lotus japonicus* is its ability to form nodules. On the contrary of *M. truncatula* the nodules of *L. japonicus* are determinate nodules. The study and the characterization of the nodulation are prerequisites to understand the cross talk between the *Lotus* host and the different strains that are able to enter in symbiosis with it.

Figure 4. *Lotus japonicus in vitro* high-density culture.

B.2. Symbiosis

As most leguminous species, *Lotus japonicus* has the potentiality to enter in symbiosis with bacteria commonly called Rhizobia. Each partner has a direct benefit from the other: Bacteria provide *Lotus* with the necessary amount of fixed atmospheric nitrogen, while in returns *Lotus* downloads into the infected cells the right amount of carbohydrates (Desbrosses *et al.,* 2005) sneeded for Rhizobia livestock and nitrogen fixation activity. The symbiotic program leads to the formation of novel root derived organs named nodules (Szczyglowski and Amyot, 2003). Legume plants can form two kind of nodules: indeterminate nodules (eg: *M. truncatula*, *Pea*) and determinate nodules ((eg: *Soybean*, *Lotus); Van Spronsen et al.,* (2001) and in figure 5). The benefit role taken by the legumes from the symbiosis, the neo-formed specialized organs are important ecological issues for the good management of the extensive cultivated areas. Thus, plant relying on such organs reduces the need for expensive nitrogen fertilizers that is an important feature of sustainable agriculture.
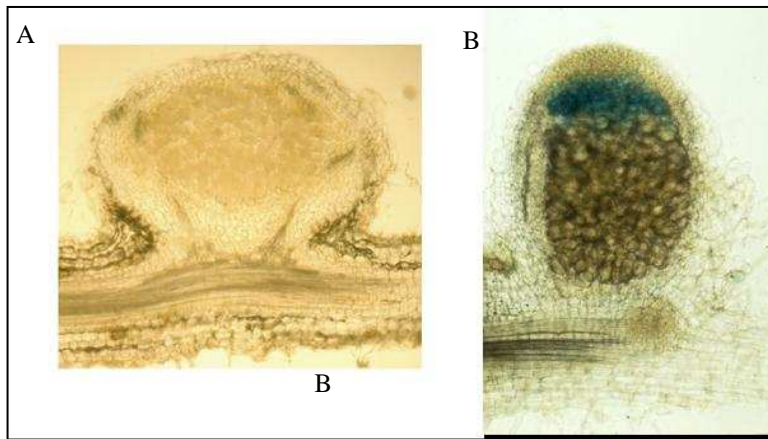

Figure 5. (A) determinate nodule and (B) indeterminate nodule types

Two important milestones were reached in the understanding of the nodulation process by the legume scientific community:

In one hand, the discovery of the bacterial elicitor called Nod factors (See § B.2.2; Denarié et al., 1996; D'Haeze and Holster, 2002) and their corresponding plant host receptors (see § B.2.4). On the other hand, the unraveling of two key central genes: (a) The Har1 receptor kinase-dependent signaling (Penmetsa and Cook, 1997; Wopereis *et al.,* 2000; Krusell *et al.,* 2002; Nishimura *et al.,* 2002). *L. japonicus* mutants carrying a mutation in the HAR1 gene fail to autoregulate nodule formation, resulting in the formation of an excessive number of nodules (hypernodulation phenotype; Wopereis *et al.,* 2000). (b) the NIN gene: Nodule inception) that encodes a master regulator protein triggering the initiation of the infection threads and the onset of cortical cell division (Shausser *et al.,* 1999). Both are essential protagonist for the establishment of the symbiosis even though many other genes are required (see § B.2.4).

Different approaches were used to unravel their existence and to characterize their role:

Lotus genetics: Many techniques participated to find out new loci as the map based cloning, the high throughput mutagenesis (Tilling; Perry *et al.,* (2003)) and genome tagging, genetic linkage map and leguminous genome (macro-micro) synteny programs.

Lotus Functional Genomics: Principally, based on the EST (Expressed Sequence Tag; Asamizu *et al.,* 2000) database and the *Lotus* sequencing project that is under the supervision of the Kazusa (Japan) program. Moreover, a gene general expression patterning was established by the production of arrays (macro, micro arrays and gene chips). Particularly, the affimetrix technology gives new insights on the symbiotic process from the expression genome screening of infected *Lotus japonicus* plants (Colebatch *et al.,* 2002)

Lotus Proteomics: One important issue was achieved by the identification of proteins present in the peribacteroid membrane and *Lotus* nodules (Winkoop and Saalbach, 2003). Tools analyzing the large spectrum of expressed proteins (Two dimensional gel electrophoresis, Liquid and Gaz chromatography) identify more than 94 known protein matching database and 24 ESTs where detected in the PBM.

Lotus Metabolomics: Metabolite profiling using GC-MS showed to profile changes in metabolites in nodules compared to roots as well as to study nodulation of mutant, non N-non fixing plants and wild-types nodules containing mutant rhizobia (Colebatch *et al.,* 2004)

B.2.1. Rhizobia: *Mesorhizobium loti*

Rhizobia designate a collective name of the genera *Rhizobium, Sinorhizobium, Mesorhizobium* and *Bradyrhizobium*. These prokaryotes colonize the rhizosphere where they perform nitrogen fixing symbiosis with leguminous plants. Both "fast growing" *Mesorhizobium loti* and slow growing *Bradyrhizobium loti* can nodulate *Lotus japonicus*. However *B. Loti* induces only infected non N-fixing nodules. By contrast, *M. loti* is able to form determinant-type globular nodules and perform nitrogen fixation on several *Lotus* species. The *M. loti* genome is totally sequenced. The project was initiated in February 2000 by the sequencing of the strain MAF303099 and the complete nucleotide sequence was achieved in December 2000 (Kaneko *et al.,* 2000). The genome of *M. Loti* consists of a single chromosome (7,036,071 bp) and two plasmids, designated as pMLa (351,911 bp) and pMLb (208,315 bp). The chromosome comprises 6,752 potential protein coding genes, two sets of rRNA genes and 50 tRNA genes representing 47 tRNA species. The genome of plasmids pMLa and pMLb, contains 320 and 209 potential protein-coding genes, respectively.

To date, the commonly fast growing strains, lab *ready to use,* are: R7A, NZP2235, JRL501 (Niwa *et al.,* 2001, Kawagushi *et al.,* 2002), MAF303099, and TONO (Kawaguchi, 2000). Most of these strains are equipped with GUS and GFP fusion reporter genes to monitor the process of infection from the beginning till the formation of the nodules. There are also other species of rhizobia that can induce nodulation on *Lotus japonicus* as *Rhizobium etli* that is the *Phaseolus* symbiotic partner but is also able to nodulate *Lotus*.
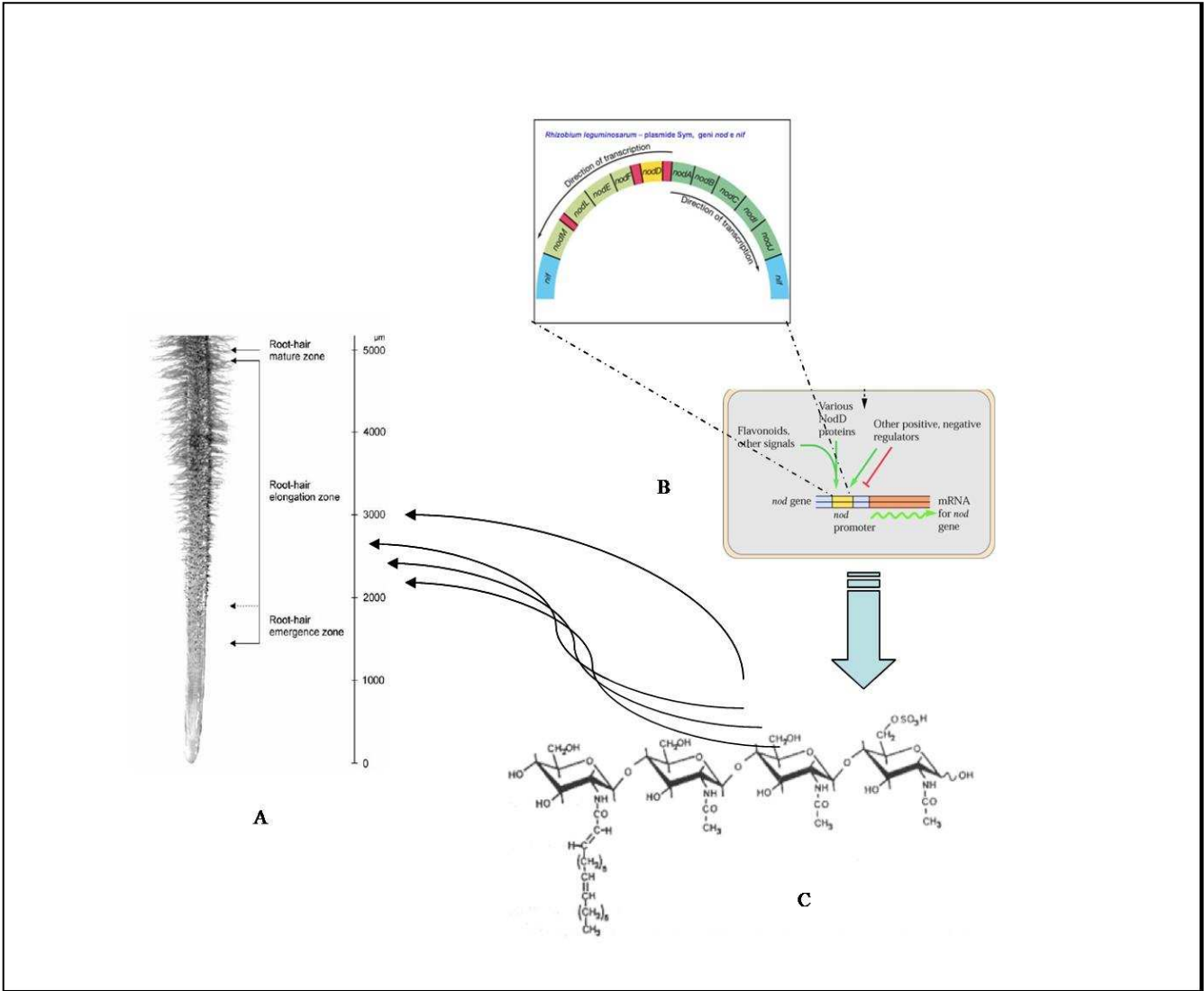
Figure 6. A. Suceptible infection zone. **B**. Rhizobia nod operon ; **C.** Nod Factor backbone

However, in this case nitrogen fixation is missing because of the defects in the cortical cells invasion and nodules senesce rapidly (Banba *et al.,* 2001). The broad host range Rhizobium sp. NGR 234 has also been reported to nodulate *Lotus japonicus*. For the understanding of the early legume-rhizobia interaction basic mechanisms, permitting a myriad of cross possibility to nodulate *Lotus* with different rhizobia strains, the recent studies of Radutoiu *et al.,* (2007) were extremely important. The authors used domain swap experiments on the plant host-Nod Factors-receptors of different legumes and the *M. loti* Nod factor acetyl end groups rendering these accessible to each other.

B.2.2. Steps of nodule formation and development

The first plant organs involved in the nodulation process are the root hairs. The root hairs of higher plant represent an important extension of the root surface. This enlarged surface is able to sense and uptake nutrient from a continuously fluctuating rhizosphere environment. During the symbiosis the structure of the root hairs contained in a fraction of the root at 0.5 cm far from the root tips (figure 6A) start a new morphogenesis process representing the first macroscopical event of the symbiotic interaction (Szczyglowski and Amyot, 2003)

The first steps involve the mutual recognition between bacteria and host plant. Bacteria are attracted by root exudates (flavonoids, sugars, volatile compounds). These plant compounds are generally synthesized when the plant is under biotic (e.g. pathogen attacks) or abiotic stress (e.g. lost of the oligo-mineral retention capacity of the rhizosphere). In particular, secreted plant flavonoids and phenolic coumpounds are able to induce in rhizobia, the Nod genes (Downie, 1998) expression (figure 6B) and subsequently the synthesis of Nod factor (NFs or Lipochitin oligosaccharides). These secreted molecules are tetramers and pentamers of the carbohydrate chitin, which are attached to a fatty acid chain (Geurts and Bisseling 20025; figure 6C). Nod factors can be purified and ingenerated. The initial response of root hairs to the NF produced by the compatible strain of rhizobia involves the establishment of *de novo* polar root hair tip growth and curling, which leads to the formation of typical ''shepherd's crook'' structures (Lhuissier *et al.,* 2001). Only root hairs localized to the susceptible zone (figure 6 A) of the root and at a particular developmental stage appear to be fully receptive to NFs (Bhuvaneswari *et al.* 1981). The curled root hairs entrap the bacteria and serve as a starting point for the initiation of the infection process, which occurs through a local invagination of the plasma membrane and establishment of a growing infection structure, the infection thread (IT). The intercellular progression of the IT through the root hair toward the underlying nodule primordium

occurs via a tip-growth-like mechanism and is guided by a specific arrangement of polarized cytoplasm in the underlying cortical cells (van Brussel *et al.* 1992; van Spronsen *et al.,* 2001). In principle, the zone of attachment of the Bacteria is the root hair. However it happens that in a few cases the mechanisms by which rhizobia colonize roots vary significantly among different legume species and various root hair-independent mechanisms of root colonization by rhizobia, including cortical intercellular invasion at lateral root bases, have been described (Boogerd and van Rossum, 1997; Guinel and Geil, 2002,).
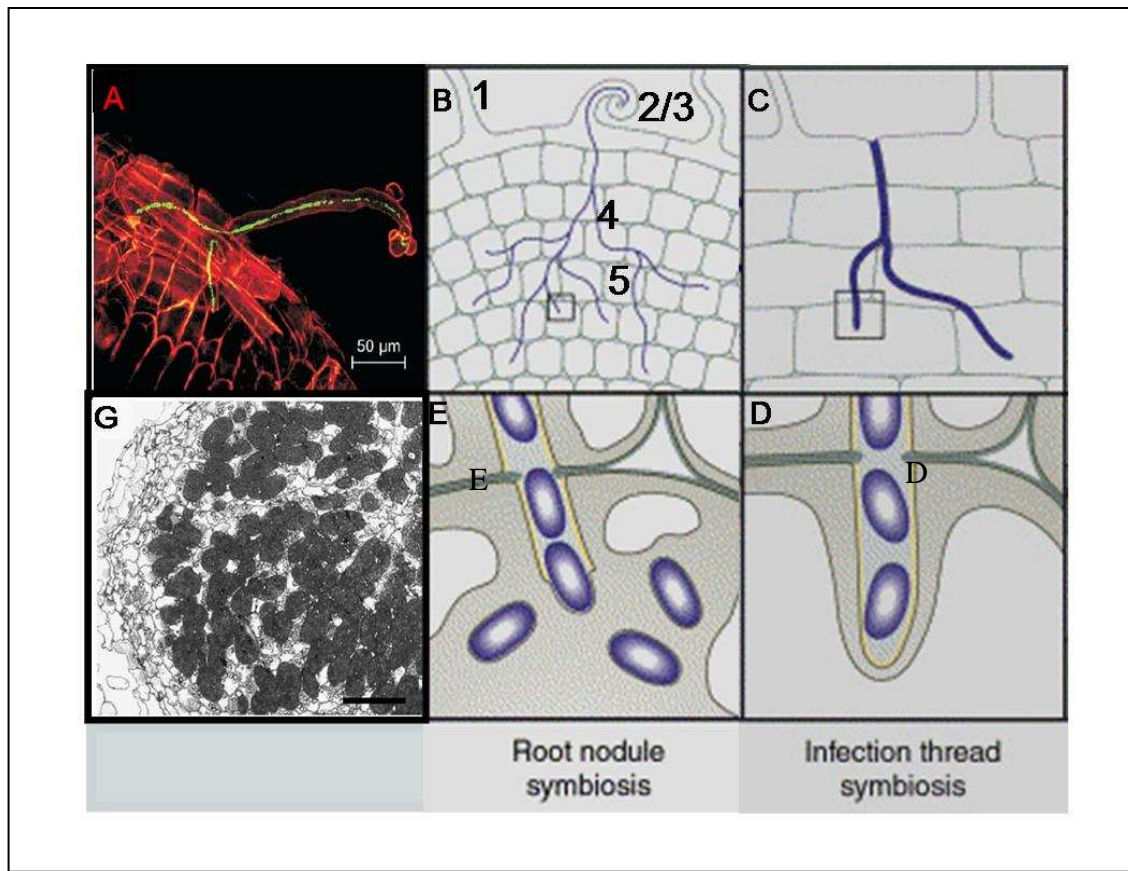

Figure 7. Different steps of the symbiotic interaction. A, scanning confocal image of an infection thread originating from a microcolony at the curled root hair tip and proceeding down into the base of the epidermal cell. *M. loti* bacteria are tagged with GFP (green fluorescence) and the root tissue has been counterstained with propidium iodide (red fluorescence) (in Karas *et al.,* 2005) B, Schematic representation of the infection thread formation steps: non infected root hair (1) infected root hair showing rhizobia entrapment (2n/3), root hair curling (4) and spreading of the infection thread from the root tip to the first cortical cell layers (5). C, sometimes the invasion occurs by cracking the root epidermal layers and then spreading of the ITs. D, the cortical cell invasion occurs first trough the destruction of the cell walls pectocellulose, followed by invagination of the cytoplasmic membrane encapsulating the bacteria inside of structures termed symbiosomes E, into the symbiosome bacteria do not divide anymore, differentiate in bacteroids and fix the atmospheric nitrogen G, a mature nodule full with symbiosome structures containing active bacteroids (black color indicates the leghemoglobin of the lively bacteroids)

B.2.3. Other type of Symbiosis: the Mycorrhizal interaction

By contrast to the bacterial symbiosis that is restricted only to the Leguminous family, Arbuscular Mycorrhizal symbiosis concerns both mono and dicotyledonous classes. The fungus, an obligate biotroph belonging to the Glomeromycota (Shüssler *et al.,* 2001) provides to the plant the necessary nutrients among which the phosphrous seems to be the main source of plant benefit (Smith and Read 1997). The process of invasion is quite different from the rhizobia threads (figure 8). Many genes which are involved in the early signals transduction pathways of the two processes are likely to be the same (See next §. B.2.4.). Both cytological changes and genetic partners were largely documented (Bonfante, 1984, Siciliano *et al.,* 2007) especially in *Medicago* and *Lotus*. However a big question mark is still raised concerning the first step of recognition between AM and the host plant. Indeed, even though the Myc factors (sesquiterpene strigolactone) were isolated (Akiyama *et al.,* 2005), the precise nature and number of plant host receptors was not elucidated yet.
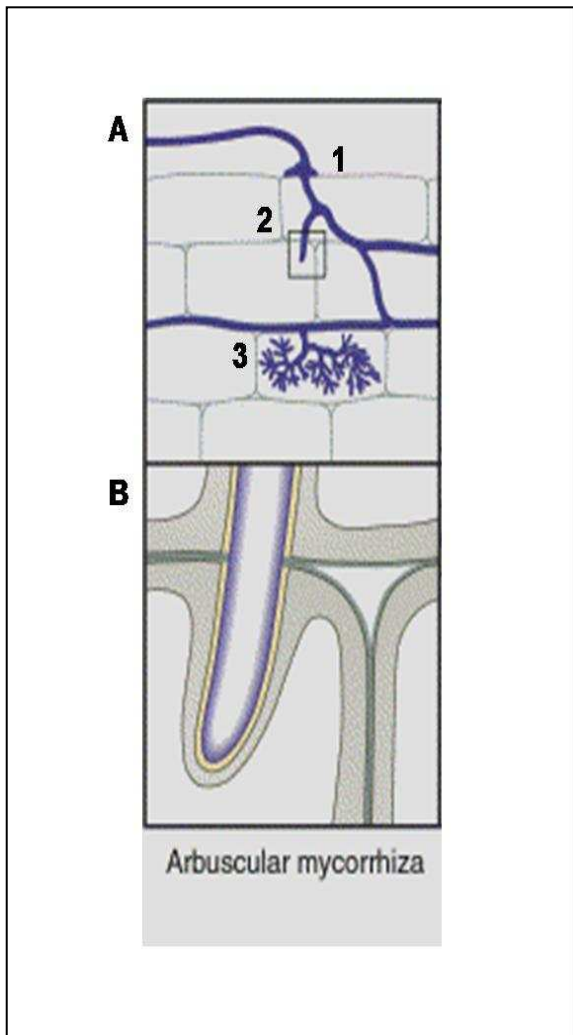

Figure 8. Arbuscular mycorhiza invasion. **A**, the appressorium is first in contact to the first epidermal cell of the root that will be subsequently destroyed (1) the progression of the tread proceed then in the extra-cellular space until the third layer of cells where the invagination and ramification process start without destroying the cells **B**, invagination of the cytoplasmic membrane without destruction. The contact between thread remain and cytoplasmic membrane is maintained, forming a micro region where nutrient exchange, mainly phosphorous and ammonium, takes place.
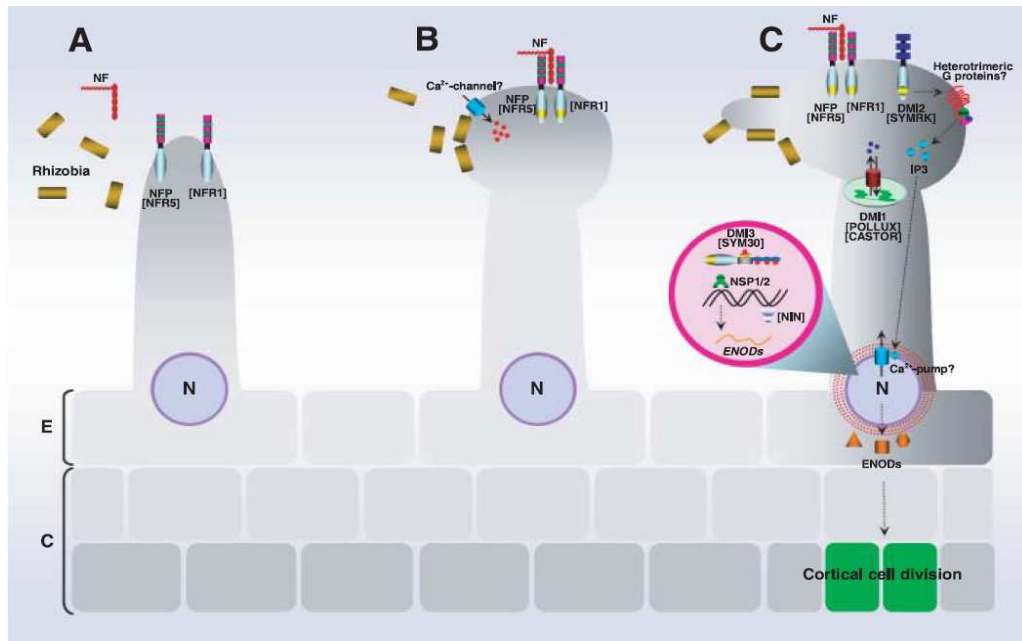
Figure 9. I. Model for early Nod factor induced responses. A, Nod factors (NF) secreted by compatible rhizobia are postulated to bind to the LysM domains of LysM receptor kinases, triggering dimerization, auto-phosphorylation and phosphorylation of downstream signalling components. B, Nod factor perception leads to a localized calcium influx, causing a reorientation of polar tip growth in root hairs in the direction of Nod factor perception. C, DMI1 and DMI2 initiate calcium spiking by way of a heterotrimeric G-protein and phospholipid module. The putative ion channels CASTOR and POLLUX localize in the plastids of pea and onion epidermal cells, but the role of plastids in signal transduction is unknown. DMI3 senses calcium concentrations and translates this into rhizobium-specific ENOD gene expression by phosphorylating the NSP1 and NSP2 transcription factors. ENOD genes activate cell division within cortical cells by a not yet identified mechanism.
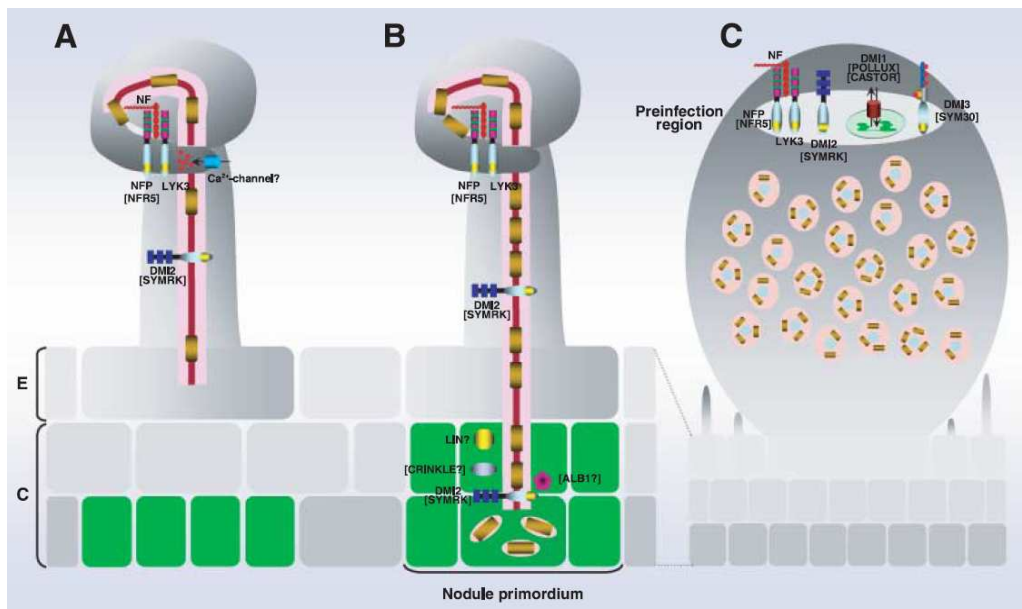
II. Model for the rhizobia root hair infection. A, pronounced root hair curling leads to the entrapment of rhizobia within the curling, creating a high, local concentration of Nod factors. The LYK3 LysM receptor kinase, perhaps in a complex with NFP, initiates infection thread growth. Bacteria penetrate the root hair and traverse plant-derived infection threads towards the developing primordia. B, upon reaching the primordium, rhizobia are released into membrane-bound sacs termed 'symbiosomes', a process that requires DMI2. Additional genes have been identified that are required for infection threads to penetrate the epidermal layer (Table 1) but the nature of these gene products is currently unknown. C, proteins required for Nod factor signalling are expressed in the pre-infection region of indeterminate nodules, suggesting that the continuous infection process in developed nodules requires constant Nod factor perception. An analogous situation may exist in determinate nodules but be limited to early developmental stages in which cell division and infection are taking place. M. *truncatula* and L. *japonicus* genes are indicated with L. *japonicus* genes given in parentheses. E = epidermis; C = cortex. *In* MOLECULAR PLANT PATHOLOGY (2006) 7(3) , 197–207 © 2006 BLACKWELL PUBLISHING LTD

B.2.4. Symbiosis pathway

All the morphological changes that occur during the rhizobia infection are under the tight control of a signaling pathway that restrict the extent of successful infections at the root epidermis and nodule organogenesis at the root cortex (Nutman, 1952; van Brussel *et al.,* 2002). The microscopical analysis of the early symbiotic steps leading to the root hair deformation and IT formation were more recently supported by electrophysiological and fluorescent microscopy investigations that allowed defining many different steps occurring within a few seconds by the addition of Nod factors and concerning its perception and transduction. These include: a membrane depolarization, an extra-cellular alkanization and a calcium influx followed by a calcium spiking in the perinuclear cytoplasmatic region of the root hairs (Harris *et al*., 2003). These early events precede the root hair swelling and deformation (branching followed by curling).

Recently, a detailed characterization of several mutants (table below) isolated by chemical mutagenesis coupled to an optimized map positional cloning technique set up jointly in *Lotus japonicus* and in *Medicago truncatula,* allowed the identification of different genes involved in the early events described above (figure 9). The mutant phenotypes have been characterized on the basis of the specific deficiencies detected in the temporal cascade of early events induced by Nod factors.

Mutant	Putative function	Symbiotic phenotype	Non-symbotic phenotypes	References
nfp(nfr5)	LysM RLK	Nod–, Inf–, Ccd–, myc+	Reduced responses to root-knot nematode	(Ben Amor et al., 2003; Madsen et al., 2003; Weerasinghe et al., 2005)
(nfr1)	LysM RLK	Nod–, Inf–, Ccd–, myc+	Reduced responses to root-knot nematode	(Radutoiu et al., 2003; Weerasinghe et al., 2005)
LYK3*	LysM RLK	Nod–, Inf–	NR	(Limpens et al., 2003)
dmi1(pollux)	Ion channel	Nod–, Inf–, Ccd–, myc–/+	NR	(Ané et al., 2004; Imaizumi-Anraku et al., 2005)
(castor)	Ion channel	Nod–, Inf–, Ccd–, myc–/+	NR	(Imaizumi-Anraku et al., 2005)
dmi2(symrk)	LRR-RLK	Nod–, Inf–, Ccd–, myc–/+	Reduced responses to root-knot nematode	(Endre et al., 2002; Stracke et al., 2002; Weerasinghe et al., 2005)
dmi3(sym30)	CaCAMK	Nod–, Inf–, Ccd–	NR	(Lévy et al., 2004; Mitra et al., 2004a)
nin	TF	Nod–, Inf–, Ccd–	NR	(Schauser et al., 1999)
nsp1	TF	Nod–, Inf–, Ccd–, myc+	NR	(Smit et al., 2005)
nsp2	TF	Nod–, Inf–, Ccd–, myc+	NR	(Kaló et al., 2005)
(sym3)	Unknown	Nod–, Inf–, Ccd–, myc–/+	NR	(Kistner et al., 2005)
(sym6)	Unknown	Nod–, Inf–, Ccd+, myc–/+	NR	(Kistner et al., 2005)
(sym15)	Unknown	Nod–, Inf–, Ccd–, myc–	NR	(Kistner et al., 2005)
(sym24)	Unknown	Nod–, Inf–, Ccd–, myc–/+	NR	(Kistner et al., 2005)
hcl	Unknown	Nod–, Inf–, Ccd+, myc+	NR	(Catoira et al., 2001)
nip	Unknown	Nod–/+, Inf–/+, Ccd+, myc+	polyphenolic accumulation, PR genes up-regulated, abnormal lateral roots	(Veereshlingam et al., 2004)
pdl	Unknown	Nod–, Inf–/+, Ccd–	NR	(Cohn et al., 2001)
lin	Unknown	Nod–, Inf–/+, Ccd–/+	NR	(Kuppusamy et al., 2004)
(crinkle)	Unknown	Nod–/+, Inf–/+, Fix–, Ccd+	wavy trichomes, short seedpods with aborted embryos, pollen tube defects	(Tansengco et al., 2003, 2004)
(alb)	Unknown	Nod–/+, Inf–/+, Fix–, Myc+	defects in vascular bundle	(Imaizumi-Anraku et al., 2000)
(Ljsym79)	Unknown	Nod–/+, Fix–, Myc+,	small pods	(Kawaguchi et al., 2002)
(lot1)	Unknown	Nod–/+, Inf–/+, Fix+, Myc+	trichome distortion, dwarf phenotype	(Ooki et al., 2005)
MtSUNN(HAR1 (GmNARK)	LRR-RLK	Nod++, Ccd++, NTS+	Reduced root length, increased lateral root (Har1/GmNARK)	(Krusell et al., 2002; Searle et al., 2003; Schnabel et al., 2005)
(astray)	TF	Nod++, NTS–	Defects in responses to light and gravity	(Nishimura et al., 2002a,b)
(klavier)	Unknown	Nod++, NTS+	Convex veins on leaf, delayed flowering, dwarf, fasciated stems	(Oka-Kira et al., 2005)
(sen1)	Unknown	Nod++, Fix–, NTS–	NR	(Suganuma et al., 2003)
sickle	Unknown	Nod++, Inf++, NTS unknown	Ethylene insensitive	(Penmetsa and Cook, 1997)

Table. Mutants affected in the infection and nodule development.

Abbreviations: Nod, nodule formation; Inf, infection process from root hair curling to the release of bacteria in cortical cells; Ccd, cortical cell divisions; Myc, mycorrhizal symbiosis; CCAMK, calcium- and calmodulin-dependent protein kinase; Fix, nitrogen fixation; TF, transcription factor; LRR, leucine rich-repeat; RLK, receptor likekinase; NR, none reported; NTS, nitrate-tolerant symbiosis. The response intensity is indicated as follows: ++, increased response; +, presence of the response; –/+, reduced response; –, absence of the response. M. truncatula and L. japonicus genes are indicated with L. japonicus genes given in parentheses. E, epidermis; C, cortex.
*LYK3 identified by RNAi, mutant not yet reported.

The Nod factors are detected through the presence of two LysM receptors like kinases NFR1/MtLYK3-MtLYK4 and NFR5 (Madsen *et al.,* 2003; Radutuoi *et al.,* 2003) as well as MtNFP (Amor *et al.,* 2003), hence acting at the top of the transduction pathway induced by Nod factors (figure 10). Both receptors could form putative heterodimers serving as docking site for the Nod factors. However, a Leucine Rich Repeat Kinase-Receptor (TOLL family, see figure 9) called SymRK (Symbiosis Receptor-like Kinase) was previously identified, having, by contrast to NFR1-NFR5, also a role in the arbuscular mycorhization (AM) (Stracke *et al.,* 2002) and possibly involved in the bacteria recognition. Recently, Yoshida and Parninske (2007) partially uncovered the mechanistic activity of SYMRK confirming that phosphorylation occurs at a serine-threonin domain. The ortologue of SymRK was also identified in *Medicago truncatula* and the closely-related crop specie *Pisum sativum*, and termed *DMI1* (Does not Make Infection). In *Lotus japonicus,* other genic determinants involved in the intracellular root hair transduction of the Nod factor signal have been recently identified as *CASTOR, POLLUX* (*MtDMI2* orthologue), *NUP133*, CCaMK (*MtDMI3*), LjSym6/30/82 and LjSym24/73/85 (Kistner *et al.,* 2005, Sandal *et al.* 2006). They are all involved in the early calcium spiking signal, a part of the signaling pathway implicated in the establishment of both mycorrhizal and bacterial endosymbioses (Catoira *et al.,* 2000).
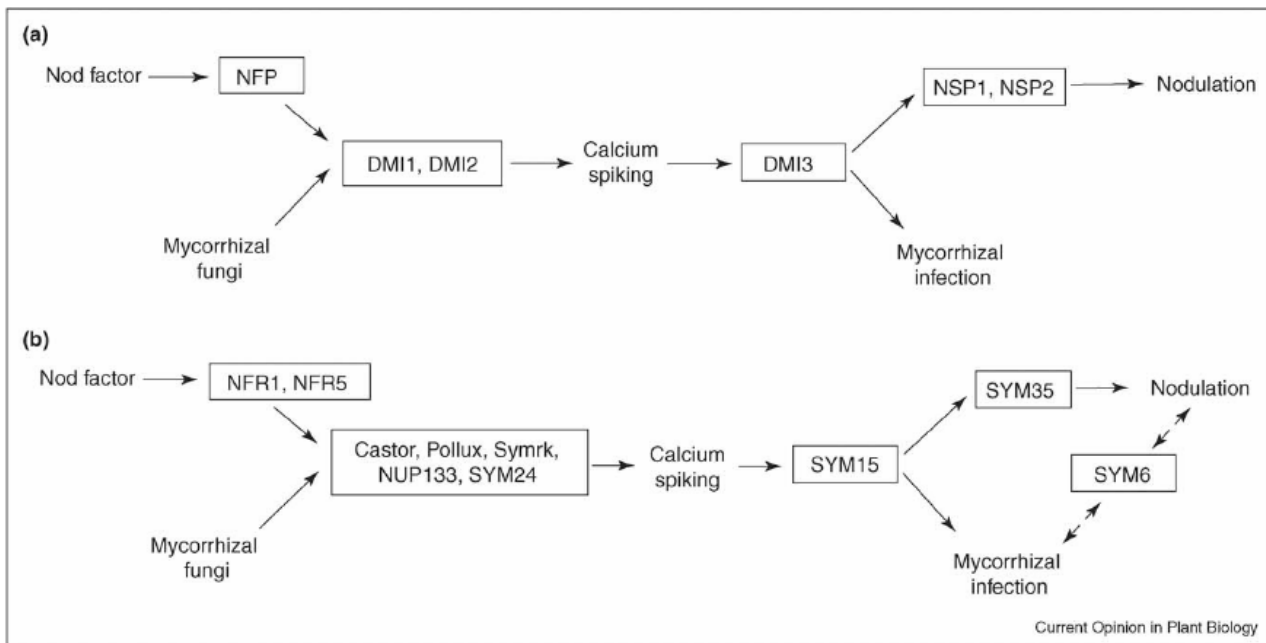

Figure 10. A. *Medicago truncatula* nod factor-depentent pathway **B.** *Lotus japonicus* nod factor-dependent pathway. Both pathways show also the potential integration, at different levels, of the Arbuscular Mycorrizal signaling. *In* Current Opinion in Plant Biology 2006, 9:1–7

The very likely mechanism for the activation of the calcium spiking is the production of a heterotrimeric G-protein and a phospholipid module (secondary messenger associated with the nucleus) that can bind to and activate the putative calcium channels identified by the *CASTOR* and *POLLUX* genes (*MtDMI1*, Ané *et al.* 2004). The sub-cellular localization of these proteins as well as their electrophysiological features is controversial. Indeed, the true amino acid sequence homology between *DMI1* and *POLLUX* is not maintained at the level of the sub-cellular localization of these proteins. While *DMI1*::GFP fusion localizes to the nuclear envelope in *M. truncatula* roots (Ané, 2007), the *Lotus japonicus CASTOR* and *POLLUX* homologs were reported to be localized in plastids. However, the plastidial localization of both proteins has been very recently corrected for a perinuclear location similar to that of *MtDMI2* (Charpentier , 2007). This sub-cellular localization raised the question of their possible mechanistic role as calcium channel. Recent Patch clamp investigations (Charpentier, 2007) are indicating a possible double affinity of *CASTOR* and *POLLUX* channels in guiding either the fluxes of Ca2+ or K+ through the nuclear membrane.

Recently a nucleoporin NUP133 was identified in *Lotus* as required for Nod-factor induced calcium spiking playing a role in both symbiotic and mycorrhiza pathways. (Kanamori *et al.*, 2006). NUP133 is homologous to a eukaryotic component forming the core of the nuclear pore complex, although its exact function is currently unknown. The NUP133 gene does not appear to be part of a gene family in plants, yet apparent null mutants show only defects in symbiosis signaling, indicating that this nucleoporin has a specific function in this signaling pathway. This protein is possibly required to transport the secondary messenger that has a target on the interior of the nuclear membrane.

While, NFR1-NFR5/NFP, SYMRK/DMI1 CASTOR-POLLUX, DMI2 and NUP133 mutants are unable to elicit calcium spiking, CCaMK/DMI3 mutants retain this capability (Wais *et al.,* 2000). CCaMK/DMI3 encodes a protein kinase harboring both calcium and calmodulin binding domains, suggesting that this protein may perceive Nod-factor-induced calcium spiking and translate it into a physiological response by phosphorylating downstream proteins (Lévy *et al.,* 2004; Mitra *et al.,* 2004).

The calcium concentration sensed by CCaMK/DMI3 is readily translated into specific gene activation through the phosphorylation of the NSP1 and NSP2 transcription factors(. Both transcription factors belongs to the GRASS family and where isolated in *Lotus*
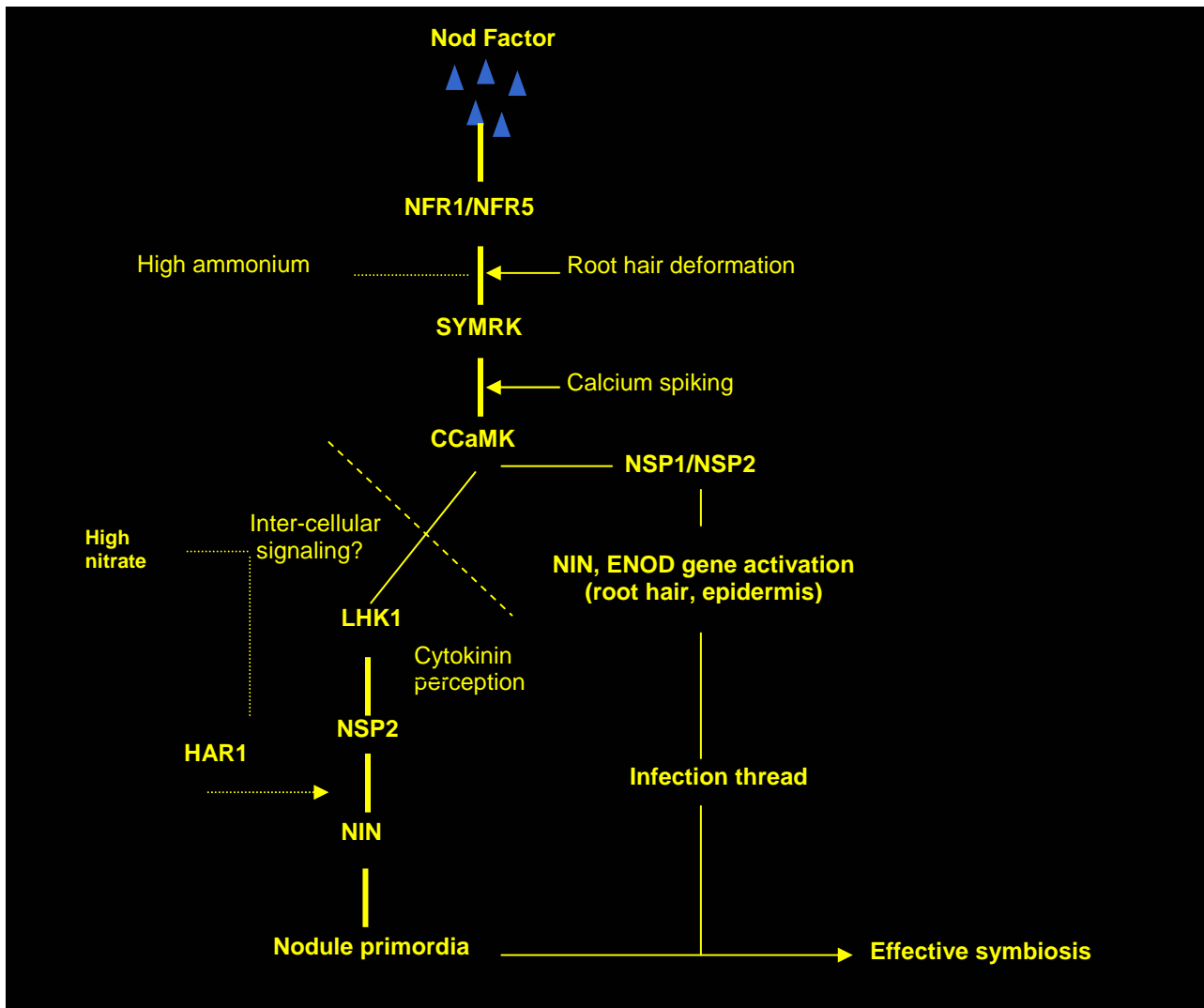
Figure 11. Nod factor-dependent and putative nitrate and ammonium signaling pathways in *Lotus japonicus* roots.

Root hair deformation is represented as NFR1 and NFR5-dependent since these are the only two mutants lacking this type of response to Nod factor treatment. The dashed line indicates the putative position of the cellular signaling event. The square dot lines indicate the putative nitrate-dependent and ammonium-dependent signaling pathways. We indicated a *NSP2*-dependent expression of *NIN* in the cortical cells, although the reported experiments cannot discriminate between the epidermal and cortical *NIN* induction. (In Barbulova *et al.*, 2007)

japonicus (Lj NSP1/2, Heckmann *et al.,* 2006) and *Medicago truncatula* (Smit P *et al., 2005*; Kalo *et al.,* 2005)   A potential master regulator acting downstream in this transduction pathway and involved in the cortical root cell division activation is termed NIN (Shausser *et al.* 1999).

The structure of NIN suggests it functions as a transcriptional activator. Although the NIN transcript was modestly up regulated 5 h after inoculation, it was found to be strongly up-regulated 24 hrs after inoculation (about 20 fold) and after a transient decline of the level of expression the peak is reached at about 10 days after inoculation suggesting a role in both early and late steps of the interaction. This dual temporal pattern of expression is coupled to a dual localization of its expression. In fact, NIN is expressed earlier in the root hairs and epidermal cells and later on in the cortical cells of the nodule primordium. Even though, the initial responses of root epidermal and cortical cells to signaling from the Nod factors-producing bacteria set off a cascade of signaling events that restrict the extent of successful infections at the root epidermis and nodule organogenesis in the root cortex (Nutman, 1952; van Brussel *et al.,* 2002), multiple levels of regulation, including local and systemic signaling events, have been implicated in this process and have been shown to involve the plant hormone ethylene and Har1 receptor kinase-dependent signaling (Penmetsa and Cook, 1997; Wopereis *et al.,* 2000; Krusell *et al.,* 2002; Nishimura *et al.,* 2002). *L. japonicus* mutants carrying a mutation in the Har1 gene fail to autoregulate nodule formation, resulting in the formation of an excessive number of nodules (hypernodulation phenotype; Wopereis *et al.,* 2000).

Very recently, two independent studies (Tirichine *et al.,* 2006 and Murray *et al*., 2006) working on two contrasted mutants respectively SNF mutant (Spontaneous nodulating mutants) and Hit mutant (Hyper infected mutant) identified two alleles of the same gene *LHK1* (*Lotus* Histidine kinase) encoding for an AHK cytokinin receptor type. Both gain of function (*snf2*) and loss of function (*hit1*) alleles were positioned before the NIN and the HAR1 genes in the Nod factors-dependent transduction pathway. In 2007, Barbulova *et al.* demonstrated in an elegant study the negative effects of both ammonium and nitrate on the Nod factor-dependent NIN induction and were able to position the independent actions of the ammonium (NH_4^+) and the nitrate (NO_3^-) in the symbiotic pathway of *Lotus japonicus* (figure 11). These results represent a prelude to this PhD thesis.
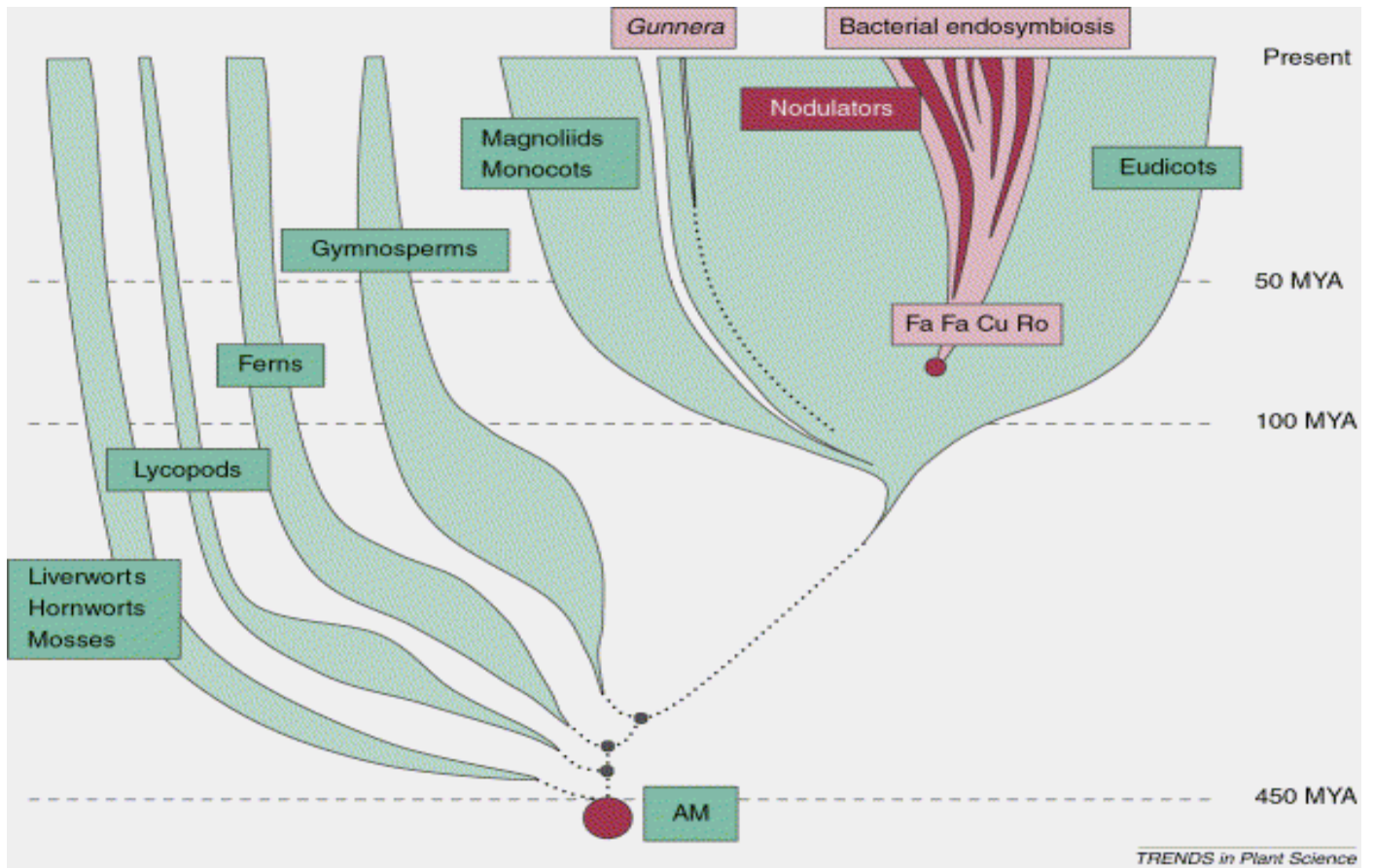
Figure 12. Evolution time scale of the symbionts and their corresponding hosts.

C. The nitrogen transport

The nitrogen is the first constituent of DNA (nitrogenous bases) and proteins (amino acids), as well as an essential source of nutrient for all the living organisms. Nowadays, Physicians and Chemists are able to easily define the different combined nitrogen forms that are available for the living stocks. By contrast, it is still up to date to uncover, the complex evolutionary mechanisms that allowed living organisms adaptation and therefore, to take benefit from different sources of accessible and inaccessible combined nitrogen. Eukaryotes and prokaryotes mostly rely on membrane proteins that are carriers of ion forms (NH_4^+/NO_3^-). Even the little number of organisms that lack ion transporters appears to be either specialized to use specific nitrogen forms, such as urea in the case of *Helicobacter pylori*, or to grow in nitrogen-rich environments. It is the case of the pathogenic eukaryotic parasites *Plasmodium falciparum* and *Trypanosoma brucei* which thrive in the blood of their obligate hosts (von Wiren, and Merrick, 2004)

"Agronomically speaking", combined nitrogen is mainly constituted by the NH_4NO_3 complex. Indeed, the ammonium (NH_4^+) represents one of the most essential mono-charged ions in plant nutrition. It is mainly complexed to other ions but in soil it shows a higher affinity for nitrate ion (NO_3) (Woldendorp and Laanbroek, 1989) and it is provided from two main soil fractions: organic and inorganic. It is well established that higher plants rely more on the inorganic fraction because of it's abundance and direct availability to the plant absorption machinery compared to the poor quantities of amino acids delivered by the organic fraction and the higher costs in energy spent for their scavenging directly from the soil, especially in absence of specialized organs (Heller *et al.,* 1996). However, the higher plant family staying on the edge (figure 12) of evolution in viridiplant superfamily: The Leguminosaea, developed an eterotrophic way for feeding themselves as an outlet solution when soils are deficient in NH_4^+ by establishing a mutualistic interaction (in preview § B.2.).

These interactions rose up the level of the mechanism complexity in soil minerals-uptake, host retrieving and final metabolism assimilation since the plant is becoming able to modulate its nutritional inputs in function of the environmental cues.
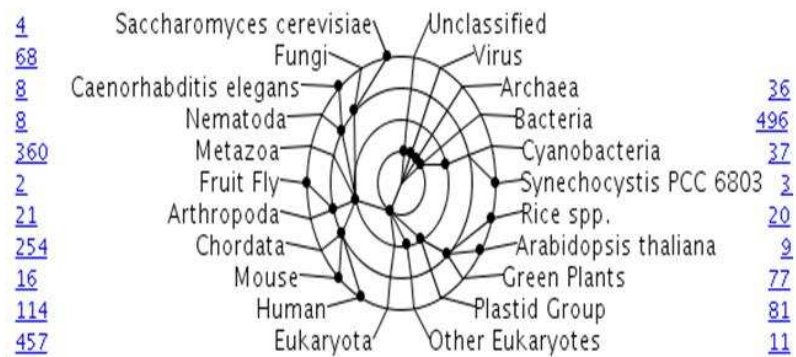
A
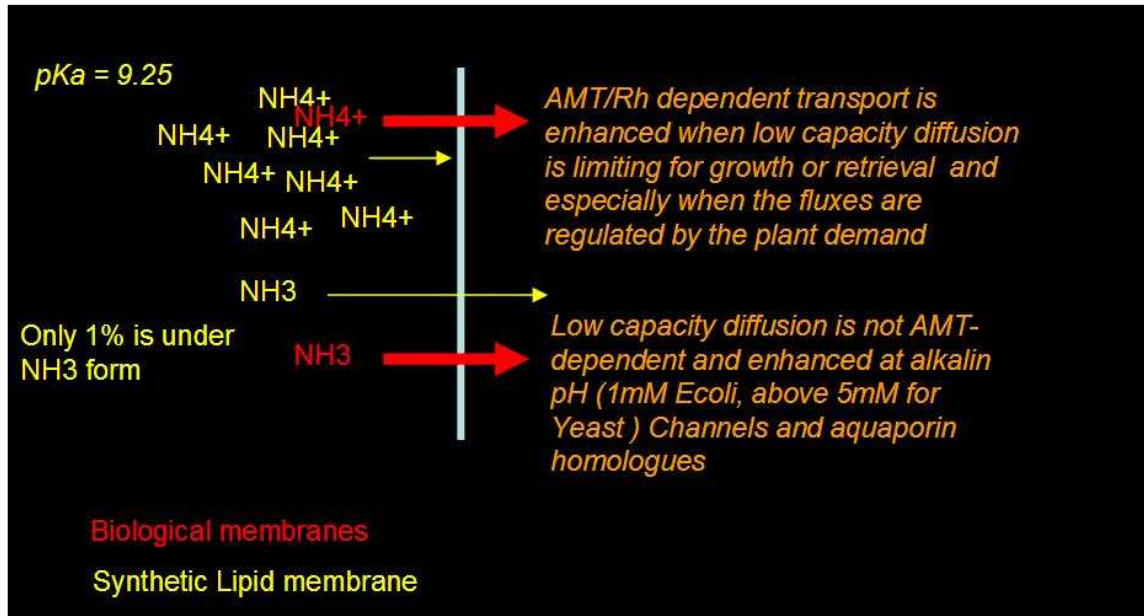
B

Figure 13. AMT transport type through two kinds of Membranes (A) and classification (B).

C.1. Ammonium transporters: Phylogeny and distribution

In plant cells, ammonium is under the control of a complex network of regulation where the ammonium transporters proteins seem to play a key role in its transport to ensure the right distribution of NH_4^+ all over the nitrogen cell cycle (Glass *et al.,* 2002). Depending on their capacity of NH_4^+ uptake (high or low), ammonium transporters are classified into two groups respectively: LATS (low affinity ammonium transporter system) and HATS (high affinity transporter system) (Howitt and Udvardi, 2000; figure 13 A). However, only the HATS members have been widely identified in nearly all the organisms (figure 13 B). In plants, high affinity ammonium transporters were genetically as well as biochemically characterized in several species and subsequently classified in AMT different families (for review, see Loque and von Wirèn, 2004). Three distinct classes are distinguishable (figure 14): the eukaryotic class where AMT members of two mainly studied plants are closely related, the prokaryotic class with known three-dimensional structure from *Archaeoglobus fulgidus* and *Escherichia coli* structural models and the specific class of human Rh glycoproteins and non-glycosylated Rh proteins. However, such a classification could under(over)-estimate the distance between AMT members because it doesn't care about the mechanism of ammonium transport that could represent an important parameter for the evaluation of similarity.
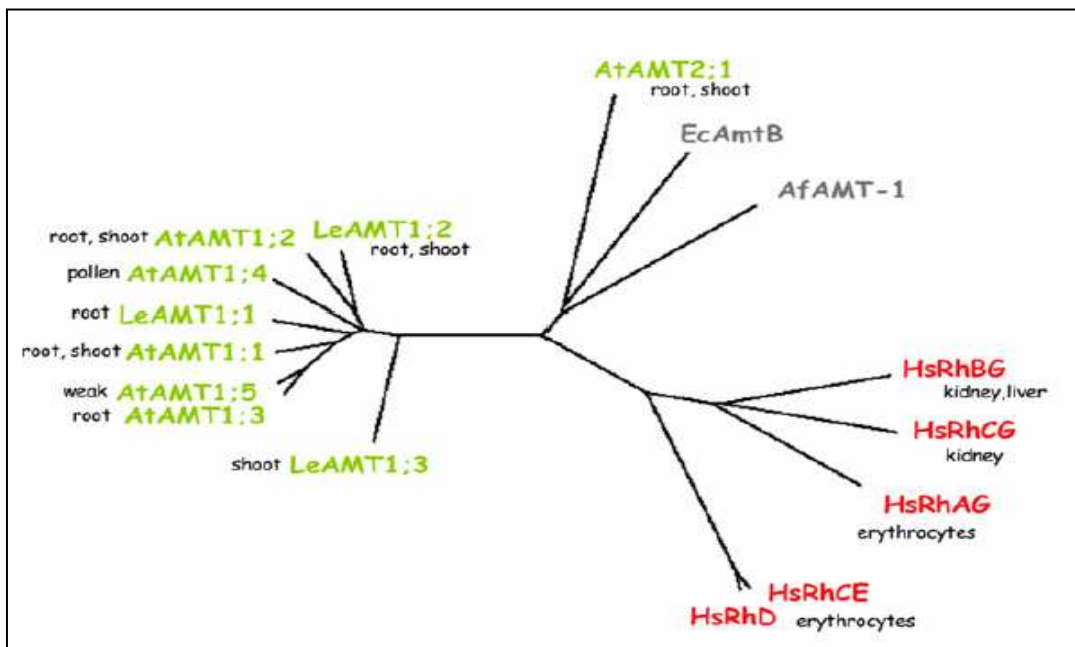
Figure 14. Un-rooted sequence distance tree of selected AMT/Rh homologs based on a ClustalW alignment. The tree contains two prokaryotic AMTs with known three-dimensional structure from *Archaeoglobus fulgidus* and *Escherichia coli* (grey); all AMTs from the plant *Arabidopsis thaliana* and three characterized members from *Lycopersicon esculentum* (tomato, green) and the human Rh glycoproteins and non-glycosylated Rh proteins. The preferential site of expression is given next to the sequence names. Only one plant member (*AtAMT2;1*) is similar to the bacterial ammonium transporter. *In* Uwe Ludewig *et al.,* (2007)

C.2. Transcriptional regulation & phenotypical analysis of AMT mutants

It has been demonstrated that the molecular basis of ammonium transport and its regulation by the nutritional status are strongly correlated and thus link high-affinity ammonium influx to *AMT* expression. In plant the first correlation of the AMT-transcripts and proteins with ammonium influx was made in the model system *Arabidopsis thaliana*. Yet it has been demonstrated in this genetic background that the transcriptional regulation is the main response to nitrogen and carbon availability and hence their respective metabolism (Gazzarrini *et al.,* 1999; Loqué *et al.,* 2006). In *Arabidopsis* 4 out of the 6 identified *AMT* genes were up-regulated by nitrogen deficiency, photosynthetic products such as sugars and are diurnally regulated, albeit to a different extent (Sohlenkamp, *et al.* 2002; Lejay *et al.* 2003). The studies of the ammonium transporters under different concentrations of combined nitrogen source (Mainly NH_4NO_3) showed that *AtAMT1.1* expression and ammonium influx were down-regulated after ammonium re-supply to N-starved plants and these effects negatively correlated with glutamine levels, suggesting that glutamine may be a feedback signal for inhibition of ammonium influx after re-supply (Rawat, *et al.,* 1999). The use of double knockout alleles of the *AtAMT1.1* and *AtAMT1.3* reduced the ammonium influx by 70% showing that both transporters acts in an additive way under N-deficiency, consistently with their plasma membrane localization and expression in rhizodermal and cortical cells of primary and lateral roots, including the root hair zone (Kaiser *et al.* 2002, Loqué *et al.* 2006. Mayer and Ludewig 2006). Despite the fact that ammonium influx under N-deficiency was reduced up to 70% by the loss of *AtAMT1.1* and *AtAMT1.3*, only a little effect on growth was observed. This is also observed when the *AtAMT2.1* member was down-regulated by RNAi (Sohlenkamp *et al.,* 2002) giving a strong support to the fact that under most conditions, the residual amount of ammonium is sufficient for growth. Thus the involvement of other high affinity transporters in ammonium influx, having inner vascular localization (*AtAMT1.2*) as well as the presence of low affinity transporters that were not yet well identified or characterized, may reflect the rescue of plant growth under stressed condition of growth.
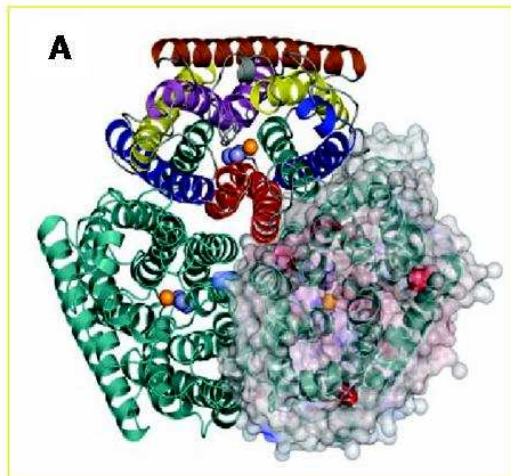
Figure 15 A, the crystallographic structure of the Ec-amtB is the consensus model for all the high affinity transporters. It shows 3 monomers forming a pore that allows the transport of NH3. **B, o**ne monomer is the product encoded by the *amtB* gene. The protein shows 11 highly hydrophobic domains with an extracellular N terminanl tail and a C-terminal tail. A single substitution in segment 5 (Histidin replaced by aspartate) of the Ec-amtB leads to partial active MeNH$_4^+$ transport.

C, importance of the C-terminal tail: a Threonin residue is crucial in the functioning of the ammonim transporter by a phosphorylation mechanism, while a single mutation in the tails is sufficient to disrupt the co-assembling of the 3 subunits.
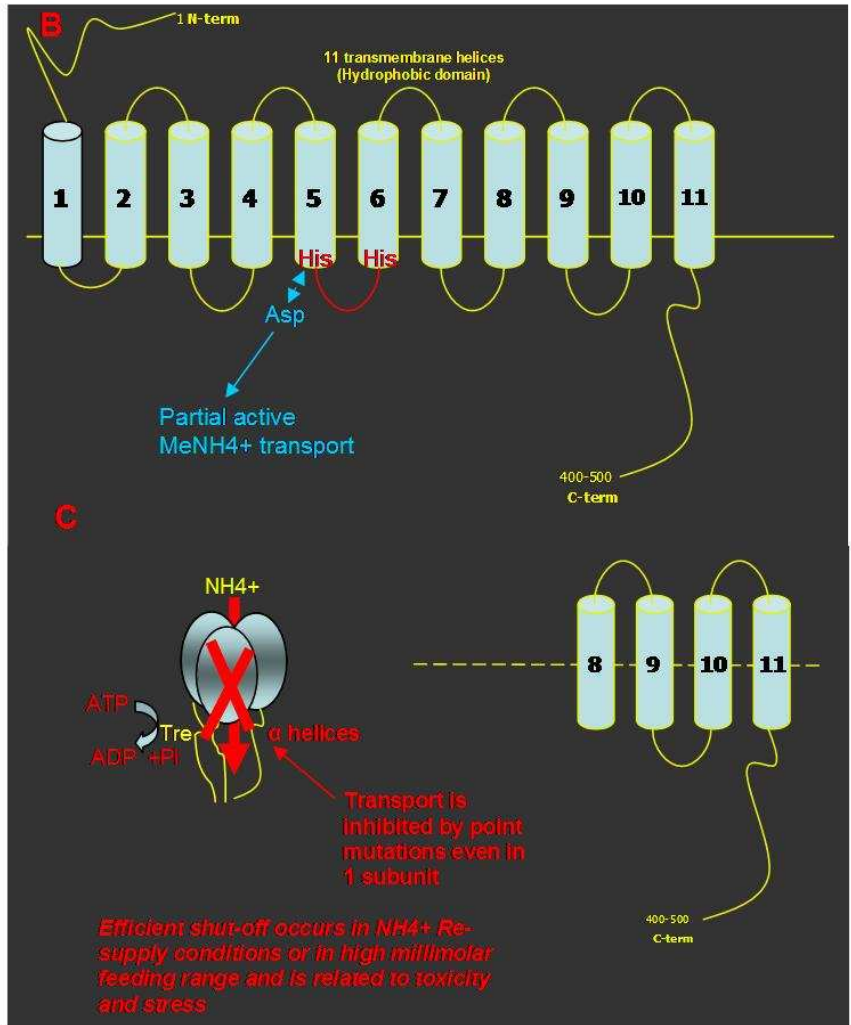
C.1.2. Crystallographic structure and post-transcriptional regulation

The crystallographic structure of the ammonium transporters was resolved in 2004 by Khademi *et al.,* (2004) using as model the *E coli* amtB transporter. The three dimensional molecular configuration of the AamtB high affinity transporter shows three amt unities of the same monomer (trimer structure; figure 15A). One monomer is formed by 11 α-helical trans-membrane α-helixes arranged in a two fold almost symmetric configuration (Khademi *et al.,* 2004; Miercke and Stroud 2004; Andrade *et al.,* 2005), an N-terminal extra-cellular domain and an intracellular C-terminal end (figure 15B). The molecules of ammonium are up-taken or released through a highly hydrophobic non polar pore. This pore shares two highly conserved Histidines (His) which form a hydrogen bond. However, the structure of the pore that is extending from the extra-cellular hole to the inner cytoplasmic part shows a high diversity pattern in amino acid composition upon organisms. Recently mutational studies showed that the replacement of the first histidine (H168) by aspartate (Asp) in the *Ec*-amtB protein yielded a partially active Methyl-ammonium (MeA) transport. Similar studies using mutation in single subunits of the plant *LeAMT*1.1 showed that transport is inhibited by point mutations in the cytoplasmic carboxylic-tail (Ludewig *et al.,* 2003). In this case, the residue responsible of the good close co-operativity (threonin 460) was revealed through a large scale phospho-proteomic study involving the *At*AMT1.1 transporter (Loque *et al.,* 2007). Therefore, the mutational exchange of the threonin by a charged amino acid that mimics phosphorylation inhibited NH_4 transport and abolish the formation of the trimer when expressed in oocytes or in yeast. (figure 15C) Despite the absence of evidence describing the reverse mechanism (dephosphorilations), these mutational studies argue in favor of a post-translational regulation of the AMT genes that it is possibly related to the control of the omo-trimerization process. Consistently, this mutated AMT1 behaves as dominant negative when co-expressed with wild type AMT1 either in yeast and xenopus leavis oocytes (Neuhauser *et al.,* 2007). Moreover, the implication of the *Ec-amtB* carboxylic tail in the post-translational regulation of the AMT through direct interactants was deeply investigated in *E.coli* (Durand and Merrick, 2006) indicating that the uptake activity of the PM-bound AMT protein is quickly regulated by interaction with the PII-homologue GLNK protein. Thus the conserved linkage of these two genes is strongly suggestive of a

functional interaction between their products (Thomas *et al.,* 2000) and it has been shown that the glnK protein is indeed sequestered to the membrane in an amtB-dependent fashion (Coutts *et al.,* 2002; Javelle *et al.,* 2004). This interaction constitutes a novel signal transduction pathway which we believe is ubiquitous in bacteria and archaea.

When external ammonium is limiting, amtB facilitates the transport of ammonium into the cell where it is converted to glutamine by glutamine synthetase. As the intracellular glutamine pool rises, the deuridylylation of the GlnK protein and its binding to amtB is triggered which in turn inhibits ammonium transport. This process occurs at external ammonium concentrations between 5 and 50uM. It is very rapid, occurring within seconds, and is fully reversible. The interaction provides a mechanism whereby not only is the activity of amtB regulated in response to the cellular demand for ammonium but the cellular pool of glnK is also modulated rapidly in response changes in the extracellular ammonium availability (Javelle *et al.,* 2004). Dynamic changes in the subcellular localisation of proteins are emerging as important factors in controlling cellular physiology and this system offers an attractive model to study one such mechanism.

In plants, the possibility of a post-translational mechanism of regulation of the AMT1 activity was first postulated in *Arabidopsis thaliana* on the basis of experiments showing that $^{13}NH_4^+$ influx declined more rapidly than root *AtAMT1;1* transcript abundance after shifting the plants from a N starvation to a N excess condition (Rawat et al. 1999). This may be related to the need for a quick and efficient inhibition of the AMT activity in the presence of high concentrations of ammonium when AMT proteins are still bound to the plasmatic membrane (Loqué, D. *et al.,* 2006, Mayer and Ludewig, 2006)

Figure 16. **A.** The RhD transporter is an etero-trimer formed with different subunits (RhD, RhC, RhC/E) having D, C, E epitopes. The biological function of AMT/Rh membrane proteins in ammonium transport, NH_3 facilitation by RhAG in human erythrocytes. By contrast, strong consumption and catabolism of glutamine may preferentially leads to release of ammonium while in the case of bacterial ammonium transporter (not reported in this figure), the NH3-facilitation is followed by metabolic trap. **B,** the *LeAMT1.1* transport system transport NH3 only in a short constricted region of the pore lumen but only NH4+ is released into the cytoplasm after re-protonation.

C.1.3. Mechanism of ammonium transport

As it's reported in § C.1., the ammonium is transported either by high affinity or by low affinity systems, each transport system being tightly related to the outside nutritional cues and inside nutritional status of the cell (concentration, pH, Temp.). The mutational studies as well as the biophysical features of the transporters (last §.) shed the light on the mechanism by which the ammonium/ammonia is uptaken or retrieved by the cells. Thus, it is possible to determine the preferential form of Nitrogen compound transported for a given transporter. For instance, *E. coli* amtB as well as human the RhAG transporter are probably structured for the NH_3 transport (figure 16 A).

Moreover, thermodynamic features could guide the transport of the preferential nitrogen form. There is for example a close co-operativity between *Ec*-amtB and the cytosolic GS to recruit a very low ammonium concentrations. GS has the key role in nitrogen acquisition avoiding NH_3 toxicity in the cytoplasm; by contrast RhAG, that shares the same *Ec*-amtB transport system, seems to recruit NH_3 through a thermodynamic antipodal mechanism that is different from the *E. coli* transport system (figure 16A).

By contrast, electrophysiological studies on the tomato LeAMT1.1, indicates that this transporter, transports the NH_4^+ form. The properties of LeAMT1;1 were examined by expressing the protein in *Xenopus laevis* oocytes and using two-electrode voltage clamp to study the transport mechanism. Micromolar concentrations of external ammonium, induced voltage and concentration-dependent currents that remained constant over a pH range of 5.5 to 8.5 (Ludewig *et al.,* 2002). This is in agreement with NH_4^+ being the transported species because if NH_3 was transported, the K_m should increase by tenfold for each unit increase in pH, considering that the pKa of the two forms NH_4^+/ NH_3 is 9.25 and hence that at physiological pH most of these are present in the NH_4^+ form. The ammonia form NH_3 is converted (protonation) to NH4+ before reaching the inner cytoplasmic part of the transporter (figure 16B). This particularity is due to the mechanistic way of transport that characterizes the *Le*AMT1.1. Indeed, it was demonstrated (Ludewig *et al.,* 2002; Mayer *et al.,* 2006) by monitoring the intracellular pH (pHi) of voltage clamped oocytes with a fluorescent dye that *Le*AMT1;1 strictly selects for net NH_4^+ transport, but excludes NH3 transport. Acidification was only

identified in voltage clamped, but not in unclamped oocytes, probably for two reasons: (i) NH_4^+ influx at normal resting potentials is small compared to the buffering capacity of the cytosol. At the cytoplasmic near neutral pH only _1% of the inflowing NH4 is deprotonated to form H+ and NH3. (ii) The transported NH_4^+ depolarizes the cell, diminishing the driving force for NH_4^+. These experiments as well as similar studies made on AtAMT1.1 in Arabidopsis background (Shelden *et al.,* 2001, Wood *et al.,* 2006; Mayer and Ludewig 2006) strongly suggested that even residual net NH3 transport is unlikely in LeAMT1;1.

Thus, the question of which is the NH_4^+/ NH_3 form to be transported by the AMT protin is still controversial with contrasting data reporting in the literature. However, the predicted model that takes in account the conclusions drawn for both Ec-amtB and *Le*AMT1;1 is that in the inner cytosolic region (figure 17A and B), NH3 is transported
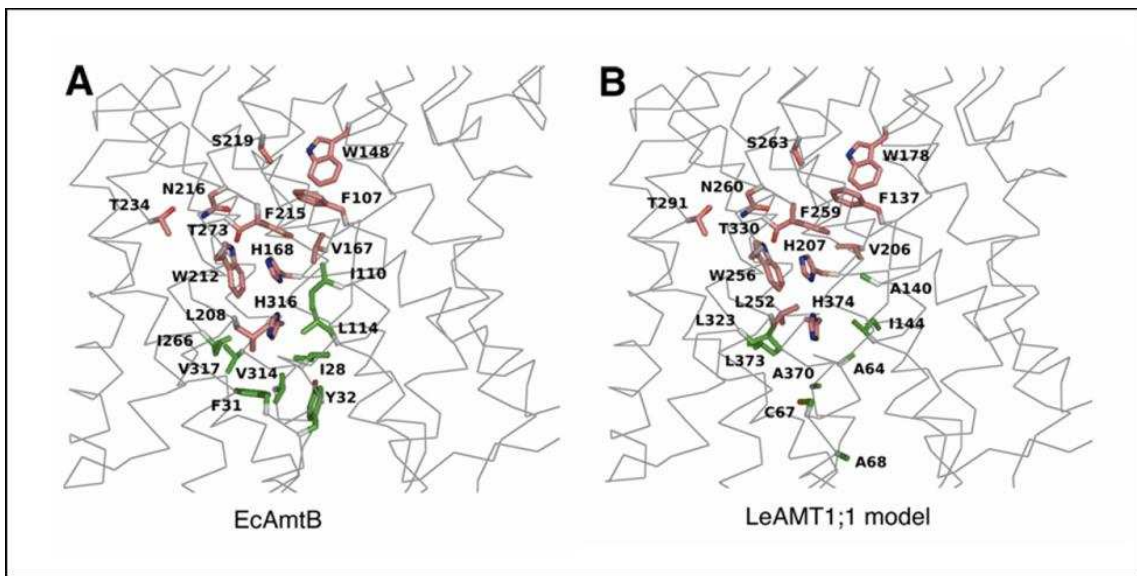

Figure 17. Comparative model of the pore zone for *Ec*amt-B (**A**) and *Le*AMT1.1 (**B**) The side chains of the pore lining residues in the structure (PDB code: 1U7G) of EcAmtB in comparison with the LeAMT1;1 homology model are explicitly shown. Identical residues are shown in salmon, divergent but corresponding residues in green. The non-polar character of the pore-lining residues is entirely conserved in LeAMT1;1. (*in* U. Ludewig *et al.,* 2007)
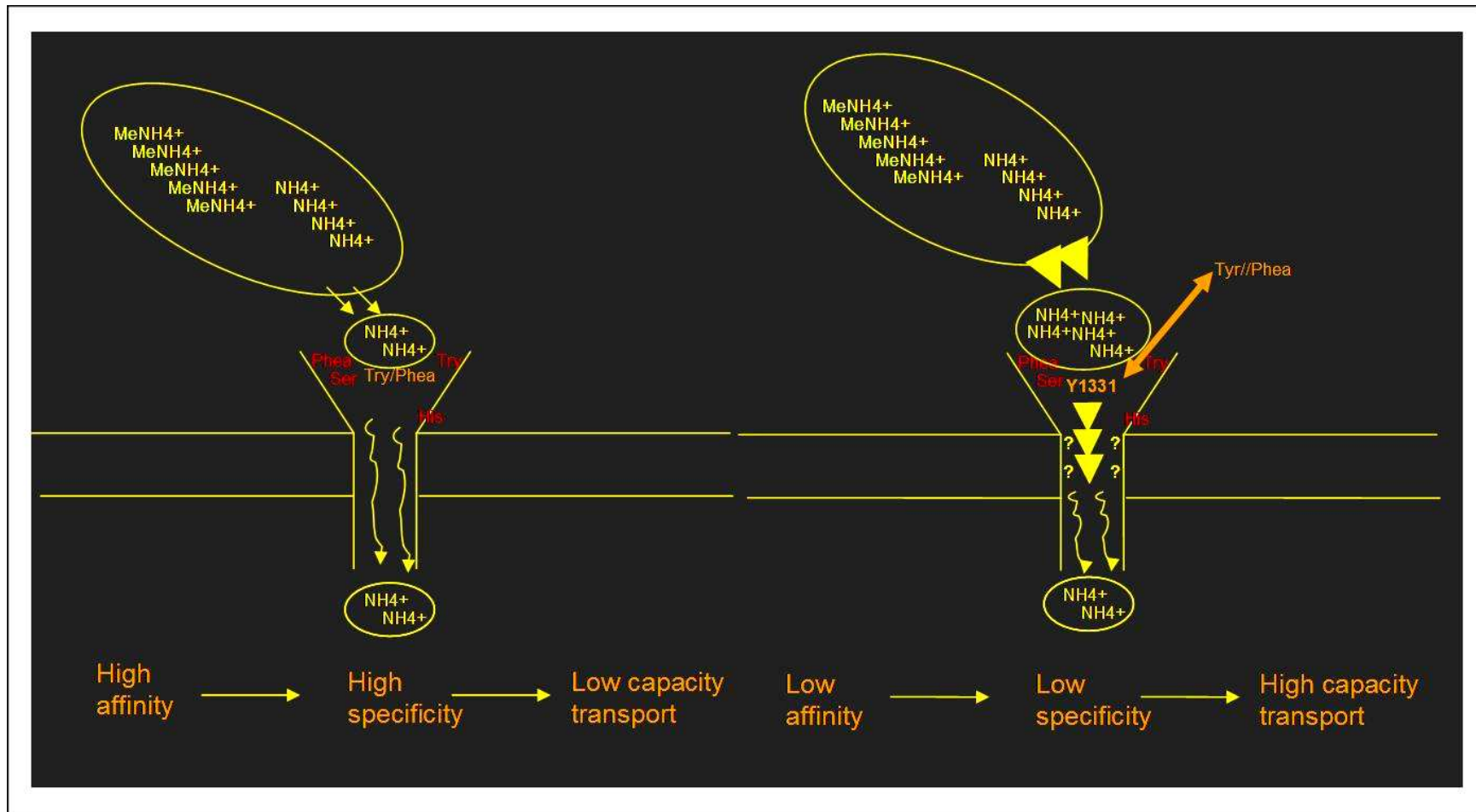
Figure 18. The physiological functioning of the plant high affinity ammonium transporter implicates the presence of aromatic residue (Phenylalanin and tryptophan) that guide the specificity to NH4+ in the outer part of the pore (left panel) and thus the replacement of just one of these residues by an hydrophobic amino acid (Y1331) leads to enhancing the capacity of uptake of about 10 fold in the outer part of the pore lowering the affinity to NH4+ and MeNH4+. However the Km is maintained indicating that other deeper sites in the pore lumen are responsible of the affinity (right panel). The study indicates that the low affinity correlating respectively with a low specificity and high capacity of pore occupancy can not be the system of transport of the wild type AMT transporters.

for a short constricted tract and meantime a proton is conducted in the same stechiometric manner. This fact could explain the selectivity of the AMT against alkali cations (Ludewig *et al.,* 2002) while the NH3 form (rapidly converted in NH4) could also be retrieved from an estimated large loss in root and shoot tissues (Nielsen and Schjoerring 1998). One relevant point explaining the affinity of the ammonium transporters to NH4+ lies into the high conservation of the residues at the recruitment site (figure 18). The disruption of the aromatic site (phenylalanine or tryptophan) by insertion of a hydrophobic amino acid (Y133I) in LeAMT1.1 increases the affinity for NH_4^+ and Me NH_4^+ by_10-fold and lowered the maximal transport capacity. Therefore, the recruitment site favors the moderate binding of NH4+ suggesting that deeper sites are involved in affinity recognition of the cation NH4+ form. This mechanism provides a brief and transient occupancy of the pore entrance and by contrast allows high rate occupancy of the pore lumen. Then the transport of the NH4+ as well as the $MeNH_4^+$ is related to the electrophysiological potential created into the inner part of the pore. Ludewig *et al.,* (2007), estimated on the basis of the homology between predicted models that it is counter productive to limit the uptake rate to very low concentrations even if no evidence of a minor specificity that correlates to lower affinity was yet reported in literature.

C.2. Pathways and nitrogen fluxes in plant

The AMT genes could be considered as a part of an assimilatory pathway monitored by the nutritional demand and the variation in Carbon/Nitrogen metabolism ratio. The first attributed role is the transport of the NH_4^+. However, other different roles could probably be assigned to the ammonium transporters.

C2.1. Ammonium assimilation

Once uptaken into the cell through the AMT, the ammonium is immediately integrated into the GS-GOGAT cycle. This assimilation is important to avoid toxic effect of the ammonium on plant metabolism (ammonium is an in vitro un-coupler of photophosphorylation (Izawa and Good, 1972). In the GS-GOGAT pathway the ammonium is assimilated directly by contrast to the nitrate ion that has to be reduced in
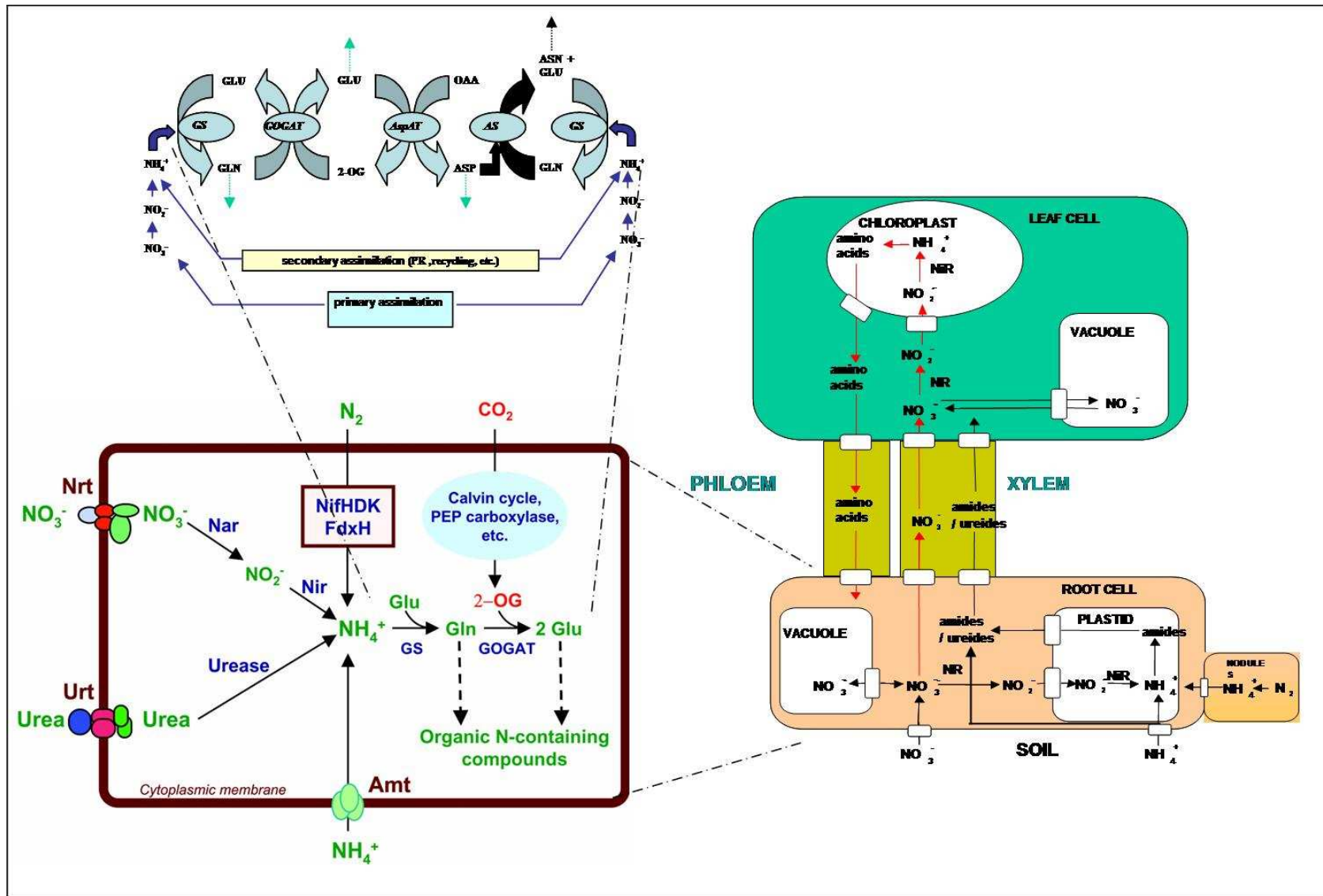
Figure 19.A. GS-GOGAT assimilation pathway showing the different amino acids that are synthesized right after NH4+ assimilation by the glutamine synthetase and their subsequent recycling or translocation in other pathway. **B.** representation of the ammonium assimilation pathways that take place in a single cell (here root cells) with the different entering ammonium sources; **C.** N fluxes in different tisues and organs. The very small white boxes represent the different transporters, essential sentries that ensures the continuum of NH4+ assimilation from soil (or nodules) till the shoot green organs.

Nitrite and then in NH_4^+ ions (figure 19A). The glutamine synthetase enzyme is then in charge to produce substantial amounts of glutamine from the NH_4^+, which requires an equally substantial amounts of α-ketoglutarate (obtained from glycolysis and mithochodrial respiration of photosynthate) as a carbon skeleton necessary for glutamate formation through GOGAT. It is well established, that plants produce significant amounts of ammonium endogenously from process such as photorespiration, phenylpropanoid biosynthesis and amino acid catabolism. The coordination of the assimilation places the GS-GOGAT in the center of a virtual sphere where transporters are the border first sentries regulating the combined nitrogen flux (figure 19B, C). Grain legumes as *Lotus japonicus* have a double origin of nitrogen sources, from the root uptake and from the nodule through atmospheric nitrogen fixation (figure 19C; Triplett, 2000, Gordon *et al.,* 2001).

Different combined N sources show some differences in their assimilation pathways. NO_3^- is translocated during light period to the shoot part or stored into the root vacuoles when it is present in strong excess in the soil. The long distance xylem sap transport is followed by the downloading of the N03- into the leaf apoplasm to reach the mesophyll cells, where NO_3^- is again absorbed and either reduced to NO2- or stored into the vacuoles (Crawford and Glass, 1998). By contrast, NH_4^+ is mainly translocated already incorporated under amid, amino acids or ureides forms. Although the process of transport of the NH_4^+ has been found to vary widely among higher plants (Bolard 1957, Reinbothe and Mothes, 1962; Patejs 1973; Peter *et al.,* 1979), recent studies showed that probably ammonium could be even translocated as the cationic form.

NH_4^+ is the major form for nitrogen retrieval after unavoidable losses from deamination or transamination processes. This could either involve the AMT proteins themselves (Loqué and von Wirén, 2004) as well as other proteins responsible for its efflux to the apoplastic compartment (loqué *et al.,* 2005). This could be also in agreement with the expression of the AMT in different organs like the petiole bases, the sink and source leaves and roots (D'apuzzo *et al.,* 2004; this PhD) and the plasma membrane protein location.
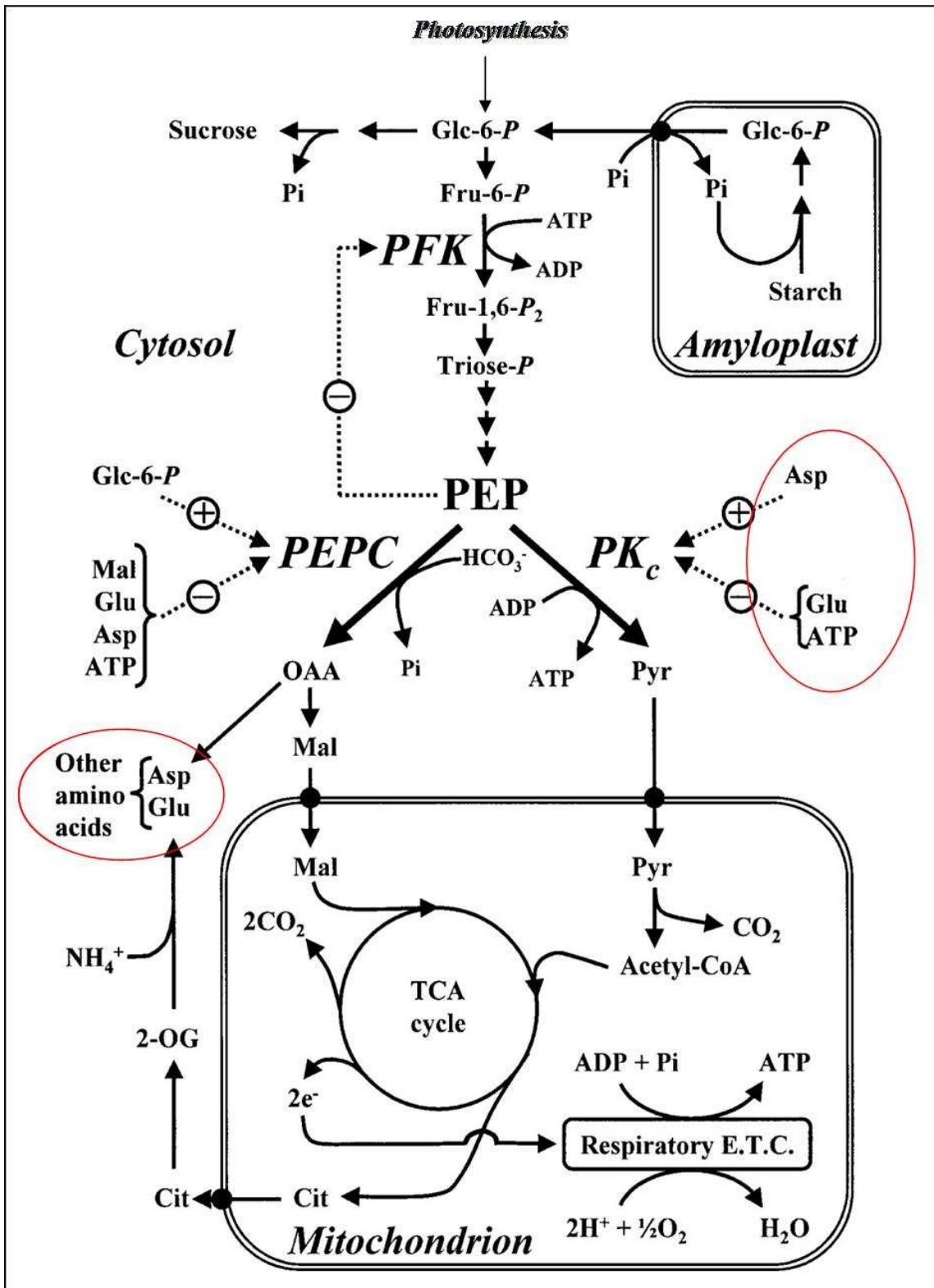
Figure 20. The GS-GOGAT assimilation cycle is tightly related to the different pathways of carbon metabolism through the PEP and its respective converting enzymes, the PEP carboxylase and the PEP kinase.

In all the cases, transport and assimilation are orchestrated by the C/N ratio (Palenchar *et al.,* 2004; Gutierrez *et al.* 2007) where the pathway of GS-GOGAT is tightly linked to the carbon metabolism/catabolism (Glycolysis) through the PEP carboxylase (figure 20). This enzyme serves to generate hydrogen ions, which are necessary to replace those extruded from root cells in exchange for incoming ammonium ions (Aznozis and Findenegg, 1986). The direct evidence of the key role played by PEP carboxylase is given by its anapleurotic action that promotes the replacement of oxaloacetate in the TCA cycle (oxaloacetate levels are depleted due to the remova1 of an α-ketoglutarate in the assimilation of ammonium via the GS-GOGAT cycle). Besides, other strong supports to the interaction at different physiological levels of carbon and nitrogen metabolism in plants are given by the phenotypes observed when growth parameters are analyzed in different condition of imbalanced C/N ratio. Since long time, it has been argued (Lindt and Feller, 1987) that the root assimilation of ammonium diverted carbon from root growth. Therefore, the reduced growth from culturing on ammonium depends by re-allocation of phloem-derived carbon to nitrogen assimilation rather than root expansion growth (Lewis *et al.,* 1989). This assumption was strongly confirmed by the quick disappearing of the limited storage carbohydrate reserves after supplying seedling plants with ammonium. This determines the need for using proteins and lipids as respiratory substrates and subsequently a rapid catabolism of chloroplast proteins and pigments in the photosynthetic tissues (Goyal *et al.,* 1982 and Mehrer and Mohr 1989). All these considerations appear to be crucial in reconsidering the general uptake of combined nitrogen sources and in particular the study of the related transporters in the framework of a C/N metabolism general panel. However recent studies (Lopez-Bucio, *et al.,* 2003, Doerner, 2007) updating the local effect of macro-mineral sources on the root growth and architecture development insist on the specific role of the phytohormones rather than that of the C/N ratio and suggests a potential signaling role played by these minerals in coordinating the mechanisms of sensing the local nutritional status (see next § C.2.2.)
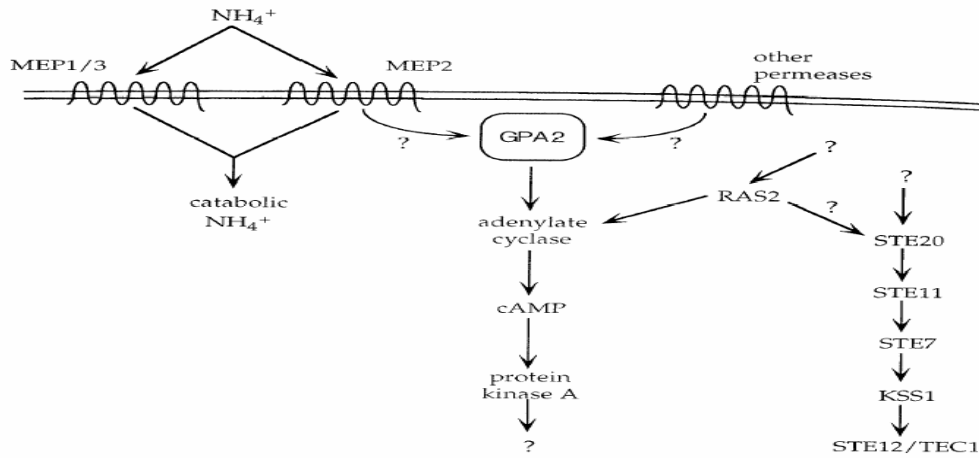
In *S. cerevisiae*

Figure 21. A model for MEP2 control of pseudohyphal differentiation. Ammonium starvation is sensed via MEP2 to produce a signal that activates GPA2 and a signaling pathway that regulates filamentous growth independently of the MAP cascade. (In Lorenz and Heitman, 1998)
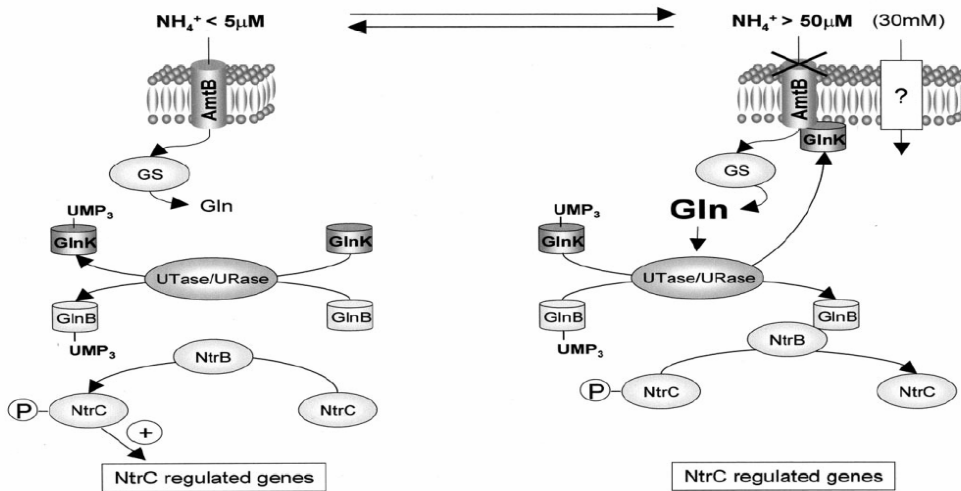
In *E. coli*

Figure 22. Model for function of AmtB and GlnK ammonium transport and their integration into E coli Ntr system. When extracellular NH4+ concentrations are around 5µM or less, ammonium enters the cell via AmtB and is converted by glutamine synthetase (GS) to glutamine, which is utilized in metabolism. The intracellular glutamine pool is low, and urydylyltransferase (UTase) uridylylates both GlnK and GlnB. NtrB phosphorylates NtrC, and NtrC-dependent gene expression is activated. When extracellular NH4+ concentration rises above 50µM, the metabolic demand for glutamine is exceeded, the intracellular glutamine rises, and uridylyltransferase deuridylylates GlnK and GlnB, GlnK complexes with AmtB, thereby inhibiting its transport activity. GlnB interacts with NtrB and activates its phosphatase activity leading to dephosphorylation of NtrC and NtrC-dependent gene expression ceases. At high extracellular NH4+ concentrations (*e.g.* 30 mM), ammonium enters the cell either, by an unidentified low affinity transport system or by free diffusion. (In Javelle *et al.,* 2004)

C2.2. Ammonium sensing

Evidence of the ammonium sensing has been established through the identification of the Mep proteins in the yeast *S. cerevisiae.* In particular, the Mep2 protein is responsible of the pseudohyphea formation in NH_4+ depleted growth medium (figure 21) as demonstrated by the phenotypical analysis of a *mep2* mutant strain. In this case, Mep2 acts, independently by its ammonium uptaking function, as a possible sensor of the external N conditions and it is crucial to link directly this signal to a precise developmental program such as pseudohyphea formation.

Recent data reported in literature suggest that this sensing function can be related to different plant transporters as in the case of the A. thaliana high affinity nitrate transporter NTR2;1. A recessive mutation in this gene is responsible of the alteration of *Arabidopsis* plants capacity to respond to specific nutritional clues such as nitrate availability in the medium. However, this function is independent by the NTR2;1 nitrate uptake activity and can directly affect the architecture of the root system and in particular the secondary root formation (Little *et al*. 2005; Remans *et al*. 2006).

An indirect signaling pathway that relies to the general nutritional status of the organism can also mediate the linkage between N conditions and growth capacity. In this case, the changes of specific metabolites concentration can be perceived by metabolic sensors that determine the right response to specific nutritional cues.

This example is well represented by the glnK protein a member of PII family proteins. that interacts with *Ec*-amtB in a nitrogen dependent fashion (Merrick et al 2004; see § C.1.2.). This year the crystal structure of the complex amtB-glnK was resolved (Conroy *et al.*, 2007) indicating that other *in vivo* compounds are likely to be necessary to produce a stable complex. The study finally gave a relevant confirmation to the existence of a new pathway monitored by the PII multigenic family that physically links the GS-GOGAT assimilatory pathway to the uptake activity of the AMT proteins (figure 22). Despite these encouraging findings, only one homologue of the PII multigenic family was found in *A. thaliana (Hsieh MH et al., 1998)* and one in *L. japonicus* (in sequence databases).
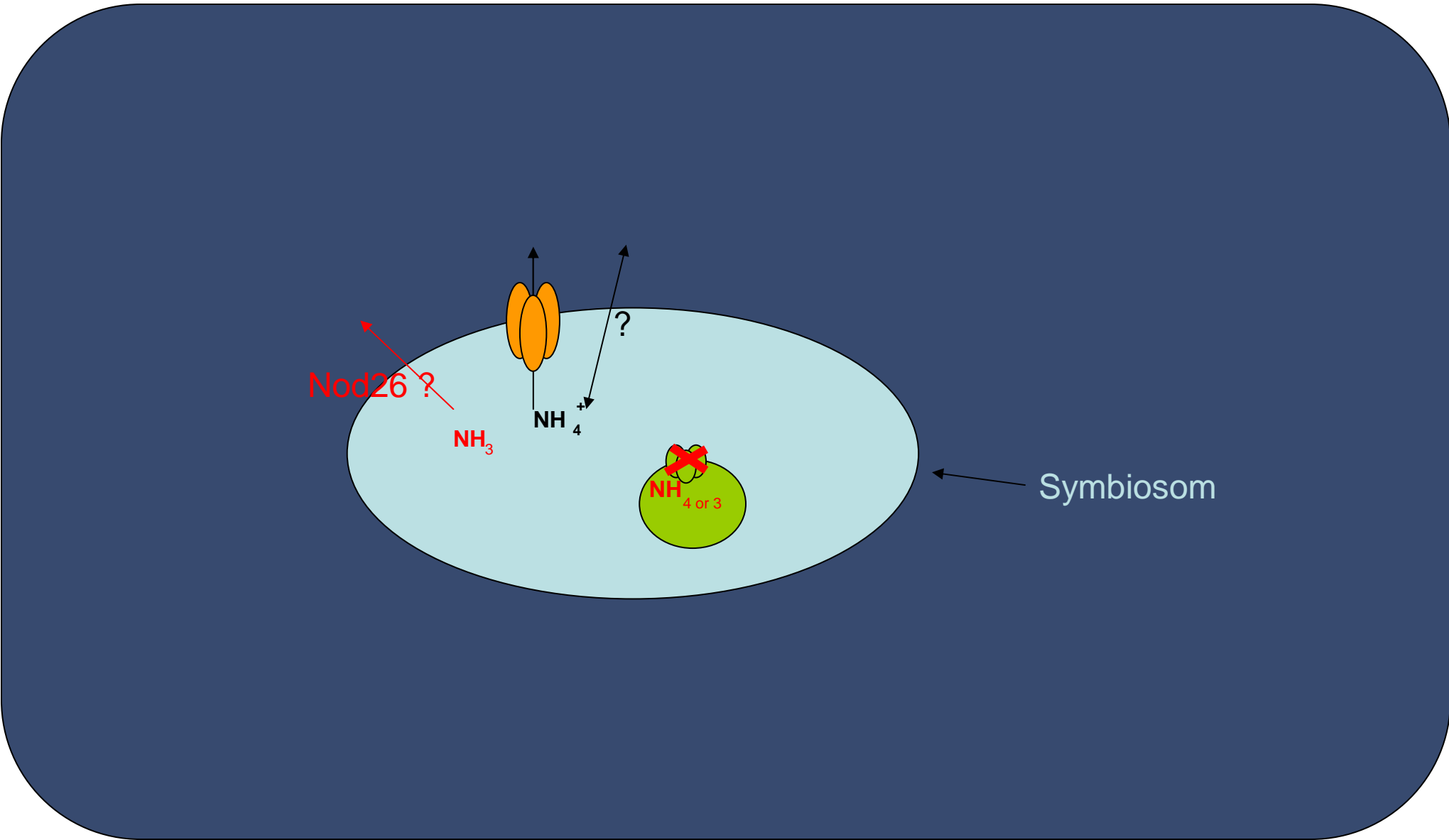
Figure 23. Infected cell showing the putative presence of a high affinity ammonium transporter on the symbiosome membrane and a putative aquaporine like transporter facilitating NH3 transport from the symbiosome to the cytoplasm of the invaded cell. The shut off of the amtB of the bacteroids once this is encapsulated into the symbiosome is also shown. Double sense arrow indicate possibility of NH4+ retrieve into the symbiosome by an unknown mechanism/transporter?

C2.3. Transport to the plant cells of the nitrogen fixation product (NH_4^+/NH_3)

Once the effective nodules are formed and the symbiotic interaction is established, a myriad of nitrogen skeleton based compounds, are synthesized by the encapsulated bacteroids inside of the symbiosome structures (Udvardi and Day, 1995). Their transfer to the plant host cells that implies, as counterpart, an inverted flux of carbohydrates, needs to cross 2 layers of different phospholipidic membranes, spatially separated by the symbiosome cytoplasm: the bacteroid membrane and the peribacteroid membrane. The mechanism by which those compounds are transported is not yet completely resolved and remains for most of the cases unclear. Nevertheless, it was demonstrated that inside of the symbiosome Rhizobia does not express the amtB gene and thus the bacterial amtB transporter do not participate to the release of the NH3 (Taté *et al.,* 1998).

Both nitrogen forms NH3 and NH4 are present inside of the symbiosom and the plant-derived peri-bacteroid membrane seems highly permeable to them (Niemietz, and Tyerman, 2000). As it is shown in figure 23, the release of NH3 may also be facilitated by NOD26, an aquaporin (water channel) homolog, present at high concentration on this membrane. The role of the aquaporin could be consistent with the capacity shown by the TIP2 proteins (aquaporin tonoplast intrinsic proteins/sub-family 2) to transport NH_4^+ for its vacuolar storage in the root cells (Loqué, *et al.,* 2003). The peculiarity of this aquaporin lies in its high similarity to the RhGA protein in terms of NH3 pH–dependent transport mechanism. However, the phenotypical analysis of an interfered *L. japonicus AMT2.1* transgenic line did not confirm such a role. In yeast an analogous vacuolar accumulation of C14::Me NH_4^+ could depend on a V-ATPase (Wood *et al.,* 2006).

C.2. *Lotus japonicus* ammonium transporters

   The *Lotus japonicus* ammonium transporters were isolated by our team in 2004. We readily analyzed different characteristics of the three isolated ammonium transporters termed *LjAMT1.1;1.2;1.3*. They belong to the high affinity transporter family as it's shown in the phylogenetic dedrogram (figure 24), far away from the second family termed AMT2 that is closer to the prokaryotic ammonium transporters (Udvardi and Howitt, 2000).
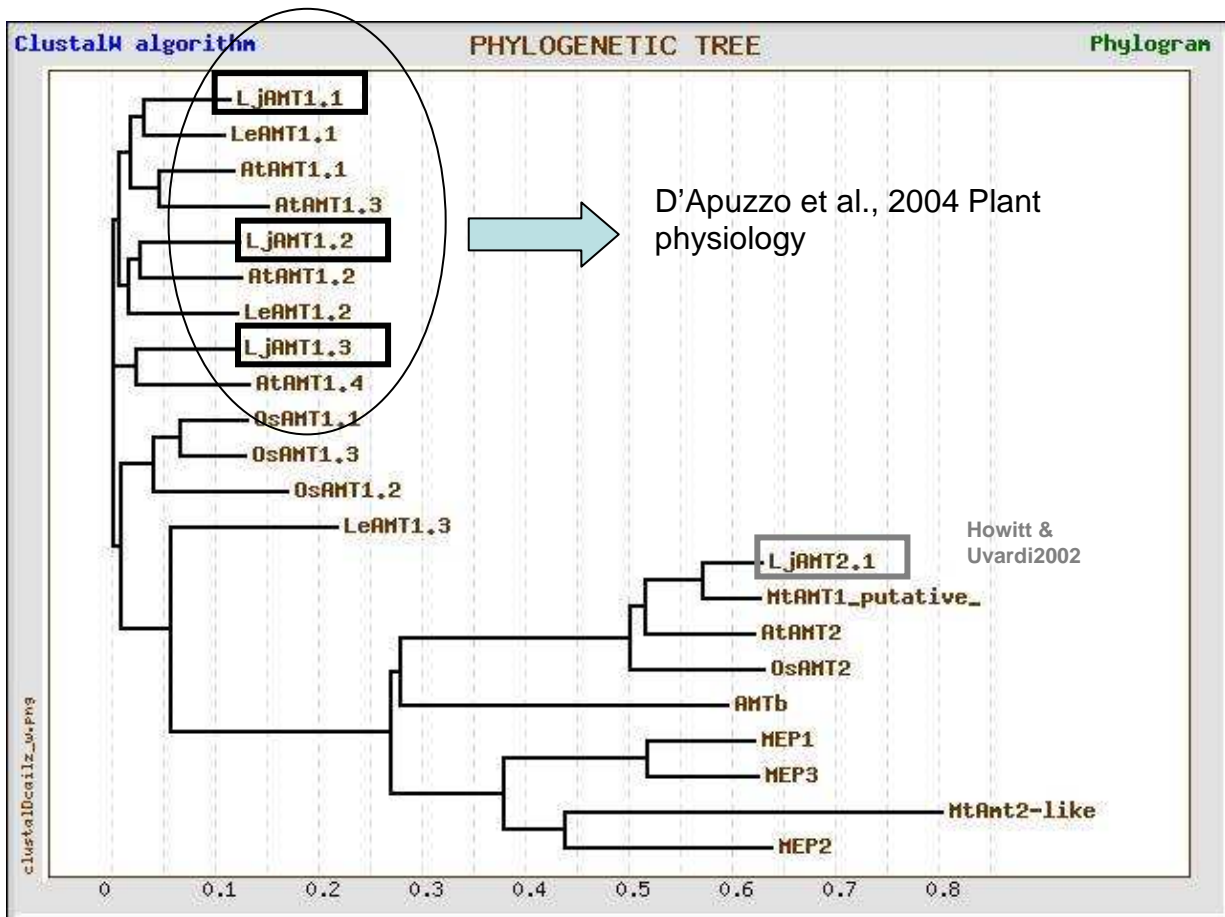

Figure 24. ClustalW dendrogram showing the speciation in the high affinity transporters where the *LjAMT1* family belongs to the plant eukaryotic clade while the *LjAMT2* member belongs to the prokaryotic one.

A

```
gi|15236300|ref|NP_193087.1|    ----MSCSATDLAVLLGPN----ATAAANYICGQLGDVNNKFIDTAFAID 42
gi|31322044|gb|AAM95453.1|      -MASLSCSATDLAPLLTATTNATATAAATYLCNQLDTISRKLSDTTYAVD 49
gi|46409004|emb|CAE01484.1|     MAAAFTCSAADLHPLLGTGAN--ATAAAEFICSRFGAISNKFTDTAYAVD 48
                                ::**:**:**  **  .    ***** ::*.::. :.**: **::*:*

gi|15236300|ref|NP_193087.1|    NTYLLFSAYLVFSMQLGFAMLCAGSVRAKNTMNIMLTNVLDAAAGGLFYY 92
gi|31322044|gb|AAM95453.1|      NTYLLFSAYLVFAMQLGFAMLCAGSVRAKNTMNIMLTNVLDAAAGGLSYY 99
gi|46409004|emb|CAE01484.1|     NTYLLFSAYLVFAMQLGFAMLCAGSVRAKNTMNIMLTNVLDAATGGIFFY 98
                                ***********:********************************:**: :*

gi|15236300|ref|NP_193087.1|    LFGYAFAFGSPSNGFIGKHYFGLKDIPTASADYSNFLYQWAFAIAAAGIT 142
gi|31322044|gb|AAM95453.1|      LFGFAFAFGAPSNGFIGRHFFGLKHYPSPTYDYSFFLYQWAFAIAAAGIT 149
gi|46409004|emb|CAE01484.1|     IFGFALAFGTPSNGFIGKHFFGLNEFPSPSFDYGFFLYQWAFAIAAAGIT 148
                                :**:****:*********:*:****:. *:.: **. ***************

gi|15236300|ref|NP_193087.1|    SGSIAERTQFVAYLIYSSFLTGFVYPVVSHWFWSVDGWASPFRTDGDLLF 192
gi|31322044|gb|AAM95453.1|      SGSIAERTQFVAYLIYSSFLTGFVYPVVSHWLWSSDGWASPTRTTGSLLF 199
gi|46409004|emb|CAE01484.1|     SGSIAERTQFVAYLIYSSFLTGLVYPIVAHWFWSSDGWGSPARTEN-LLF 197
                                **********************:***:*:**:** ***.** ** . ***

gi|15236300|ref|NP_193087.1|    STGAIDFAGSGVVHMVGGIAGLWGALIEGPRLGRFDNGGRAIALRGHSAS 242
gi|31322044|gb|AAM95453.1|      GSGAIDFAGSGVVHMVGGIAGLWGAFIEGPRIGRFDRTGRSVALRGHSAS 249
gi|46409004|emb|CAE01484.1|     GSGVIDFAGSGVVHLVGAVAGFWGAFIEGPRMGRFDHAGKPVPLRGHSGT 247
                                .:*.**********:**.:**:***:*****:****. *:.:.*****.:

gi|15236300|ref|NP_193087.1|    LVVLGTFLLWFGWYGFNPGSFNKILVTY----ETGTYNGQWSAVGRTAVT 288
gi|31322044|gb|AAM95453.1|      LVVLGSFLLWFGWYGFNPGSFLTIAKAYGNNGENGNYYGQWSAIGRTAVT 299
gi|46409004|emb|CAE01484.1|     LVVLGTFLLWFGWYGFNPGSFITILKSYGES-GSGNYYGQWSAIGRTAVT 296
                                *****:************** . * :*    .*.* *****:******

gi|15236300|ref|NP_193087.1|    TTLAGCTAALTTLFGKRLLSGHWNVTDVCNGLLGGFAAITGGCSVVEPWA 338
gi|31322044|gb|AAM95453.1|      TTLAGCTAALTTLFSKRLLEGHWKVLDVCNGLLGGFAAITSGCSVVEPWP 349
gi|46409004|emb|CAE01484.1|     TTLAGCSAALTTLFGKRLQTGHWNVTDVCNGLLGGFAAITSGCSVVDPWA 346
                                ******:******* *** :.**:* *** .. ** ** . ***

gi|15236300|ref|NP_193087.1|    AIICGFVAALVLLGCNKLAEKLKYDDPLEAAQLHGGCGAWGLIFTALFAQ 388
gi|31322044|gb|AAM95453.1|      AIVCGFVAAWVLIGLNLVAAKMKYDDPLEAAQLHGGCGAWGVLFTGLFAK 399
gi|46409004|emb|CAE01484.1|     AIICGFVAAWVLIGCNVLAEKFHYDDPLEAAQLHGGCGTWGIIFTALFAK 396
                                **:****** **:* * :* *::************:**::** :***:

gi|15236300|ref|NP_193087.1|    EKYLNQIYGNKPGRPHGLFMGGGGKLLGAQLIQIIVITGWVSATMGTLFF 438
gi|31322044|gb|AAM95453.1|      GEYVAEVYG-SAGRPYGLLMGGGGKLLAAQVIEILVVCGWVTATMGPLFY 448
gi|46409004|emb|CAE01484.1|     KQYVNEVYAGLPDRPYGLLMGGGWRLLAAHVVQILTIAGWVSVTMGAVFF 446
                                :*: ::*.  .. **:**:**** :**.*::::*:.: ***.***.:*:

gi|15236300|ref|NP_193087.1|    ILKKMKLLRISSEDEMAGMDMTRHGGFAYMYFDDD--ESHKAIQLRRVEP 486
gi|31322044|gb|AAM95453.1|      GLHKTKLLRISEDDETAGMDLTRHGGFAYAYHDDDDVSTKRGVMMSRIGP 498
gi|46409004|emb|CAE01484.1|     VLHKLNLLRISPEEEMAGLDMTSHGGLAYEYHEDVG-SVQKALKF--VFD 493
                                 *:* :***** ::* **:*:* ***:** *.:*    . ::.: :  :

gi|15236300|ref|NP_193087.1|    RSPSPSGANTTPTPV----- 501
gi|31322044|gb|AAM95453.1|      GSSSPSTMNTPAASAAANDC 518
gi|46409004|emb|CAE01484.1|     FYCKGNYYKTLLE------- 506
                                .  . :*
```

B

Figure 25. **A**, clustalW alignment of the three *Lj*AMT1 transporters AMT1.1 gi 15236300 ; AMT1.2 gi 3132044 ; AMT1.3 gi 46409004. **B,** domain conservation comparison (http://www.ebi.ac.uk) showing a less conservation in the C-terminal and N terminal ends (red lines) and high conservation in the hydrophobic part (blue line).

C2.1. Molecular and biochemical features

The three *Lotus japonicus AMT1* genes: *LjAMT*1.1, *LjAMT*1.2 and *LjAMT*1.3 share a high level of nucleotidic as well as amino acidic identity (figure 25A) where the maximum conservation is observed in the hydrophobic part while the maximum divergence is reached in the N terminal and C-terminal part (figure 25B). The hydrophobic domain spans 11 α helixes. The N-terminal is predicted to be out whereas the C-terminal tail is intra-cytoplasmic. A signal peptide with a weak cleavage site is predicted for *Lj*AMT1.1 (between residues 23-24), while a strong one is predicted for *Lj*AMT1.2 (between residues 27-28) and *Lj*AMT1.3 (between residues 26-27). The cleavage site is preceded by a putative N-glycosylated site (NAT). The affinity for the methylammonium (K_m $MeNH_4^+$) is highest for *Lj*AMT1.1 (0.16 mM; Vmax= 6.5±2.25 nmol min-1 mg-1 protein) followed by *Lj*AMT1.3 (0.47 mM; Vmax= 24±2 nmol min-1 mg-1 protein) and *Lj*AMT1.2 (1.72 mM; Vmax= 73±0.5 nmol min-1 mg-1 protein). The affinity for NH_4^+ is highest than for $MeNH_4^+$ as competition uptake rate experiments gave the following Ki: 1.7 µM for *Lj*AMT1.1, 3 µM for *Lj*AMT1.2 and 15 µM for *Lj*AMT1.3. The promoter region described in D'Apuzzo *et al.* (2004) spans fragments of respectively 496 bp, 593 bp and 689 bp for *LjAMT*1.1, *LjAMT*1.2 and *LjAMT*1.3, respectively. The main motives that were reported are: TGACTT motifs that bound the TGA1 related protein in tobacco (Fromm et al., 1991); GAT(A/T)A motifs identified in promoter region of genes responsible for N metabolism (Howitt and Udvardi, 2000)

C2.1. Functional characteristics

Real time experiments indicated a relative abundance of transcripts in different organs as follows: *LjAMT*1.1 > *LjAMT*1.2 > *LjAMT*1.3 in leaves, roots and nodules. The spatial localization of the *LjAMT1* genes expression in the different plant organs was determined by promoter::*gus*A fusions. Thus the visualization of the GUS activity (blue staining) indicated the very likely localization of the proteins in different plant organs: p*LjAMT*1.1::*gus*A shows GUS activity in leaves, in peripherical zone of root cap and columella cells, root epidermis, pericycle, root hairs, and in the nodule central zone as well as the nodule attachment and vascular bundles zones. The GUS activity of the p*LjAMT*1.2::*gus*A was observed in the root epidermal cells (slightly in the cortical cell layer) and in the outer cortex of the nodule while the GUS blue staining of the p*LjAMT*1.3::*gus*A construct was detected only in the region of the root vascular cylinder consistently with the low level of transcript detected.

Despite a huge amount of collected data, only indirect evidence through physiological or genetic studies were obtained to understand the transcriptional regulation of the *AMTs* in response to the dark/light cycle (Von Wirèn *et al.,* 2000) or to sucrose availability (Lejay *et al,* 2003) in plant kingdom. These investigations have to be updated in a leguminous background as that of *Lotus japonicus* to help to unravel the role of the *LjAMT1* genes in the framework of the symbiosis.
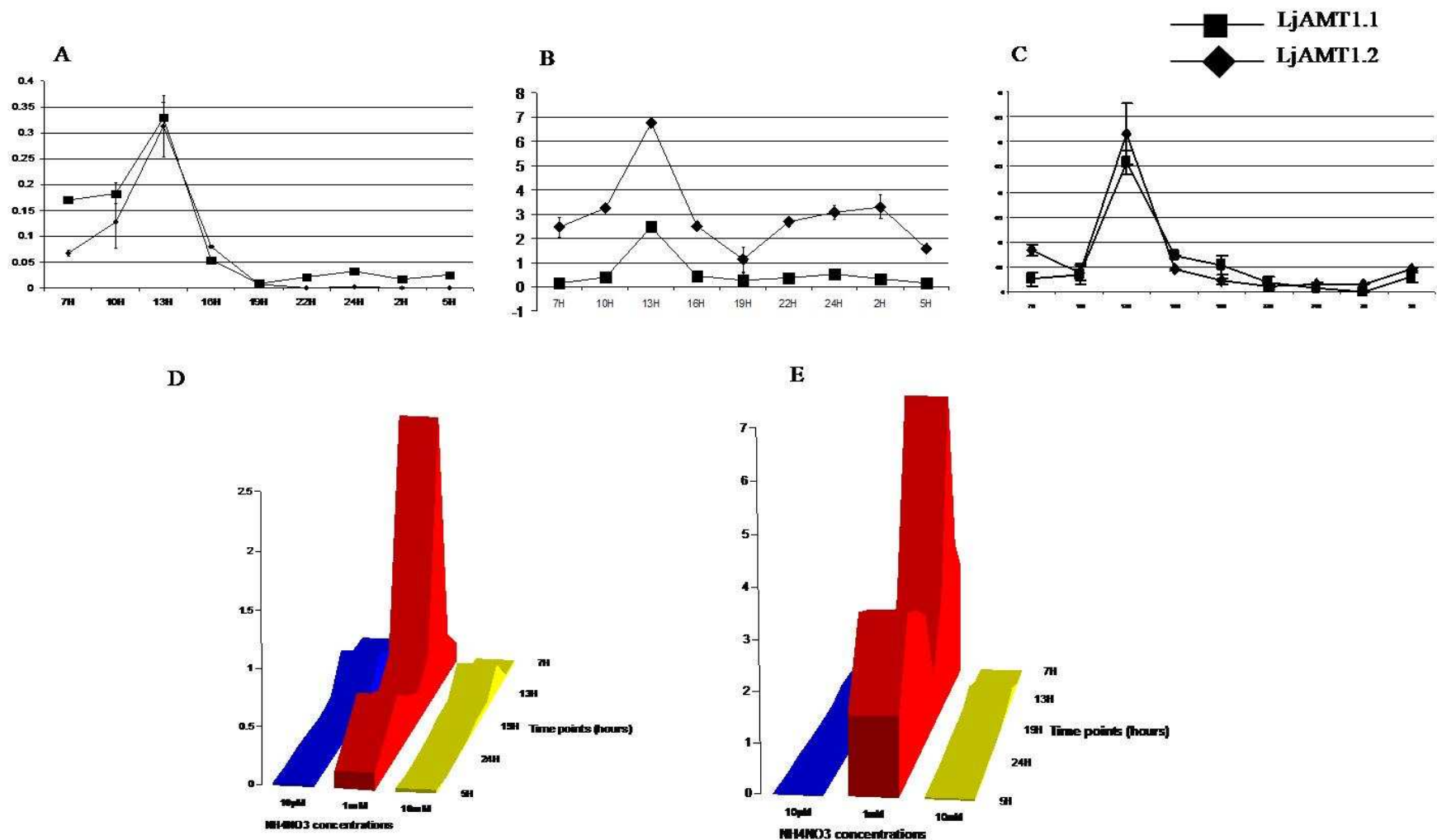
II. Results

Figure1. Expression of *LjAMT1.1* and *1.2* in roots of *Lotus* steady state hydroponics' cultures grown in 10µM NH$_4$NO$_3$ (A), 1mM NH$_4$NO$_3$ (B) and 10 mM NH$_4$NO$_3$ (C). The light/dark cycle is indicated in the figures (7H-24H = light; 24H-7H = dark).

Comparative representation of the *LjAMT1.1* (D) and *LjAMT1.2* (E) root expression data obtained according to the media composition and time points indicated in A, B, C), .

A. Steady state experiments

A.1. Analysis of the *LjAMT1* transcriptional regulation during the light/dark cycle

To have more insights on the pattern of regulation of the *LjAMT1* transcripts and to investigate the relationship between the N regime of growth and the light/dark cycle a detailed analysis was carried out on the following experimental system: L. japonicus seedlings were incubated during 5 weeks in three steady state conditions of growth:

- B5 liquid medium supplemented with 10µM NH_4NO_3
- B5 liquid medium supplemented with 1mM NH_4NO_3
- B5 liquid medium supplemented with 10mM NH_4NO_3

Two replicated samples of steady state hydroponic cultures were grown in the conditions listed above (8 seedlings/Magenta). Different time points were taken all over night & day cycle at: 2 a.m., 5 a.m., 7 a.m., 10 a.m., 13 p.m., 16 p.m., 19 p.m., 22 p.m. and 24 p.m. Once the RNA was extracted from root and shoot parts, gene expression was quantified by semi-quantitative as well as by Real-Time RT-PCR, and normalizing against the *Lotus ubiquitin* gene.

The pattern of expression of the ammonium transporters was analyzed only for members *LjAMT1.1* and *1.2* because the *LjAMT1.3* shows a very weak level of expression detected by Real Time RT-PCR. The pattern of expression in root tissue of *LjAMT1.1* and *1.2* members showed a progressive increasing during the light period extending from 7 am in the morning till a spike around 13 p.m. Thereafter, in the afternoon a progressive diminishing in intensity till the complete knock down of the expression around 19 p.m. could be revealed (figure 1A, B, C). Only a low, basic expression was detected during dark period (24 p.m. till 8am). This pattern of LjAMT1;1 and 1;2 expression was observed in all the three NH_4NO_3 concentrations (figure 1A, B, C). The highest expression level was detected in 1 mM NH_4NO_3 while a lower expression was observed in 10 mM as well as 10µM NH_4NO_3 steady state conditions for both *LjAMT1.1* and *LjAMT1.2* (figure 1.D and E). Interestingly the level of expression of *LjAMT1.1* in 1mM NH_4NO_3 is 2-3 fold less intense than that of *LjAMT1.2* all over the light/dark cycle. These patterns of expression are conserved on shoot organ for the three NH_4NO_3 concentrations (data not shown). The root expression of *LjGLN1* in the same steady state conditions appeared to follow the same pattern, with a 6 fold higher level than that of the AMT genes (data not shown).

A.1.1. Effect of the sucrose addition on the *LjAMT1* transcriptional regulation & plant growth phenotypes.

In order to test whether the observed pattern of *LjAMT1.1* and *1.2* expression (in § A.1.) was obeying to a circadian rhythm or not; the effect of the addition of a carbon source was investigated. The carbon regulation described was followed by adding 1% sucrose (29 mM) to the B5 derivative medium (see Materials and Methods) supplemented with 10mM NH_4NO_3, and the expression of *LjAMT1.1* and *LjAMT1.2* was analyzed at 7 a.m. (corresponding to the end of the dark period) and 13 p.m. The inhibition of the expression of the *LjAMT1.1* as well as *LjAMT1.2* at the end of the dark period (7 a.m.) was lifted by the addition of 1% sucrose (figure 2A). The pattern of *LjAMT1.2* in root in the dark seems to be more induced by the addition of sucrose than that of *LjAMT1.1*. Surprisingly a slight inhibition in the pattern of expression was observed for both genes at 13 pm when sucrose was added. By contrast, the pattern of expression of the *LjGLN1* (coding for the cytoplasmatic glutamine synthetase) is always enhanced when 1% sucrose is added to the medium during either dark or light period. Accordingly, the high concentration of sucrose (29mM) strongly affected the growth phenotype (Figure 2B and C) by increasing the fresh biomass in both shoots and roots organ of plants grown in 10mM NH_4NO_3.
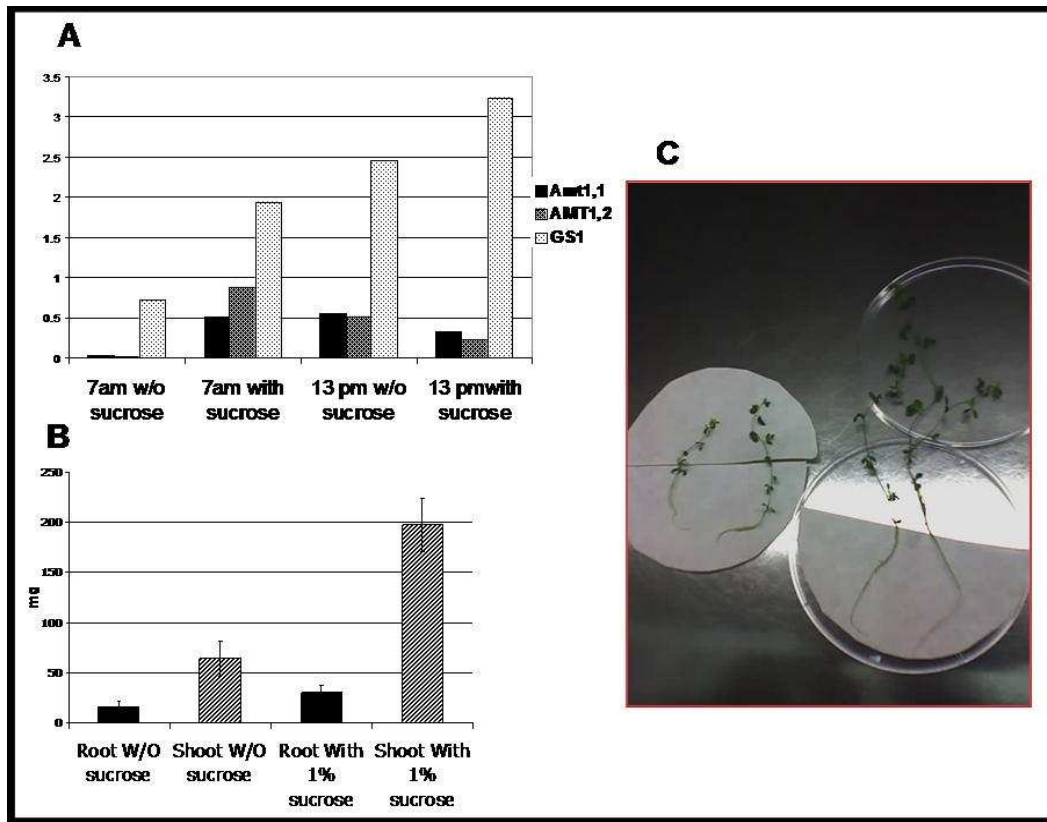
Figure 2. Effect of the sucrose (1%) on gene expression of genes involved in N metabolism.

A. Diurnal transcriptional regulation in root of *LjAMT1.1*; *LjAMT1.2* and *LjGLN1* (coding for the cytoplasmic glutamine syntethase) genes relative expression. *LjAMT1.1* (black bars), *LjAMT1.2* (black dotted bars) and *LjGLN1* (white dotted bars).

B. 5 weeks wild-type plants grown hydroponically in B5 medium supplemented with 10mM NH4NO3 without sucrose (left plants) or with 1% (29 mM) sucrose (right plants). **C.** Fresh root (black bars) and shoot weight (dashed bars) of the plants shown in panel B.
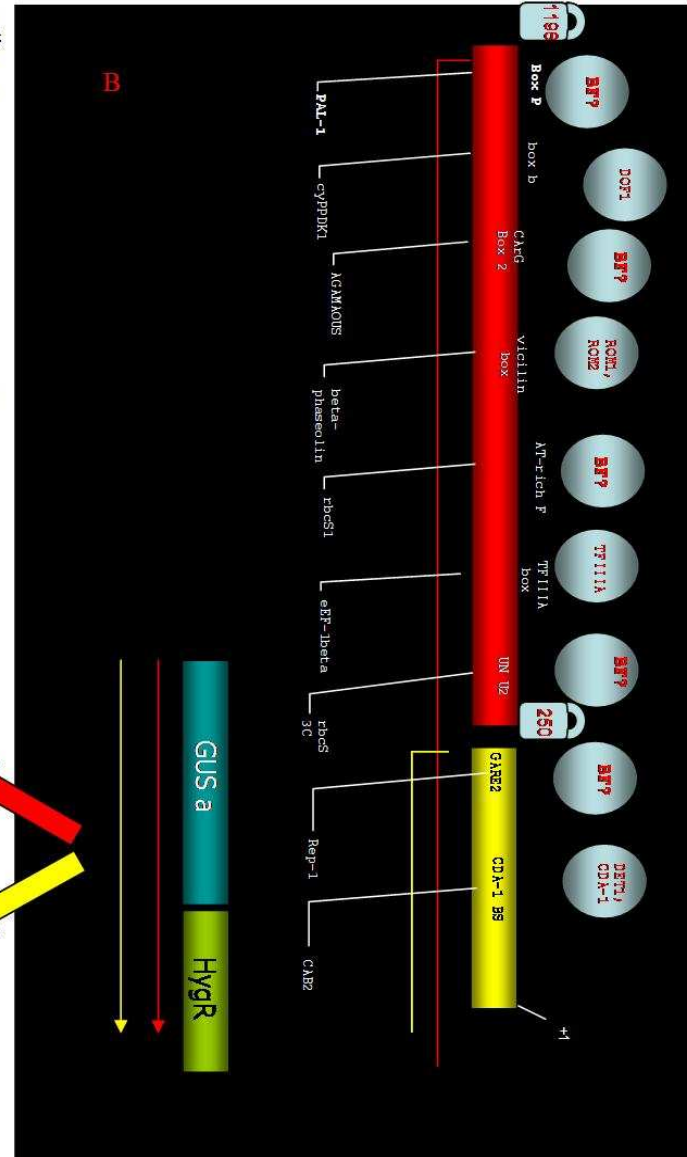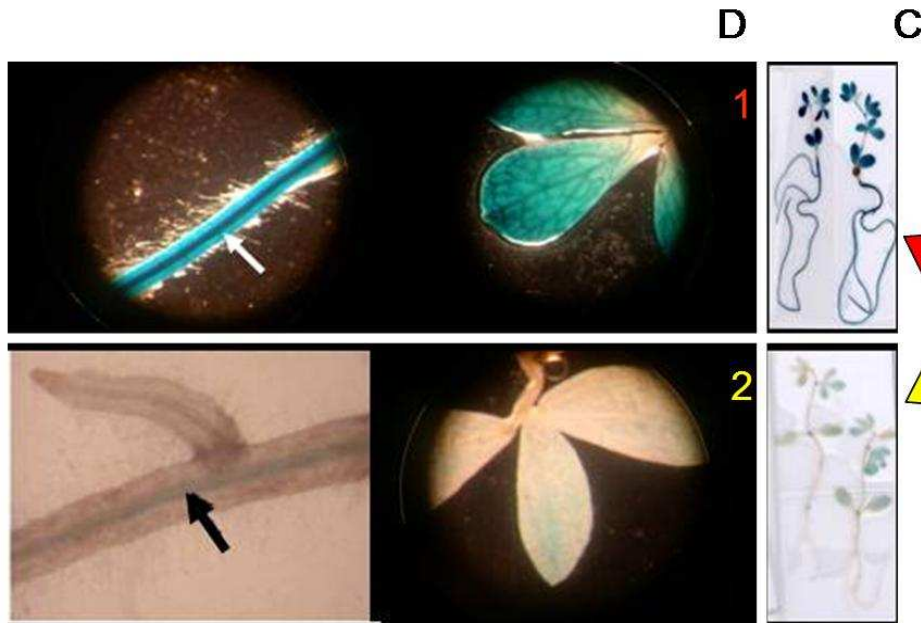
Figure 3 A. 5' regulatory regions (RE) of LjAMT1;1 and LjAMT1;2. .All the RE are mentioned in **the annex** B. Schematic representation of the predicted regulatory elements present on the .*LjAMT1.1* promoter region from the ATG (+1) till -1198bp. C. Analysis of the *pAMT1;1*prom.*gus*A fusions activity of the 1198 promoter region(Yellow +Red portion). and 250bp (only Yellow portion) are fused to GUS cassette (C). An intense blue staining of the 1198bp-prom.*gus*A fusion (1) is observed when compared to the weak spreading of the the 250bp-prom.*gus*A fusion. (2). D. Relative magnification of (1) top, and (2) bottom, showing the staining in leaves and root vascular tissue.

A.1.2. *In silico* analysis of the promoter regions

In order to associate the pattern of transcriptional regulation described in A.1 and A.1.1 to the features of the 5' regulatory region of the investigated genes, we carried out a detailed *in silico* analysis (softberry software) of the *LjAMT1.1* and *1.2* promoter regions to screen for the presence of regulatory elements. The *in silico* screening revealed a series of motifs that were not previously described (D'Apuzzo *et al.,* 2004; figure 3A). The 5' regulatory sequences of *LjAMT1.1* and *LjAMT1.2* were markedly imprinted by regulatory elements, binding putative factors affected by light availability (*in* annex). In particular, the presence of three putative GT-1 transcriptional factor binding sites, were found in the *LjAMT1.2* promoter region whereas the DET1 binding sites and an AT rich region was found in the *LjAMT1.1* regulatory 5' sequence. Other binding sites responsible for C/N metabolism (DOF1) and the biotic/a-biotic stresses (PAL1; ROM1-2) are also present in the *LjAMT1.1* sequence. Interestingly, the density of the regulatory elements is higher in *LjAMT1.2* sequence than in the *LjAMT1.1*.

A.1.3. Deletion analysis of the *AMT1.1* promoter activity

On the basis of the in silico analysis, two different fragments of the *LjAMT1.1* promoter region (-250 bp and -1198 bp counting from the +1 ATG) were used to drive the GUS cassette in transgenic *Lotus* lines. *LjAMT1.1prom.*::*gus*A lines were grown for 2 weeks on solid B5 medium supplemented with 10mM NH_4NO_3 without carbon source and harvested for GUS staining at 13 pm. The fixed lines carrying both constructs (figure 3B) were analyzed for the blue staining released by the GUS activity. The lines having the 1198 bp promoter region showed an intense blue staining in the shoot organ where it was revealed in leaves mesophyll cells and vascular zones of the leaves, while in the root organ the intense blue staining decreased from the vascular tissue to cortical cells whilst the root hairs appeared weakly blue stained (figure 3 C (1) and D (1)). By contrast the lines carrying the truncated promoter (215 bp) showed a very weak spreading of the blue staining in these same tissues (figure 3C (2) and 3D (2)). In particular the staining in the leaves (figure 3D (2)) was restricted only to the veins. In roots the expression was observed in the vascular tissue and in the root hairs.
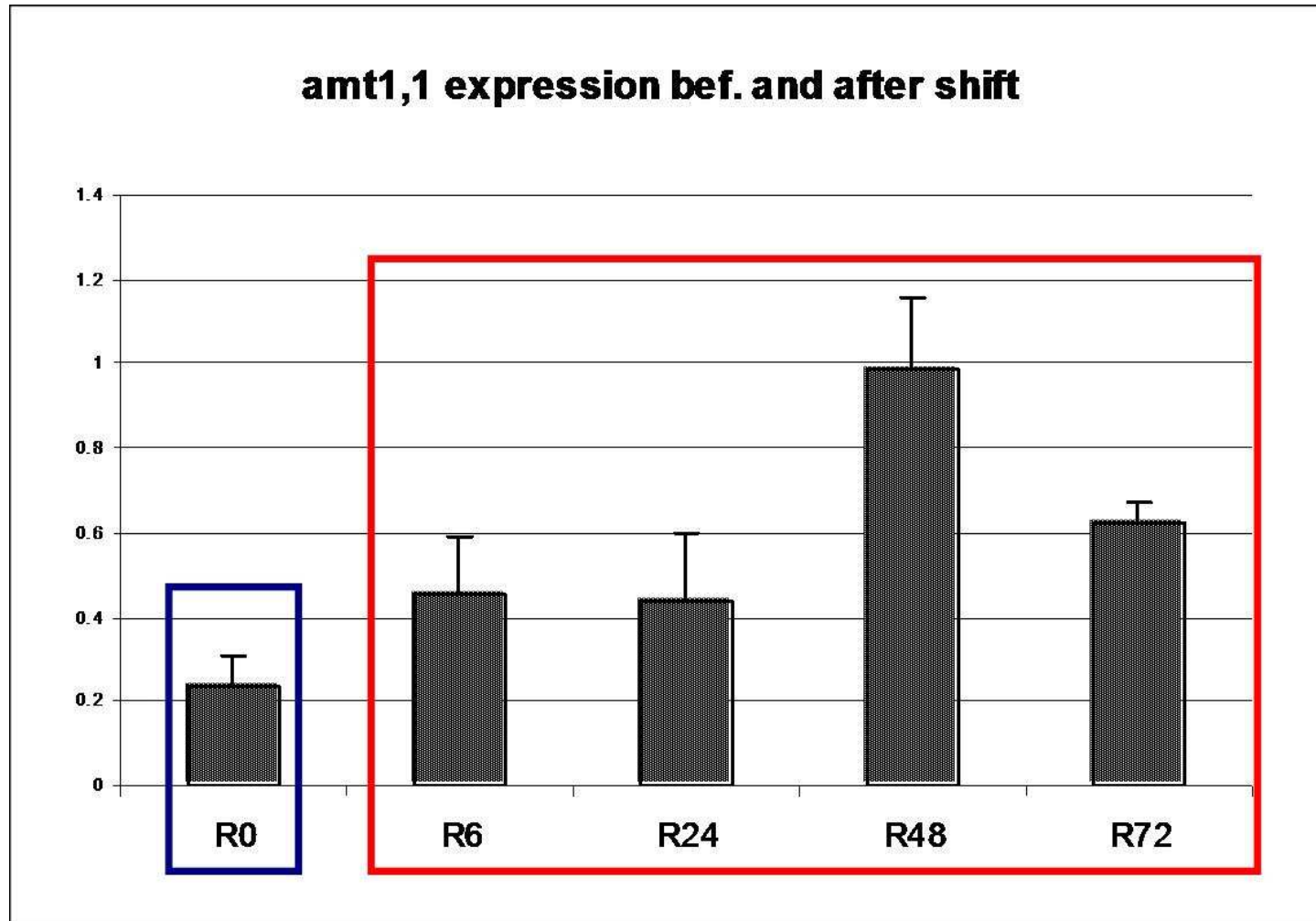
Figure 4. Pattern of expression of the *LjAMT1.1* gene in root tissue during the time course (numbers indicate the hours) after shifting the plants from 10 mM (R0,/Blue) to 10μM NH4NO3 (6h, 24h, 48h and 72h/red) conditions. The R0 is taken at 10 a.m. in the morning and the first time point in N starvation is taken 6 hours after (R6=16 pm)

B. Shift from high to low ammonium concentration
B.1. One marker gene for an array global overview

As a prerequisite to have a general overview of the metabolic quick adaptation to the Nitrogen starvation which also represents the *sine qua non* condition for initiating the symbiotic program in *Lotus* plants, the *LjAMT1* variation in expression was used as an indicator of the *Lotus* nutritional status. Only the evaluation of the expression of *LjAMT1.1* was used since it is the *LjAMT1* family member with the highest level of expression in the N starvation conditions represented by the 10 µM NH_4NO_3 regime in the steady state condition tested (see figure 1A). Besides, it is known that the transcription of several plant AMT1 genes is induced in roots, after shifting the plants in a N-starvation and in the case of *Lotus*, the *LjAMT1.1* showed the highest level of induction (D'Apuzzo et al. 2004). However, in order to test the range of time needed to induce the *LjAMT1.1* expression, after shifting the plants from a N excess to a N starvation condition, it was necessary to set up a time course experiment with *Lotus* hydroponic cultures taking in account the results of the time course experiment shown in figure 1 (this chapter). The expression of the *LjAMT1.1* in root tissue was checked at different time points after the shift (T0 = 0H) from 10mM NH_4NO_3 to 10µM NH_4NO_3 conditions and in particular at 6 hours, 24 hours, 48 hours and 72 hours after the shift. To have a more significant picture of the pattern of *LjAMT1.1* induction after the shift, it was taken into consideration the previous data, concerning the diurnal pattern of *LjAMT1.1* regulation in steady state conditions (see § A.1.). Indeed, it was important to avoid a confusion between the peak of expression revealed at 13 pm in 10µM as well as 10mM NH_4NO_3 steady state growth condition (see figure1A and C in see § A.1) with that due to the shift in N starvation conditions (red group of time points in figure 4). For this reason, the T0 time point was harvested at the beginning of the light period at 10 am and the second time point at 16 pm to compare two points with a similar low level of *LjAMT1.1* expression (respectively R0h and R6h) and to ensure that *LjAMT1.1* is obeying to the shift induction rather than to the steady state diurnal pattern of regulation. Besides, no carbon sources were added to the media to avoid any additional external nutritional cue that could interfere with the expression after the shift (see § A.1.1).

As it is shown in figure 4, the expression of the *LjAMT1.1* showed a progressive increase after the shift in N starvation conditions with a peak of about 5 fold induction at 48 hours after the shift. This peak is transient and it rapidly decreases at 72 hours after the shift. Thus, the RNA samples of the two contrasted time points T0H and T48H were subsequently exploited for a full transcriptomic analysis based on an array approach.
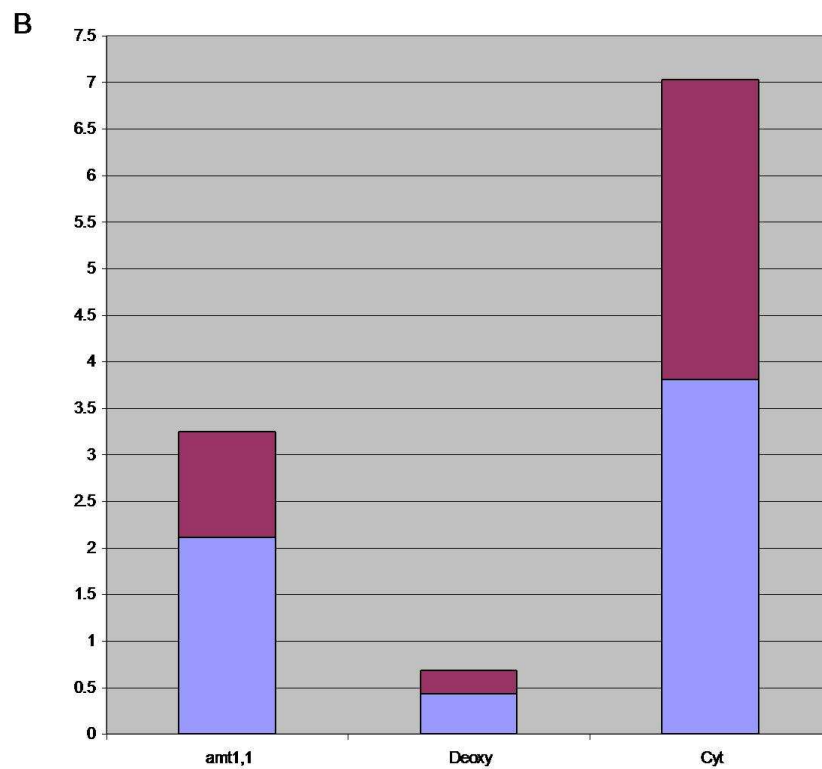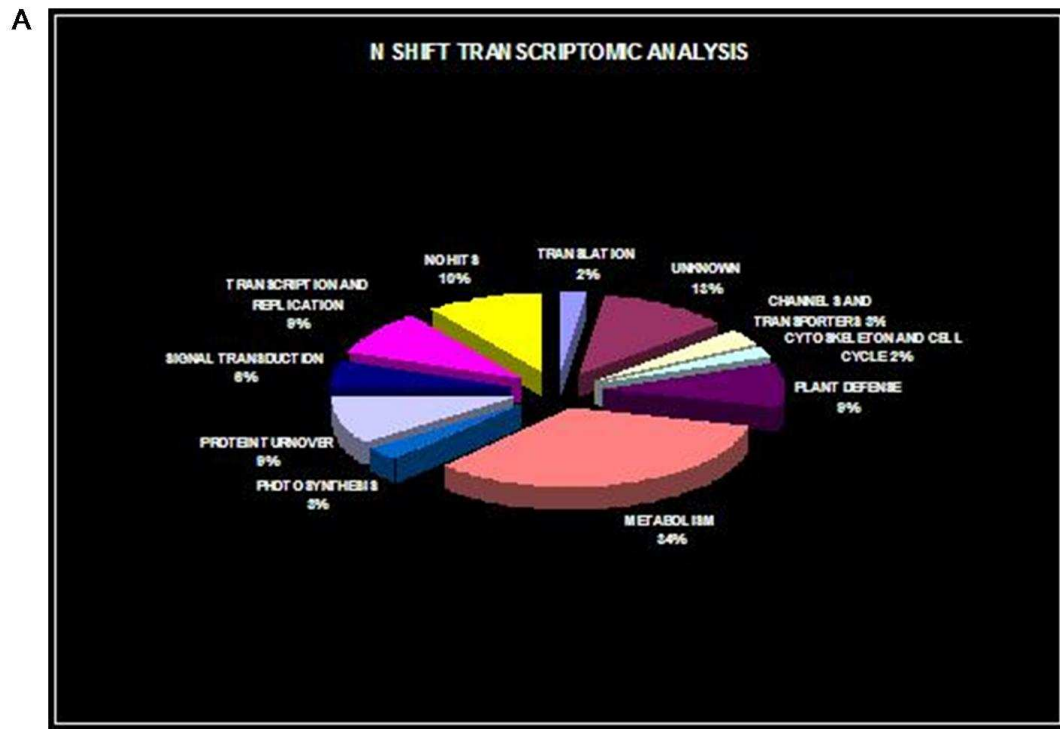
Figure 5 A.. Pie representing the different classes according to the gene annotation clustering. Eech group includes either the up regulated TCs and/or the down regulated ones.
B. Ratio T48H/T0H obtained by Real time RT-PCR (blue bars) and combimatrix technology (red bars). The analyzed TC encodes are LjAMT1.1, the downregulated putative Deoxycyclate desaminase indicated. Under the bars . The Blue bars indicate the Real time ratio (T48/T0) of each gene compared to the ratio obtained by combimatrix gene chip fluorescence (red bars)

B.1.2. Shift gene chip results

A total of 12469 TC* of *Lotus japonicus* recovered from TIGR data base (http://compbio.dfci.harvard.edu/tgi/, go to plant entry and then *Lotus* entry) were used to design synthesized oligos on the surface of the combimatrix chip, serving to be hybridized to RNA samples of the T0 and T48 points from the shift experiment (two biological replicas) (see Materials and Methods). After the SAM analysis (FDR < 5%), the results of the array showed a total of 39 TCs having from 1.8 to 3 folds induction 48hrs after the shift on 10 µM and 48 TCs having from 0.5 to 0.25 folds down regulation. These TCs were classified upon their respective annotations retrieved from tiger database (figure 5A). The majority of the TC belongs to gene actively involved in C/N metabolism (37%). A big portion shares no hits or missing function (26%) while the rest concerns mainly genes involved in protein turnover, transcription and replication, signal transduction, transport system and cell organization as well as plant defense. Interestingly, in this last portion 3 TCs belonging to putative nodulin gene s were identified: **TC8247** similar to the early nodulin 36A (Q02918), partial (25%); **TC16612** similar to the nodulin putative protein (Q8LEI9), partial (39%); **TC12598** similar to the nodulin putative protein (Q8LEI9), partial (7%) . These TC were 0,5 fold down regulated before the shift at T48 time point compared to their expression 48 hour after the shift.

B.1.3. Methodology for increasing the TC number

The poor number of up and down regulated TCs raised the question of the FDR stringency that was applied upon the fluorescence. Moreover the *LjAMT1.1* gene was not mentioned in this list whilst it was asserted to be induced (in § B1). In order to understand this discrepancy in expression between combimatrix and Real Time analysis of the *LjAMT1.1*, we decided to verify, by Real time RT-PCR, the level of down- and up -regulation of two genes that were identified as significantly regulated on the basis of the combimatrix analysis. On one hand, this analysis confirmed the down- and up-regulation of the two chosen genes, the putative deoxicylclate desaminase and the putative Cytochrome P450, respectively validating the combimatrix results. On the other hand, this analysis revealed that the number of fold of up and down regulation identified by combimatrix was clearly over-estimated when compared with Real Time results (figure 5 B). Thus, the stringency of the FDR could underestimate the potentialities of the small variation in expression in which our *LjAMT1.1* is

---

* Tentative consensus sequence is created by assembling ESTs (expressed sequence tags) into virtual transcripts. TCs contain information on the source library and abundance of ESTs and in many cases represent full length transcript.

included too. To recover the potential lost information, a new filtering was applied on the data released by the combimatrix analysis for the expression between T0h and T48h around ratio 1 (no variation in expression). The calculation was based on the T-test formula:

$$\frac{\displaystyle\sum_{X=1}^{a/b} \dfrac{[Pn_x(T48/T0)]}{n_x \text{ pop}}}{\dfrac{S}{\sqrt{n_x}}} = 3.29 \text{ (value T test for } \alpha \text{ classes P=0.01 (Student T-99.9\% CI)}$$

Implementation:

Find "n" giving the ratio Pn_x that determine a T-test observed value = 3.29 (highly significant).

Where n_x = number of the Pn_x ratios and S the Standard deviation of the n spots

Remark:
This operation is performed twice with:
x_a = All the ratio spot > ratio 1 (up-regulated TC)
and
x_b = All the Log_2 (ratio) < ratio1 (down-regulated TC)

This because the number "b" of down regulated TC is <<< to "a" of the down regulated and thus to stay in a gap of acceptable T-Test at the P=0.01
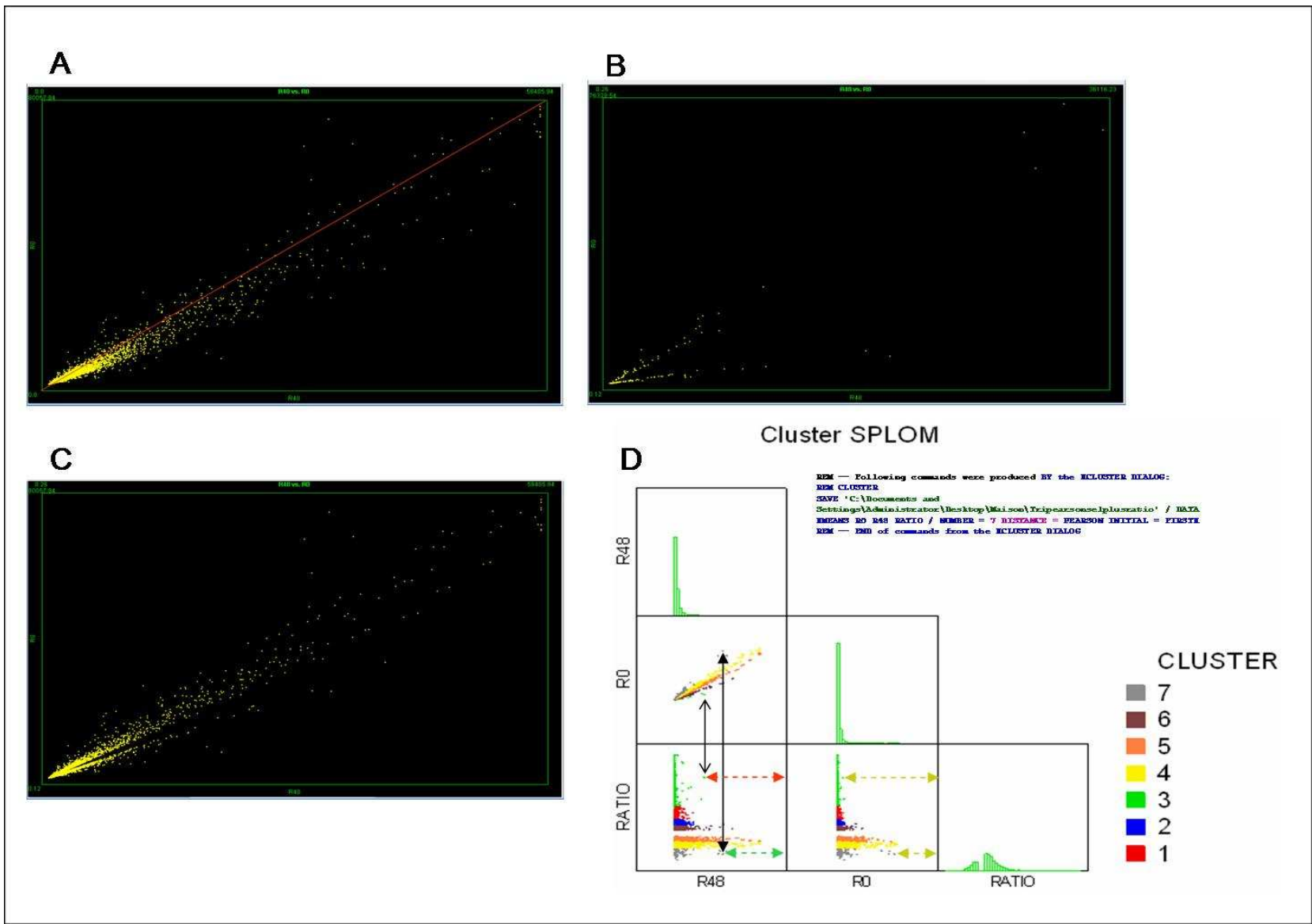
Figure 6 Scatter plot reporting the whole data set of TCs (12469; T48h vs. T0h) is compared to **B** a scatter plot of the data after FDR 0.5 and then to **C** addition of the data set after T test.

D. Cluster SPLOM indicating the 7 clusters (Kmeans, 20 iteration). The cluster that has the lowest variation in expression (ratio T48h/T0h) is n° 1 while that of the highest variation is n° 3. The black double arrow indicates the position of a chosen TC while the colored double arrow indicate its pattern of expression an up regulation (red) or a down regulation of the selected TCs.

This re-analysis of the whole data based on the new statistical method approach allows looking inside to the small differences. A parametric T-test (P=0.01) was used "to magnify" the small variations in expression.

In figure 6, is reported a comparison between the scatter plot reporting all the 12469 TCs (T48H against T0H; plot A) with that after the original FDR data filtering (plot B) and with that obtained with the additional data of the T test (plot C). By this statistical modification, it was possible to enrich the first list with 6501 up regulated and 2187 down regulated TCs and therefore only 4781 TCs were considered as being false positive spots.

This massive increasing in statistically accepted TCs raised the subsequent question of their direct clustering (grouping) around ratio 1. Using SyStat software (web Demo version available for free) the values of the TC at 0H were plotted against those of the TC at 48h after shift (Cluster SPLOM *in* figure 6 D). During the plotting a clustering was established by the use of the K means algorithm (20 iterations, K=7 groups (clusters) chosen according to the first classification) and applied to a Pearson correlation for the definition of the limits of each group. The plotting of the ratio against R48h or against R0h magnifies the difference of the small variation for TC that is clustering very tightly around 1 (plotting R48/R0).
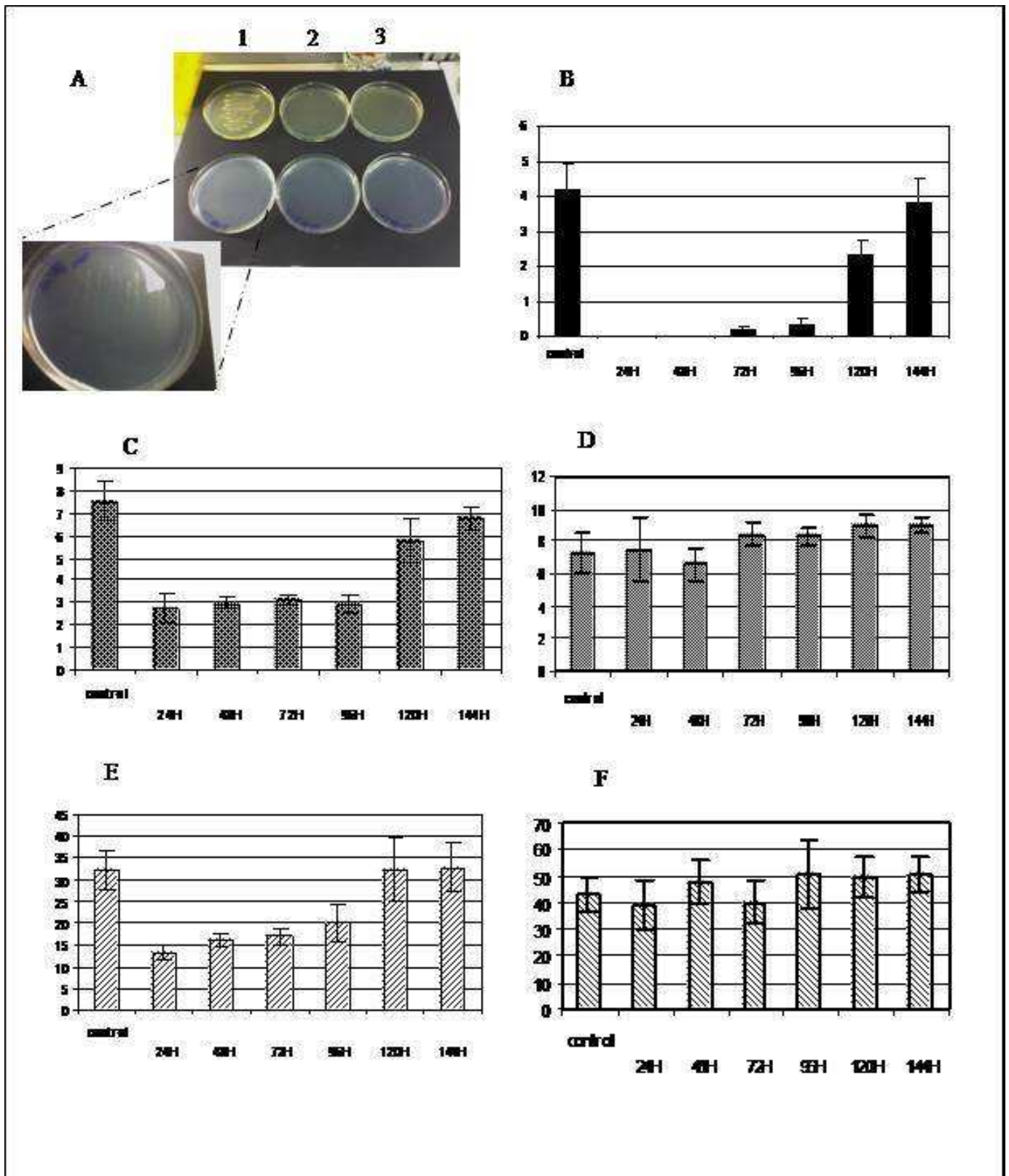
Figure 7. **A.** Rhizobia killing curve. The R7A rhizobia strain was streaken on TYR or B5 medium supplemented with 10mM NH₄NO₃ and 0.2% sucrose (we approximate the sucrose concentration to the sugars concentrations released by L. esculentum root root exudates described in Lugtenberg *et al.,* 1999). **1, 2 and 3** indicate the results of bacteria streaking in absence of cefotaxime or in the presence of 50 mg/L, 100mg/L, respectively. 50 mg/L is the minimal concentration required to kill bacteria on TYR medium as well as B5 medium. Magnification shows the bacteria growth on B5 medium. **B** Time course addition of cefotaxime (50 mg/L) to test the effects on nodule formation (number of nodules per plant, on an average of 20 nodulated plants). The cefotaxime has a decreasing effect at 24H, 48H, 72H, 96H, 120H post inoculation whereas at 144H p.i. the plants present the same number of nodules than control untreated with cef. . The same time points were scored for the shoot length **(C),** root length **(D),** shoot fresh weight **(E)** and root fresh weight **(F)** phenotypes.

C. Re-acquisition of the nodulation potentialities

As it was reported in the previous paragraphs, N-starvation is a crucial condition for the occurrence of the symbiotic interaction. Thus, in order to ensure the identification of the putative genetic determinants (*in* §B.) that could affect the competence of legume plants for symbiotic interaction in the presence of N excess (inhibitory conditions) and N starvation (permissive conditions), we implemented the shift array experimental scheme (*in* §B.) with new parameters to link the phenotype due to a general N shift to that specifically correlated to the symbiotic program. Therefore, a new specific experimental scheme had to be set up. In particular, the objective of this new experimental design wanted to discriminate between plants grown in the presence 10 μM NH_4NO_3 that are able to interact with Rhizobium and plants grown on 10 mM NH_4NO_3 that are not competent for symbiosis, reproducing the previous array experiment, but in this case to investigate the precise timing after shifting the plantlets in permissive condition (N starvation), necessary to re-acquire the right normal nodulation phenotype.

C.1. Prerequisite

In order to draw the right experimental design and to unambiguously investigate the plant capacities for entering the symbiotic pathway after growth in N/excess and N starvation conditions it is necessary to evaluate the plant competence at the time of the inoculation avoiding any possible nodule formation due to the maintainment of bacteria in the rhizosphere. A series of checking were set up. Firstly, the evaluation of the right minimal amount of antibiotic cefotaxime that needed to kill bacteria. This was tested on both bacterial rich medium and plant agar plates. Notably, a minimal concentration of 50mg/L cefotaxime was sufficient to get rid of rhizobia in both kinds of media (figure 7A). Secondly, it was crucial to investigate the right timing of cefotaxime supply. This has to be properly temporally applied, to avoid the negative effect of the antibiotic, that could affect the normal process of nodulation. In this order, we determined through a curve of nodule formation as well as other phenotypic parameters (figure 7B,C,D,E and F), that the cefotaxime supplement could be added to the plant growth media 144hrs (6 days) after the first infection. In fact, as it is shown in figure 7B the addition of cefotaxime at the concentration of 50mg/l) 6 d.p.i. doesn't affect the nodulation capacity of *Lotus* seedlings.
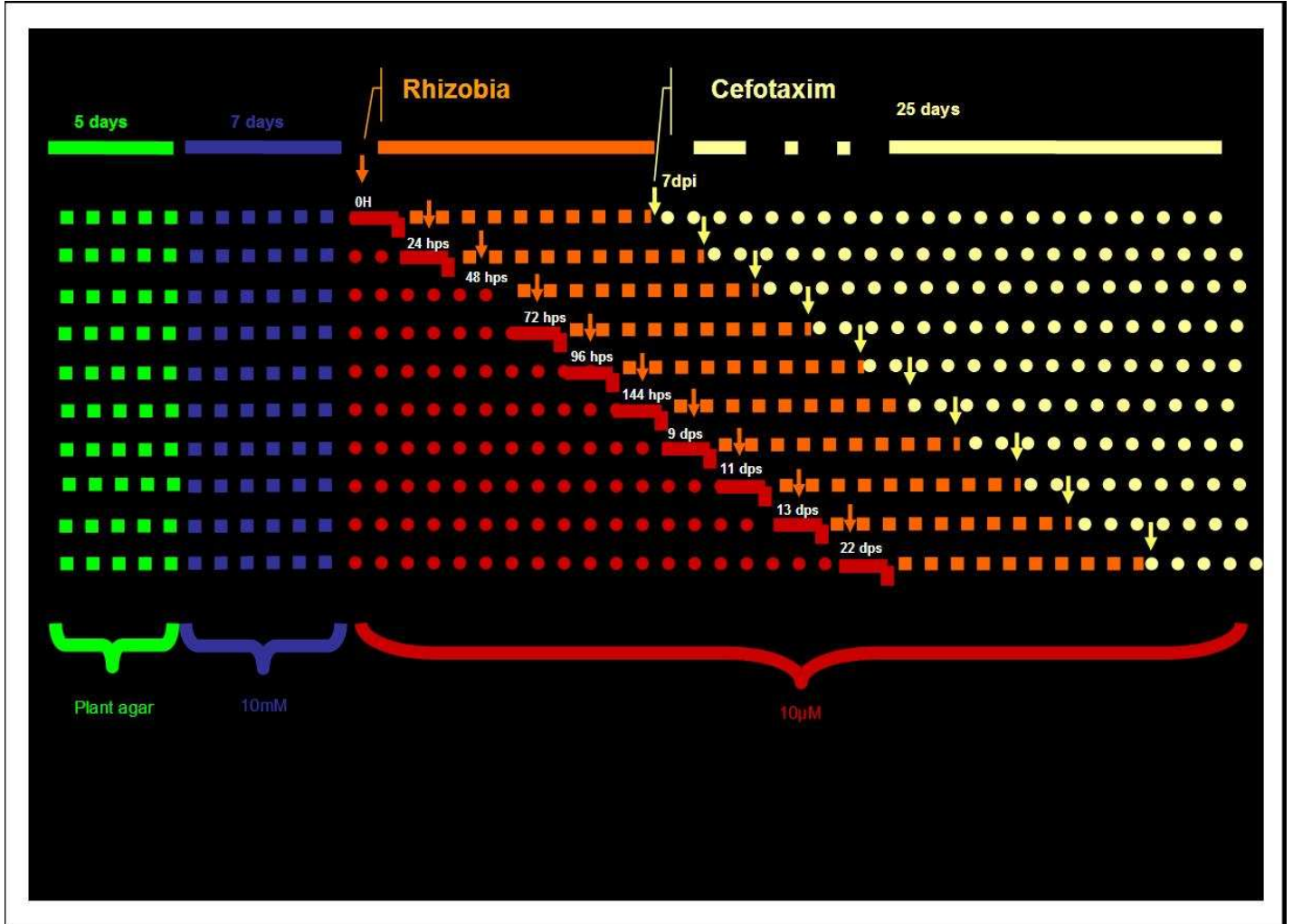
Figure 8. Experimental design for the P1 pool treatment.

Each dotted line represents a set of 10 wt plantlets with their respective replicas on independent Petri dishes. Green dotted line indicates the germination procedure that takes at the minimum 5 days (seeds sterilization, vernalization and sowing on plant agar). The blue square dotted line represents the incubation time (1 week) on B5+10 mM NH_4NO_3 for each set and their respective replicas. Red round dotted line indicates the length of the incubation time of the plantlets on B5 + 10 µM NH_4NO_3, after the shift. The orange arrows indicate the time of the rhizobia inoculation event for each set of plants. Notice that the infection series are chronologically distributed with a 24h interval from T0 till T22 days post shift. The orange dotted lines show the incubation time necessary from each infected set to complete a successful infection cycle. The pale yellow arrow indicates the time of the cefotaxim addition to the B5+10 µM NH_4NO_3 at 7 days post infection (see prerequisite.) The pale yellow dotted line indicates the last step of the experiment where plants are kept on 10 µM NH_4NO_3 and scored for nodulation as well as for shoot and root weights (at 34 dpi). Note that in the P2 experiment is identical, except that only the one week incubation on B5+10 mM NH_4NO_3 (blue dotted lines) is replaced by **10 µM NH_4NO_3**.

C.2. Experimental design for testing the re-acquisition of the nodulation potentialities

The seedlings were incubated into two different conditions of growth that were indicated as two diffrent Pools (P1 and P2 in figure 8):

- **Shifted Pool 1 (P1):** seedlings were first incubated for 1 week on B5 solid medium supplemented with 10mM NH_4NO_3 before to shift them on B5 solid medium supplemented with 10µM NH_4NO_3. In this pool the young seedlings were infected with *Mesorhizobium loti* strain R7A, according to the data shown in figure 8, at 9 different time points: T0 (at the moment of the shift); T1 (1 <u>day post shift</u>), T2 (2 dps), T3 (3 dps), T4 (4 dps), T5 (5 dps), T6 (6 dps, T9 (9 dps), T11 (11 dps), T13 (13 dps) and T22 (21 dps).

The data obtained for each time point correspond 5 seedlings incubated on the same Petri dish and its respective replicated sample. The whole experiment was repeated twice only for time points T0, T6, T9, T11 and T13.

- **Control Pool 2 (P2):** All the steps described for the P1 pool are maintained except that this time, the seedlings were incubated for the first week, on B5 medium supplemented with 10µM NH_4NO_3. In this case the seedlings are infected on the same medium (figure 8) and therefore no shift was applied. In this case, the adequate terminology used to characterize the corresponding times of the P1 plants is **"transferred"** instead of shifted. In fact, to avoid any possible artifact due to a different manipulation of the P1 and P2 plants, the latter were moved to new Petri dishes as for the shifted conditions. However it was also retained dps (days post shift) for P2 to avoid multiple terms that designates the same moment.

For each pool, a phenotyping analysis was achieved at 7 dpi (for each infected seedling set). It consisted of the measurement of the root and shoots lengths and the counting of the nodule number. Nodule primordia (Small bumps) were scored under microscope (ZEISS SV11; 1,0X) but only subsequently formed, small, young or mature nodules were taken into account for the quantitative phenotyping results (see § C3).
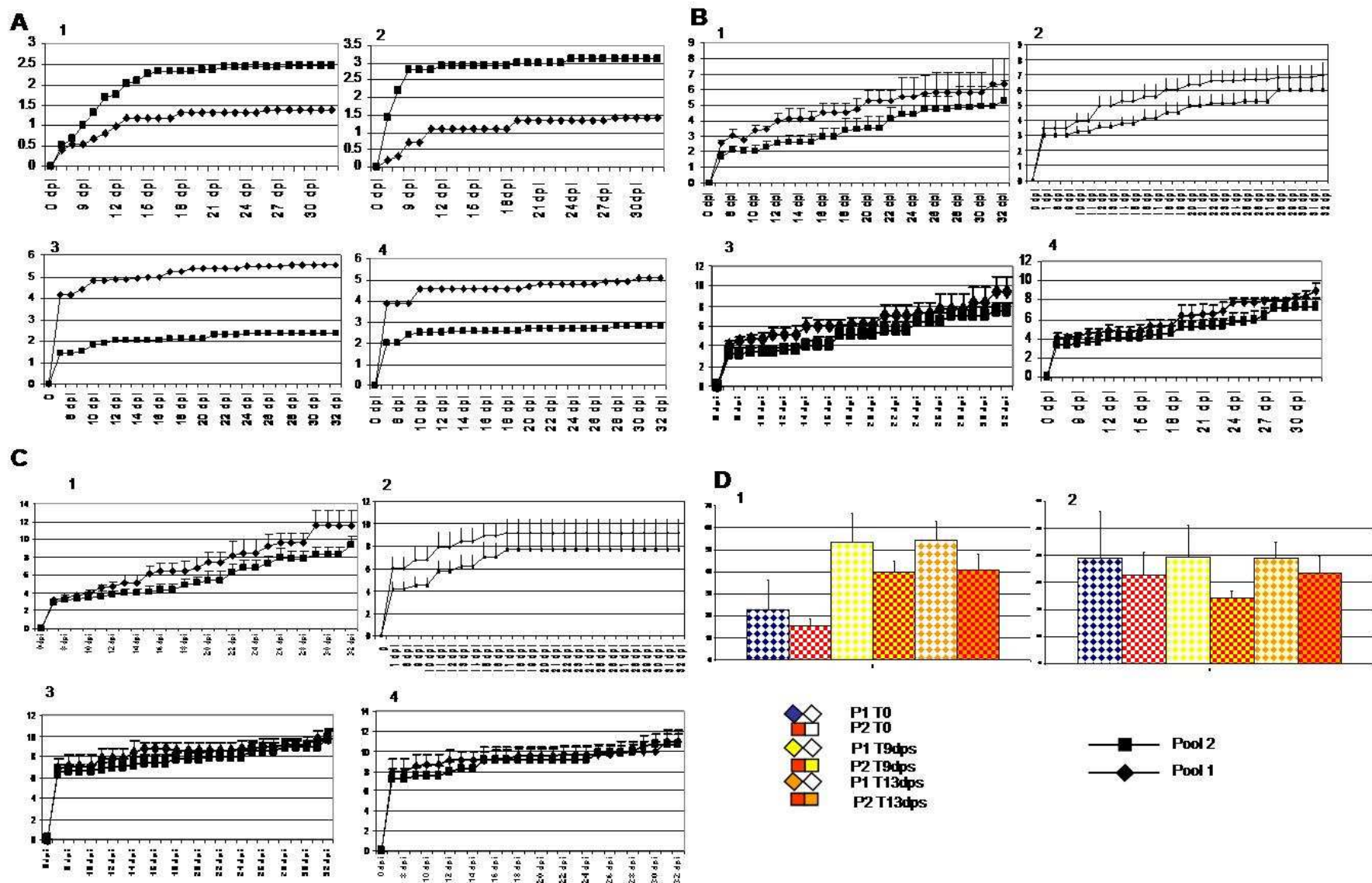
Figure 9.
A. Nodule number per plant (average of 20 plants per conditions) at T0 (panel 1), T6 dps (panel 2),T9 dps (panel 3) and T13 dps (panel 4).
B. Shoot length (cm) (average of 20 plants per conditions) at T0 (panel 1), T6 dps (panel 2), T9 dps (panel 3) and T13 dps (panel 4).
C. Primary root length (cm) per plant (average of 20 plants per conditions) at T0 (panel 1), T6 dps (panel 2), T9 dps (panel 3) and T13 dps (panel 4).
D. Fresh weight (mg) of shoots (panel 1) and root (panel 2).

By contrast, the very early events that precede nodule formation (range from 0dpi to 7dpi) where further investigated by optical microscopy by exploiting fluorescent strains and lacZ strains (T0; in § C6 and C5).To ensure the normal progression of the infection process, the Nin gene expression was evaluated by semi-quantitative Real Time 24 hours after the different infection time point events on independent set of plants (data not shown).

C.3. Comparative phenotyping of P1 and P2 pools

Seven days post inoculation, started the observation of different parameters such as: nodule number, shoot length and root length for each of the mentioned time points and this was carried out till 32 dpi (Figure 9). The average of shoot and root biomass was surveyed only at the end of the experiment (at 34 dpi). The average of nodule number was significantly higher (2 folds) in the control (P2 plants) compared to the shifted plantlets (P1 plants) at time points T0 (Figure 9A, panel 1) and T6 (Figure 9A, panel 2) and the same pattern was observed at T2, T3, T4 and T5 (data not shown). By contrast, the nodule number of the shifted (P1 pool) plantlets infected at T9, T11 and T13 days after the shift from 10mM NH_4NO_3 to 10µM NH_4NO_3, showed an inversion in the nodulation pattern with an increased number of nodules in the P1 shifted plantlets when compared with the P2 control plants (figure 9A, panels 3 and 4). Thus, 9 days on 10 µM NH_4NO_3 is a range of time sufficient, for plants pre-incubated for one week on N/excess conditions, to re-acquire the nodulation competence. As expected, the effect of cefotaxime imposes an early plateau in the kinetic of nodule formation (not more than 4 nodules in average for P1 and P2) in all the conditions ensuring that the number of nodules scored are only the results of the primary infection cycle performed at the different time points and hence reflect the plant competence at those times. The different growth conditions utilized do not affect significantly the shoot and primary root elongation rates in P1 and P2 plants in all the time points analyzed (Figure 9B and C panels 1, 2, 3, 4).

The results shown in Figure 9D indicate, as expected, different amount of shoot biomass for P1 and P2 plantlets at 34 dpi. In particular, the fresh shoot weight is increased in both P1 and P2 plantlets at T9 and T13 days post shift compared to the T0 plants (Figure 9D, panel 1),. The same pattern is not observed for root biomass (Figure 9D, panel 2). The P1 plantlets show a slight increase (about 15%) in both shoot and root biomass when compared to P2 plantlets (Figure 9D, panels 1 and 2).

A

Phenotypes of the P1 plants (T0):
Rare nodules
Stress symptoms (black arrow)
Root hair re-growth near the tips
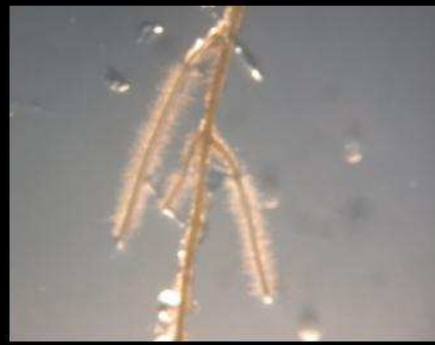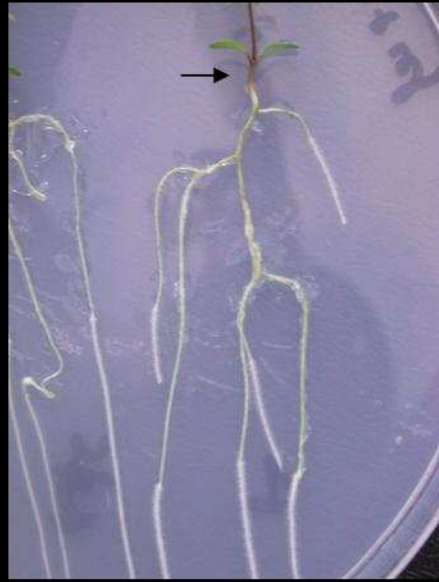
B

Phenotypes of the P2 plants (T0):
Nodules formation
Stress symptoms (black arrow)
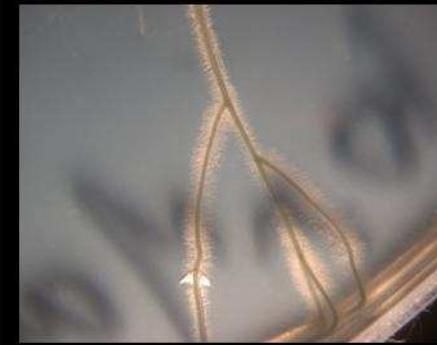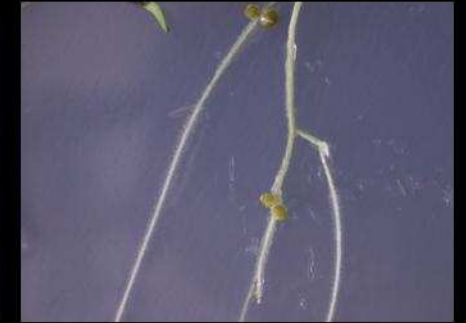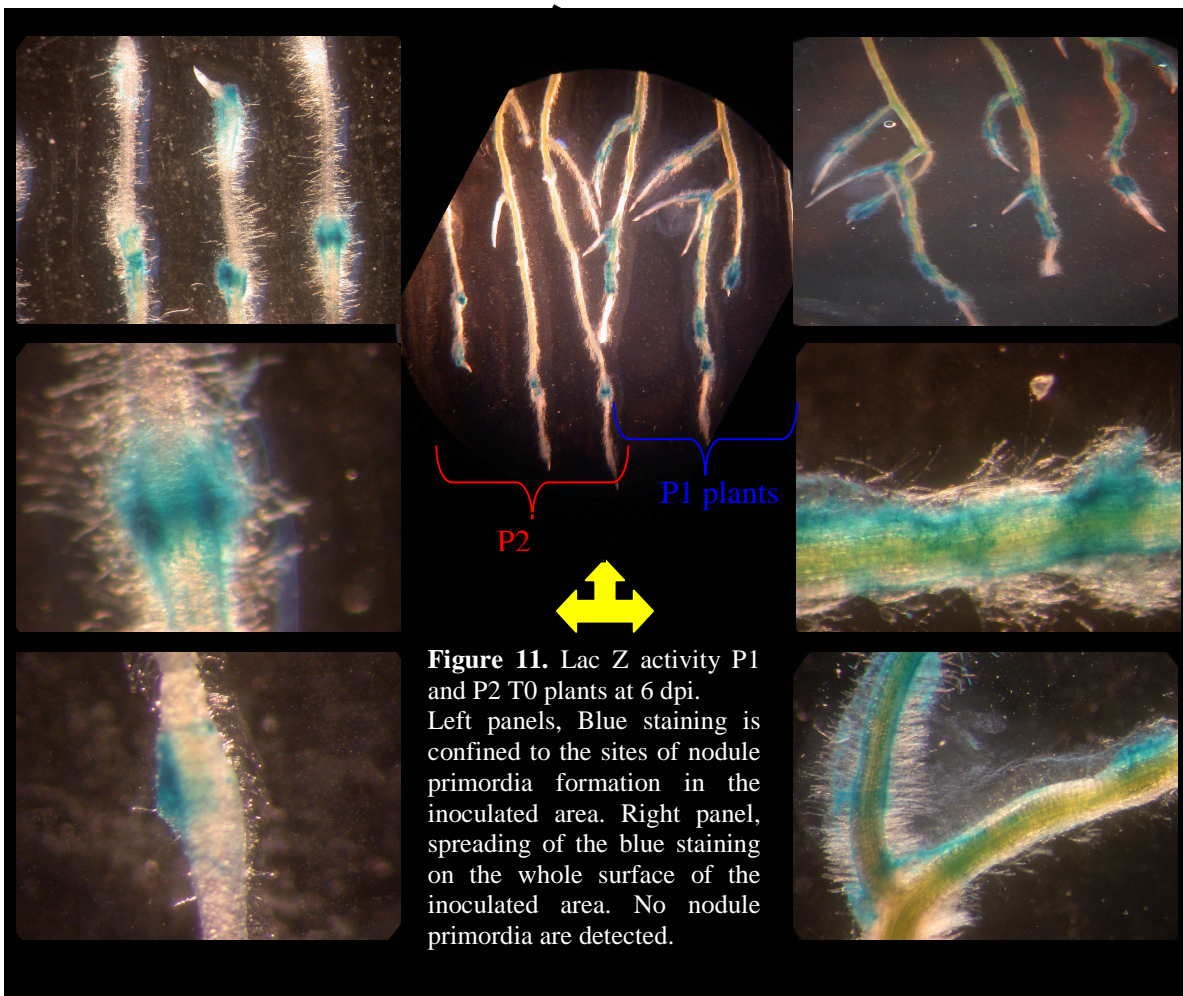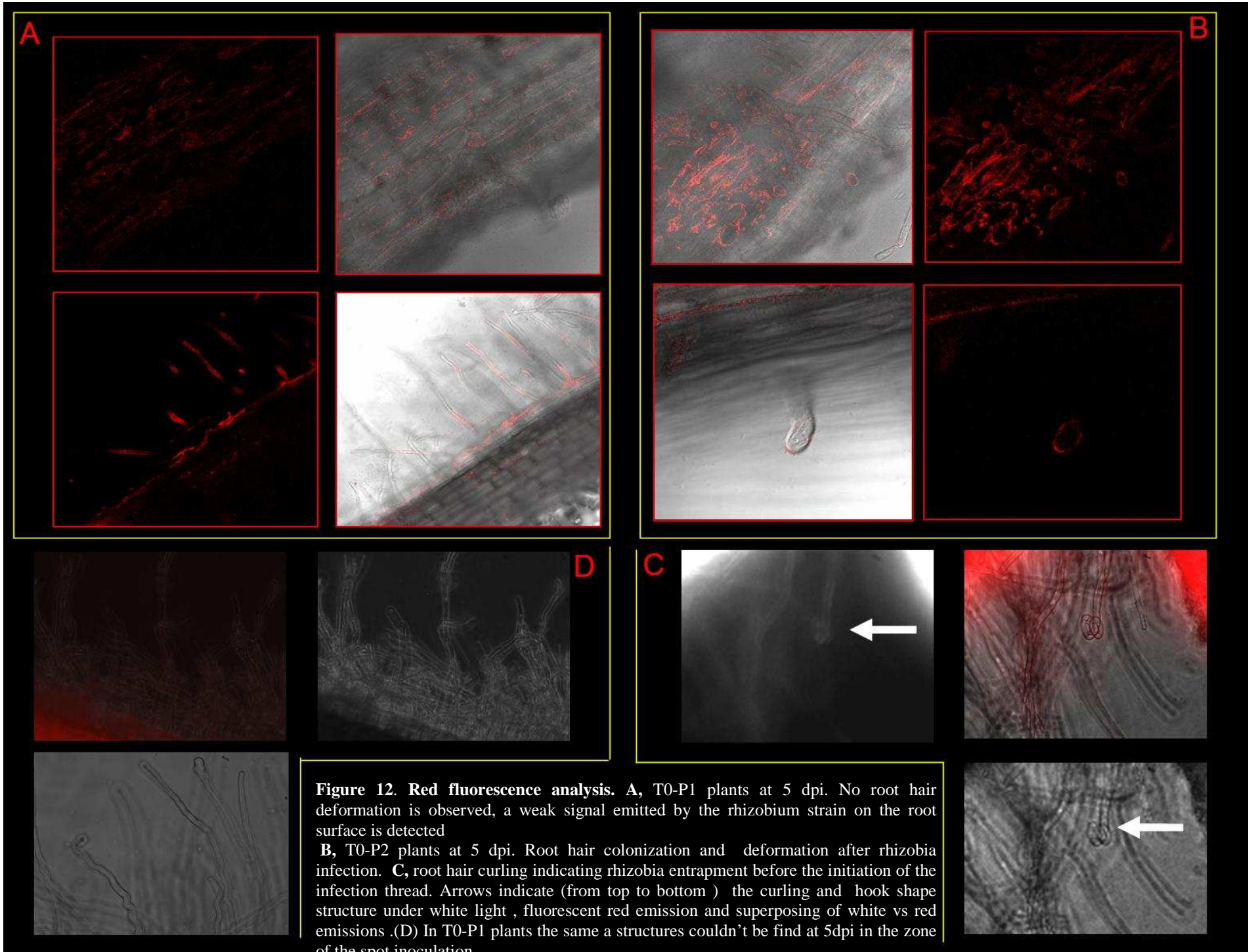**Normal pattern of root hairs formation**

Figure 10 Phenotypical observations of P1 and P2 plants.

A, P1 plantlets; B, P2 plantlets.

Interestingly, looking roughly, at the 34 dpi plantlets phenotypes , P1 plants show a re-growth of root hairs on the newly formed segments of roots (Figure 10A) while the P2 plants root apparatus was entirely covered by roots hairs (Figure 10B). Besides, the root system in the P1 plants showed more branching and secondary root formation (Figure 10A) than that of the P2 plants which present in general only 2-3 very long secondary roots (Figure 10B). Stress signals due to anthocyanin accumulation were present for both P1 and P2 plants at the level of the hypocotyl and often extending in the shoot area till the second internode. These differences in root phenotypes were observed for all the time points.

Figure 11. Lac Z activity P1 and P2 T0 plants at 6 dpi. Left panels, Blue staining is confined to the sites of nodule primordia formation in the inoculated area. Right panel, spreading of the blue staining on the whole surface of the inoculated area. No nodule primordia are detected.

Figure 12. **Red fluorescence analysis. A,** T0-P1 plants at 5 dpi. No root hair deformation is observed, a weak signal emitted by the rhizobium strain on the root surface is detected
 B, T0-P2 plants at 5 dpi. Root hair colonization and deformation after rhizobia infection. **C,** root hair curling indicating rhizobia entrapment before the initiation of the infection thread. Arrows indicate (from top to bottom) the curling and hook shape structure under white light , fluorescent red emission and superposing of white vs red emissions .(D) In T0-P1 plants the same a structures couldn't be find at 5dpi in the zone of the spot inoculation.

C.4. Optical microscopy investigation

In order to analyze the effects of the shift on the early steps of the *Rhizobium* infection, an optical microscopy investigation was carried out on both P1 and P2 plants after inoculation with rhizobia strains expressing RED fluorescent proteins or LacZ markers (See Material and Method). The microscopy studies indicate that, for the T0 plants, the spreading of the LacZ strain on the root surface at 6 d.p.i. is larger in P1 compared with P2 plants (Figure 11). In particular, at 6 dpi the blue staining was restricted only to the root nodule primordia sites in the P2 plants (figure 11). This phenomenon was confirmed by the RED fluorescent analysis carried out after inoculation with a *Rhizobium* strain equipped with a constitutive RFP construct. The results shown in Figure 12 indicate for the P1-T0 plants at 4 dpi the spreading of the red emission on the whole surface of the inoculated roots but not on the root hairs (Figure 12 A and D). By contrast, the root hairs of the P2-T0 plants at 12 dpi were already colonized by the strain showing root hair deformation as well as curling structures (Figure 12 B and C).
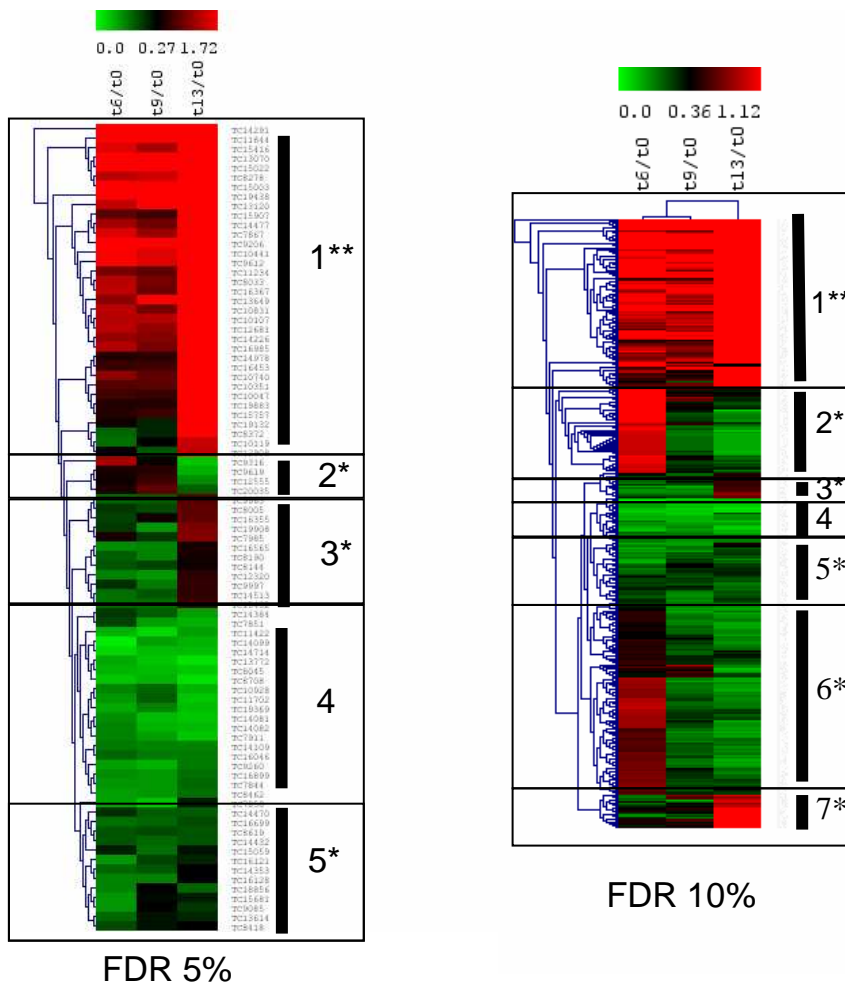

Figure 12. Cluster analysis showing regulatory tendencies of TCs expression from the T0 through T6, T9 and T13 P1 plants. The Time point T0 is not reported since it was considered as the common denominator of the other time points (respectively T6, T9 and T13). Groups of tendencies are delimited and numbered for both FDR 5% and FDR 10%. Although the numbering indicates similarity between both FDR panels (e.g. the conserved group 4), it is not appropriate to consider that all the TCs are strictly the same since when the stringency of the FDR decreases from 5 to 10 % the number of TC to be clustered increases and the groups too. The green color indicates ratio (Log$_2$ =0)=1 which means no variation in expression; black color means ratio= 0.26 for FDR 5% and 0.36 for FDR 10% (median of the down regulated values); red color means ratio= 1.72 for FDR 5% and 1.12 for the FDR 10% . The groups sharing 2 stars are those where there is the maximum of contrast between the time points. The groups sharing 1 star are those with less contrast. Groups without stars show a very weak contrast.

C.5. Combimatrix analysis
C.5.1. Genetic tendencies

Root RNA samples were extracted for each of the time points before the Rhizobium inoculation, as described in the previous paragraph (§. C.3). On the basis of the re-acquisition of competence results interpretation, the more significant time points that were picked up for the combimatrix gene chip analysis were T0, T6, T9 and T13 from the shifted P1 plants whereas only T0 was utilized from the P2 plants. A first statistical analysis for microarray (SAM) was performed by comparing the profile of expression of the P1 plants at the selected time points. This can allows to obtain a general tendency in the transcriptomic background of these plants that could give us a genetic interface of the nodulation phenotyping reported in §.C.4. In this specific SAM, the normalization that was used to get a general tendencies of differential regulation upon the four time points T0, T6, T9 and T13 was obtained by reporting the intensity of a selected TC (Log$_2$ centered values for the selected TC) at a given time point to the median of the intensity of that TC at all the rest of time points. For instance, if the intensity of expression of a TC at time point T0 is "x" and respectively "y" at T6, "z" at T9 and "w" at T13, the obtained values for this TC will be: x/(x+y+z+w) at T0 time point, y/(x+y+z+w) at T6, z/(x+y+z+w) at T9 and w/(x+y+z+w) at T13. Then, two different FDR were fixed out to select the significant TC ratios for each time point: one at 5% and the other at 10%. Subsequently, two different lists of significantly regulated TCs (upon the 12469 TCs spotted on chip) were carried out. The FDR 10% enriched the list of the FDR 5% by lowering the stringency of the selected TCs filter but remaining in a reasonable frame of TC value significance.

Thereafter, to find out the groups of tendencies, each of those values was grouped by a vertical hierarchical clustering, linking the different time points to the first T0 time point (T6/T0; T9/T0; T13/T0). In the mean time the tendencies were sorted out by an horizontal hierarchical clustering that clearly discriminated blocks of TCs allowing the identification of different groups of Tcs. A group were down regulated in T0 and then progressively up regulated at T13 and *vice versa* (numbered groups in figure 12). In particular, the clustering showed groups with high contrasted conditions between T0, T6, T9 and T13 time points (groups with numbers sharing 2 stars in figure 12) in either cases of down and up regulatory directions.
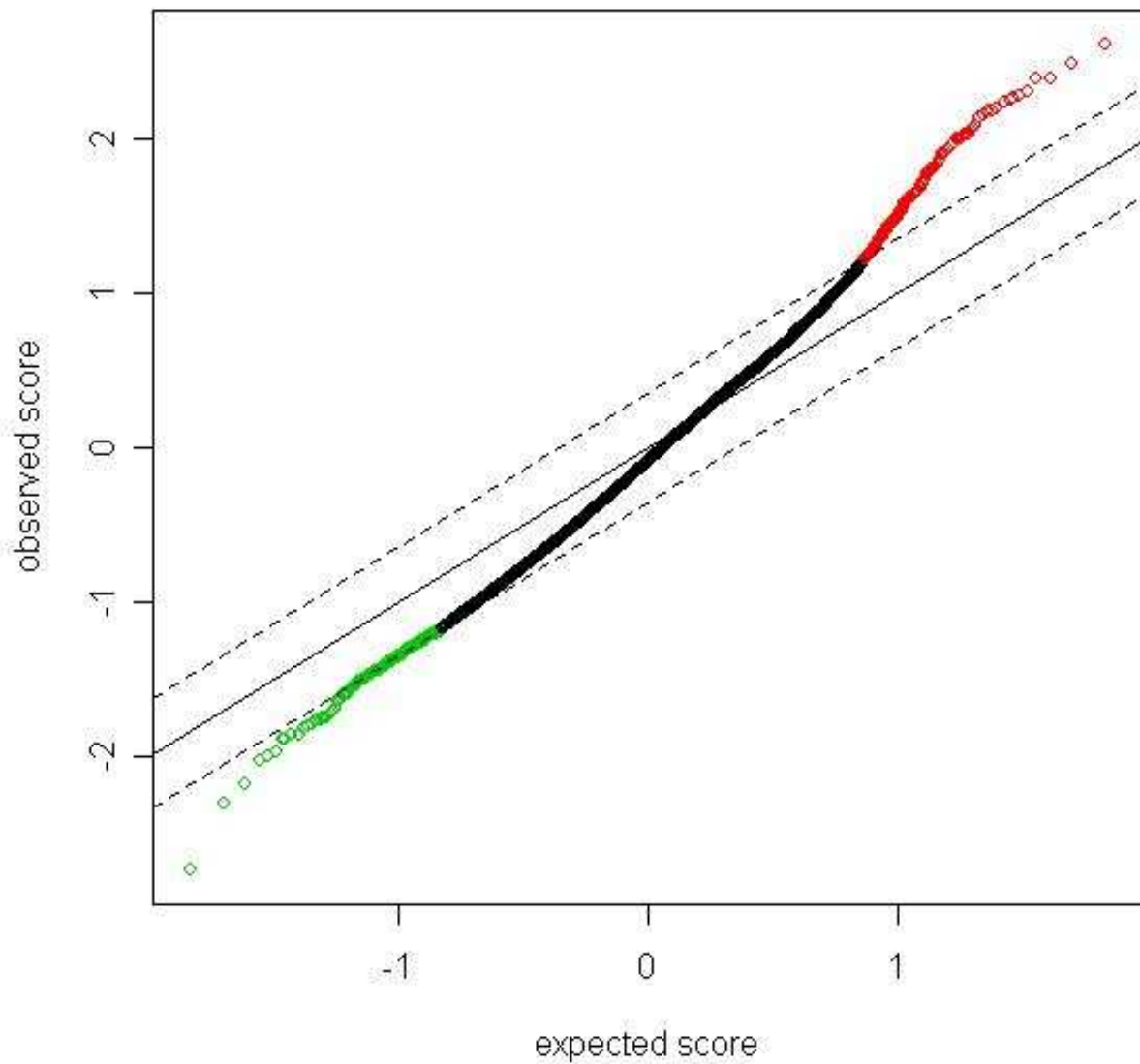
Figure 13. SAM plot indicating the ratio T0(P1)/T0(P2) in Log2 base. At FDR 6%, a very little fraction of TCs were regulated as it was the case in the previews combimatrix experiments. Thus only 156 up regulated (red spots) TCs and 200 down regulated ones (green spots) upon the 12469 on-chip spotted TCs.

By contrast other groups showed a weak but progressive regulation between time points (numbered groups sharing 1 star) while only the group 4 seems to concern a set of TCs with a very weak fluctuations in expression at all the time points. Ambiguous tendencies, reflecting parabolic or hyperbolic regulatory tendencies upon time points (*e.g.* 0 fold change at T0; 1 fold change at T6, 1.5 at T9) but retained after the FDR filtering were not anymore considered when correlated to the expected physiological cues given by the phenotyping and the experimental growth conditions. These data would be treated in a second lecture of the panel.

Besides, the clustering of the data selected after FDR 10% filtering showed as expected a major number of groups compared with those released after selection with FDR5% (group 6 for example). The observed tendency was that the Tcs that were moving up or down in the diagram in both senses T0 to T13 and *viceversa* concerned mainly TCs putatively involved in protein turnover of C and N metabolisms but also involved in biotic and abiotic stresses (classification under progress; see Discussion section).

C.5.2. Genetic modulation of P1 pool compared to P2 pool

In order to assess the discrepancy in nodule number between P1 and P2 at the transcriptomic level and hence to reflect the nodule inhibitory condition of 10mM NH_4NO_3 pre-incubation week, in a corresponding picture of genetic determinants; the transcriptoma of the two T0 times, respectively at the moment of the shift (P1) and transfer (P2), were compared. In this case the experiment was made *de novo* and extemporary from the one related to the tendency. The phenotyping showed also in this new experiment a clear two fold change of the nodule number in P2 plantlets compared to P1, ensuring the reliability of the experimental design. In this specific case a given TC value "x" is given by the ratio T0(P1)/T0(P2) that provides an estimation of fold changes between P1 and P2 (similar ratio was performed in § B. to evaluate T0 compared to T48). If the ratio gives a positive outcome this means that the TC is up-regulated in P1 and therefore down-regulated in P2. For instance if "x" = 3 the TC is 3 fold up-regulated in P1 compared to P2. Fixing the FDR to 6% it was possible to retrieve 156 up regulated TCs and 200 down regulated ones (figure 13). Interestingly, two contrasted categories of nodulins were found. ***The first category*** includes TCs that are induced in P1 and respectively, repressed in P2:

1)   TC8260, similar to Q94ES8 a nodule extensin (Fragment), partial (79%) with a 9.18 fold induction

2)   TC8247, similar to Q02918, an early nodulin 36A, partial (25%) with 2.22 fold change.

   The second category is repressed in P1 and respectively, induced in P2:

1) TC13120, weakly similar to Q8LRB6, a nodulin-like protein, partial (22%) with a 0.23 fold

 repression

2) TC8310, similar to Q9SPM8, a Nod factor binding lectin-nucleotide phosphohydrolase, complete (100%) with a 0.23 fold repression

3) TC13386, similar to AAS55542, a Ca2+ and calmodulin-dependent protein kinase (Fragment), partial (24%) with a 0.36 fold repression

4) TC16117, homologue to O80673, a CPDK-related protein (Calcium/calmodulin-dependent protein kinase CaMK3), partial (6%) with a 0.39 fold repression. Excitingly☺, all these TCs confirmed this behavior in the tendency experiment (§. C4.1.).In particular, the ones included in the category # 1 (up regulated in P1), showed a progressive decrease in their expression from T0 till T13 in the tendency experiment. By contrast, those included in the category # 2 (down-regulated in P1) they showed a progressive increase in their expression from T0 to T13. Only the calmodulin like TC(s) showed ambiguous pattern.

C.6. Additional support: The Split root system derived shift/cef experiment

The split experiment basically reproduces the experimental design of the shift/cefotaxim for the T0 plants. In addition we addressed the question whether the effects of different combined N sources on both, plant growth and symbiotic interaction can be discriminated. The root split plants were obtained as indicated in the Materials and Methods section. In this experimental design, one side of the root system (about 50% of the whole root apparatus) is maintained on 10mM ammonium nitrate, or 10 mM potassium nitrate, or 10 mM ammonium succinate (AS) while the other side is maintained or shifted at the time of the inoculation on a concentration of 10μM of the same combined nitrogen sources: NH_4NO_3, KNO_3 and $NH_4OOC(CH_2)_2COONH_4$. Only one side of the split root system (the one growing on 10μM) is then inoculated.

 The roots pre-incubated either in 10 mM ammonium nitrate, potassium nitrate, or ammonium succinate and shifted at the T0 on 10μM concentrations show in all the cases a reduced number of nodules compared with the plants having both sides of the root system maintained in N starvation conditions (10μM).
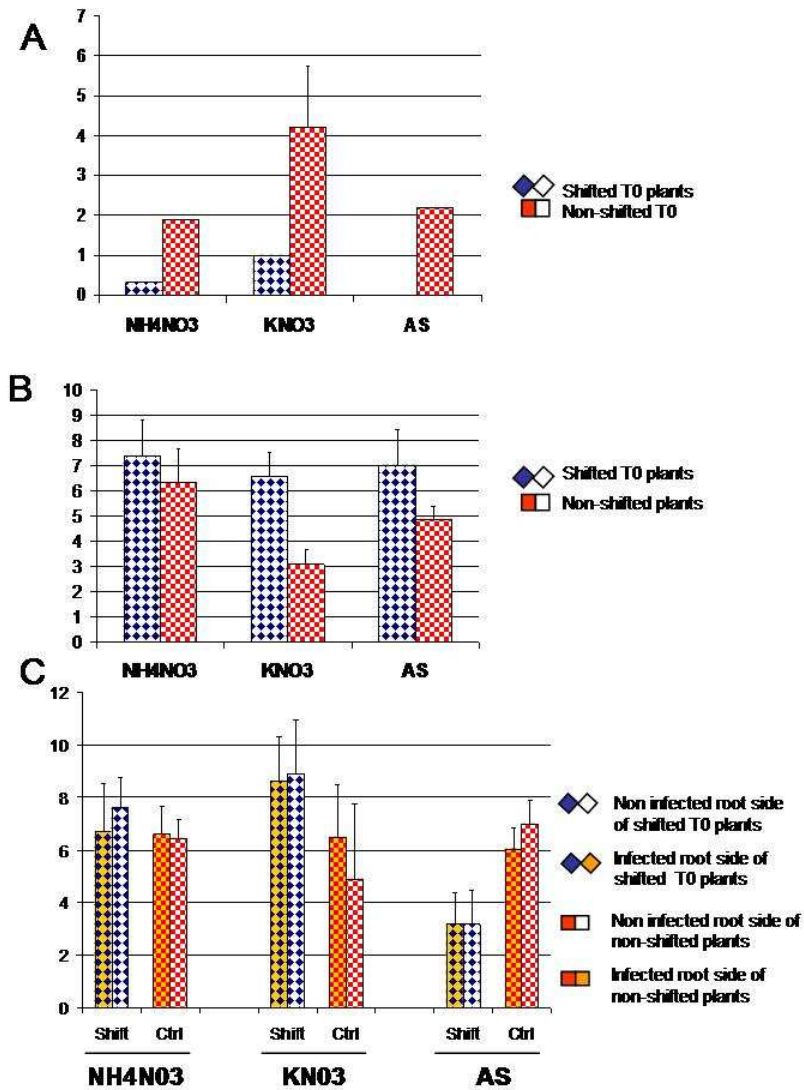
Figure 14
A. Average of nodule number (per root side) in splitted plants where half root system was shifted in 10μM at the time of the infection (T0) versus split plants where both sides where maintained in a 10μM concentration regime.
B. Average of the shoot length in split-shifted and split-unshifted plants.
C. Average of the primary root length (both infected and non infected root) in split-shifted and split-unshifted plants.
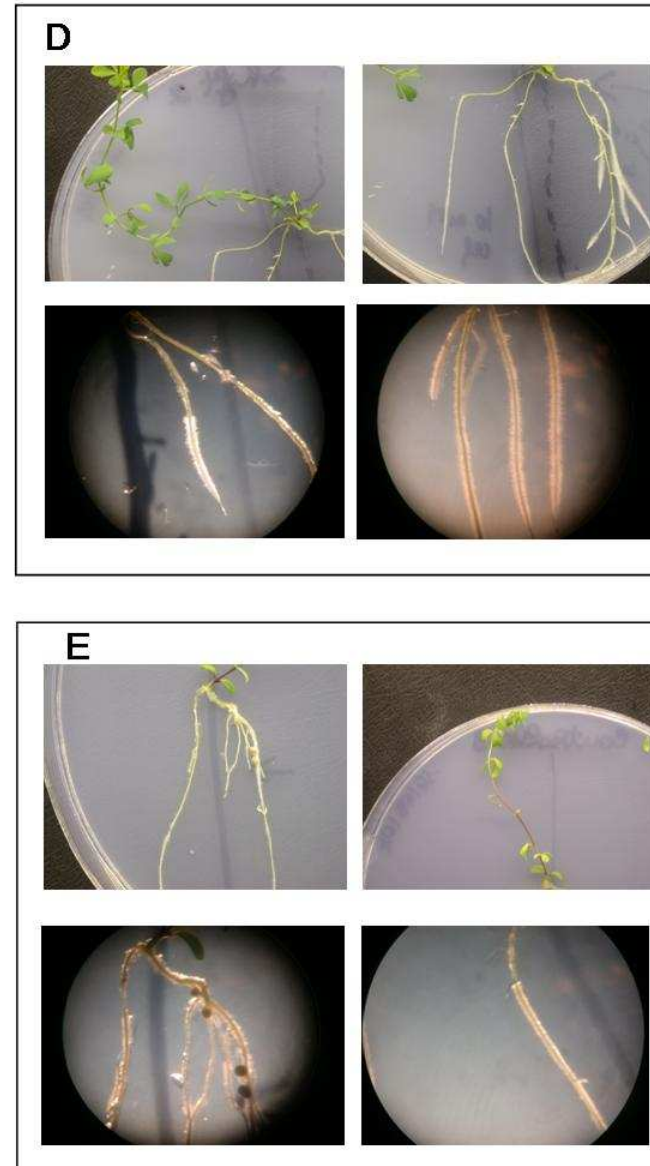
D. Root phenotypes in high concentration of combined nitrogen sources (here in 10mM NH4NO3). Shoot phenotype appeared unstressed and bushy while the root phenotype showed root hair re-growth.
E. Root phenotypes in low concentration of combined nitrogen sources (here in 10μM NH4NO3) **Shoot** phenotype appeared stressed (anthocyanin production) and chlorotic while the root phenotype showed root hair growth all over the root system. Nodules are visible on the infected root.

However the number of nodules at 15 dpi, according to the media composition was highest in roots pre-incubated on KNO_3 for both control and shifted split plants (figure 14A). The pre-incubation on 10 mM AS and NH_4NO_3 completely inhibit nodule formation (figure 14A). Contrasting, the split plants in all the 10µM concentration conditions showed stress symptoms starting at the hypocotyls and extending to almost the whole shoot as indicated by chlorotic symptoms (figure 14E). The reduction in shoot length was significant in 10µM KNO_3, followed by 10µM AS and 10µM NH_4NO_3 (figure 14B). The smaller shoots detected in the presence of 10µM KNO_3 indicating a starving nutritional status is also consistent with the higher nodulation capacity reported in Figure 14A. By contrast, the shoot part of the plants with the split roots growing into 2 different concentrations (10µM and 10mM), appeared healthy in the green part developing larger leaves and longer shoot organs with no significant differences between the different N sources (figure 14B).

The analysis of the primary root length shown in figure 14C indicates an interesting phenotype for plants grown in the presence of AS as N source. In fact, only the pre-incubation in the presence of AS at high concentrations (10mM) inhibits significantly primary root elongation (compare root length of shifted and non shifted plants) (figure 14).

The phenotype of the root apparatus revealed (as shown for a different experimental system in figure 2) a re-growth of the root hairs on the surface of the roots that have been incubated on 10mM of all the combined nitrogen sources (figure 14D). On the contrary, this root hair re-growth phenotype was diffused on the whole root apparatus of the split plants incubated in the 10µM concentrations in both infected and uninfected roots (figure 14E). A marked increase in the number of secondary roots was also noticed in the presence of 10µM of all combined nitrogen sources as compared to the root apparatus incubated on 10mM concentrations.
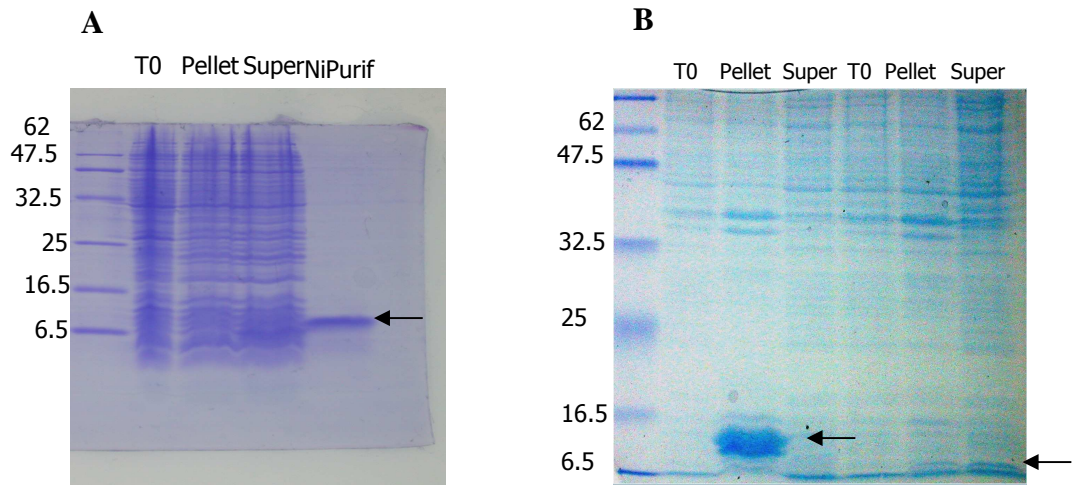
Figure 15. C-termAMTs protein purification. A. C-termAMT1;1 purification. T0, before IPTG induction (1mM); pellet after centrifugation of the clear lysate; supernatant of the 3 hours post induction sample. B. Expression of the C-term1.2 leads to its precipitation into the inclusion bodies pellet, while C-term1:3 was weakly induced.

Putative Myosin heavy chain (O. sativa japonica cultivar Group)

Pr 8.3e-001

Cov % 34

Mw 171,94

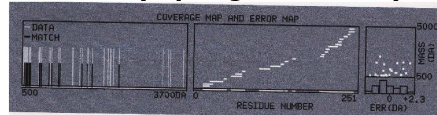**Conserved hypothetical protein (Onion yellows phytoplasma OY-M)**

Pr 1.0e+000

Cov % 44

Mw 48.81

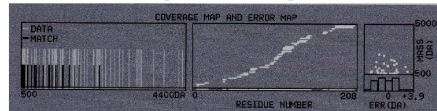**RPS6-40S (Asparagus officinalis)**

Pr 1.0e-000

Cov % 45

Mw 28.45

RPS4-Chloroplast 30S/putative L19- (Arabidopsis thaliana)
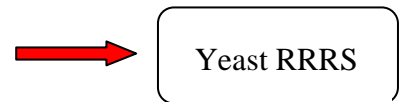

Pr 1.0e-000

Cov % 61

Mw 24.18

Yeast RRRS

Figure 16. Tripsin mass blasting. Among the four putative interactants only the RPS6 was tested in yeast Reverse trasncripton

D. LjAMT1 interactants

D.1. *In vitro* fishing

A part of my thesis was focused on the fishing of possible interactants of the LjAMT1 cytoplamic C-terminal tails. The C-terminal tails of the three LjAMT1 members were subcloned into the pET22 (b+) expression vector fused to a 6-Histidine tag. Only the AMT1.1 C-terminal end was sub-cloned in two different conformations (C-term and N-term fusions) as described in Materials and Methods. The over expression of the three AMT1 C-terms into the BL21 expression strain gave three different patterns (Figure 15A, B). The *LjAMT1.2* C-term precipitated entirely into the inclusion bodies while the LjAMT1.3 showed a very weak signal in the soluble fraction (Figure 15B). Only the LjAMT1.1 C-term, when sub-cloned in both conformations, showed a reasonable over expression in the soluble fraction (Figure 13A) and therefore used for the *in vitro* fishing as binding bait to a Nickel-column. The co-loading of the LjAMT1.1 C-term (His-tag at the end of the C-term) with crude extracts into the Ni-column gave a total of 4 putative interactants (Figure 16). A Trypsin digestion was performed on the extracted bands and an analysis of the mass of the digested fragments was carried out. The data were blasted against a mass finger print data base (program), and IDs were assigned to each of the 4 putative interactants. The first interactants matched a putative myosin heavy chain (*O. sativa*) with a partial coverage of 34%; however a low significance was assigned by the software (P 8.3e-0.01).

The second ID identified a conserved hypothetical protein (phytoplasma) with a partial coverage of 44% and a high significance (P 1.0e-000). The third ID was a ribosomal protein Segment 4 (Chloroplastic localization in *Arabidopsis thaliana*) with a high coverage of 66% and a high significance (P 1.0e-000). Finally, the fourth ID was a ribosomal protein Segment 6 (RPS6, *Asparagus officinalis*) with a partial coverage of 45% and a high significance (P 1.0 e-000).

D.2. *In vivo* conformation

Upon the 4 putative AMT1.1 C-term interactants only the RPS6 was retained for assessing its interaction with the LjAMT1 protein. In fact, this was the only ID-predicted protein that was found in its full length version in the Lotus sequence database (tiger database).

The interaction between the whole LjAMT1;1 and RPS6 proteins was analysed in the *S. cerevisiae* heterologous system that is exploited for fishing specifically membrane-bound protein interactants (Cdc 25 strain; see material and method). As a prerequisite to the protein interaction it was necessary to test whether the LjAMT1.1 construct (pMet450::AMT1.1) used for the double transformation of the Cdc25 strain produced a functional protein and this was asserted by complementing the (Δ Mep1,2,3) yeast on 1mM NH_4SO_4 restrictive ammonium source of feeding (figure 16). Then the co-transformation of the Cdc25 strain using the pRAS::RSP6 prey and the pMet450:: LjAMT1.1 procedure was followed as described in Material and Method; Unfortunately the rescue of the growth capacity of the co-transformed Cdc25 strain on the restrictive galactose medium (see procedure in Materials and Methods) was not obtained hence indicating the lack of proteins interaction.

Figure 16. LjAMT1.1 full sequence complementing the Δ Mep1,2,3 yeast strain on minimal Ynb medium supplemented with 1mM NH_4SO_4 as sole N source. The untransformed Δ Mep1,2,3 yeast strain is unable to grow on such a minimal medium (left side of the Petri dish)

III. Discussion

A. Prologue

At the beginning of this PhD thesis the objectives were clearly drawn out in the Dr Chiurazzi Laboratory. The starting point of the project concerned the further characterization of a family of *Lotus japonicus* ammonium transporters previously isolated in the lab (See introductive chapter) and published by D'Apuzzo *et al.* (2004). In this case the "further characterization" means that the molecular and physiological analysis of this *Lotus* gene family, will be considered as a tool to unravel the general mechanisms governing the plant response to different abiotic signals and to link these features to the specific potential of legume plants to start a symbiotic interaction with soil bacteria of the genus rhizobia.

Thus, it appeared necessary to "dig" deeper in the roles attributed to the *AMT1* multigenic family by D'Apuzzo *et al.* (2004) on the basis of the:

1) investigation of the biochemical features of the single family members;
2) analysis of a very little range of physiological fluctuating conditions of plant growth and study of their effects on the transcriptional regulations;
3) analysis of the spatial localization of the AMT1 genes expression.

Two kinds of newly unexplored tracks were followed concerning the regulation of these transporters in regards to the direct environmental conditions of *Lotus* growth and especially in regards to the peculiarity of the *Lotus* genetic background that offers the possibility to investigate the modulation of the AMT features in a symbiotic cross talk context involving the bacterial endosymbiont partner. Therefore, in order to understand the contribution of each abiotic factor, the research scheme that concerned this PhD thesis has followed the effects of different conditions of growth on the AMT gene expressions, by setting up the ones that allowed correlating separately the effects of different abiotic factors to the regulation of the AMT gene expressions. These conditions will be then exploited for the precise investigation of the symbiotic pathway modulations. In other words, the activity status of the *AMT1* genes could be the key reflector of the physiological adaptation that allows the plant to enter and assume a sustainable symbiotic program.

Since now few years, the terminology of N Sensor was appended to the *AMT* genes (Lorenz and Heitman, 1998; Yakunin and Hallenbeck*,* 2002; Javelle *et al.,* 2003) and in prokaryotes, their N dependent post-translational regulation by direct interactants was irrefutably demonstrated (Merrick and Durand 2006). As consequence, this project aimed to have also a parallel study that would determine whether the plant eukaryotic *LjAMTs* could have such a regulation. In this instance, the project showed through multiple experimental designs a clear possible role of the AMTs as first

sentries, indicators of the N/C status but it did not provide any strong evidence allowing the assignation of this kind of hazardous denomination (sensors).

B. *Corpus diatribae*

B.1. Uniformity of the experimental designs ensures data reproducibility

To reach these kinds of conclusions, we determined a step by step methodology. First of all, we characterized the pattern of expression of the *LjAMT1.1* and *1.2* genes to investigate their behavior under different combined N sources before drawing more complex experimental designs. Thus, we showed that plantlets grown under three steady state conditions of NH_4NO_3 (10µM, 1mM and 10mM) expressed *LjAMT1.1* and *LjAMT1.2* in a specific way with a pick of expression after 5 hours of light (13pm) and a rapid decrease, maintained in dark period (figure 1A, B, C *in* chapter Results). The same pattern of expression was observed in shoot (data not shown). This kind of regulation is, for the first time, reported in root plants contemporarily for two *LjAMT* members at three distinct concentrations of NH_4NO_3. A similar pattern of diurnal regulation was reported for the *OsAMT1;3* gene with an increased amount of transcript during the light period and a peak around 14 p.m. followed by a decrease toward the end of the day, and these changes corresponded with diurnal changes of $^{15}NH_4^+$ influx (Kumar *et al.,* 2003). Von Wiren *et al.,* (2000) showed also a similar (but not completely equal) regulation in the shoot part only for *LeAMT1.2* and the authors briefly mentioned the strong expression level of *LeAMT1.1* and *1.2* in roots observed under another kind of experimental design involving N starvation followed by N re-supply. Besides the expression of *LjAMT1.1* and *LjAMT1.2* in roots showed clearly an absolute higher expression in 1mM NH_4NO_3 compared to 10µM and 10mM NH_4NO_3 concentrations. This latter result could suggest that at the transcriptional level, 1mM concentration represents the ideal range in which the high affinity members are needed in steady state conditions and actively transcribed in roots. At that concentration the expression of *LjAMT1.2* was significantly higher than that of *LjAMT1.1* by contrast to the equal level of transcript abundance shared by both *LjAMT1.1* and *1.2* in the other conditions. Lejay *et al.,* (2003) reported a diurnal regulation for the three *Arabidopsis thaliana* ammonium transporters *AtAMT1.1*, *AtAMT1.2* and *AtAMT1.3* showing the highest expression of *AtAMT1.1* followed by *AtAMT1.2* and *AtAMT1.3*. Interestingly, the only data concerning the expression analysis in steady state conditions published by D'Apuzzo *et al.* (2004) confirmed the highest level of *LjAMT1.2* transcript while *LjAMT1.1* was the more induced after shift in N starvation conditions.   Thus, *Lotus* plant could utilize differentially its repertoire of high affinity ammonium transporters, soon after a change of N conditions and in a steady state situation. However, the changes in the steady state expression of genes belonging to the same phylogenetic

group render the concept of the experimental design of a high importance for the adequate reproducibility of the results. Besides, in D'apuzzo *et al.,* 2004 the authors used an *in vitro* condition that adds to the B5 medium, a carbon sources (Sucrose 1%) and hence, another variable in the study of regulation of genes tightly regulated by the C/N metabolism (Guttierez *et al.,* 2007). In our steady state conditions only the light period was different from that used by Lejay *et al.,* since we inverted the durations 16H light/8H dark instead of 8H light/16 dark. Surprisingly, this slight increase of the duration of light period showed that prolonged light period did not significantly affect the *LjAMT1* pattern of expression as it was demonstrated in Lejay *et al,* and raised the question of the possible circadicity of the tested *LjAMT1.1* and *1.2* pattern of expression.

Subsequently, in order to investigate the global effect of the N/C ratio on the expression of the *LjAMT1* genes, we first investigated separately the C and N effects. As preliminary observation, we noticed that the addition of high quantity of sucrose (1% = 29mM) to hydroponic *Lotus* cultures grown in presence of 10 mM NH_4NO_3 as sole N source, produced a fresh biomass exacerbation of the wild-type *Lotus japonicus* seedlings after 5 weeks growth in Magenta compared to the ones grown without sucrose (figure 2B, C; *in* Results chapter). As a matter of result we showed that a sucrose-dependent effect was also revealed on the *LjAMT* expression and *LjAMT1.1* as well as *1.2* was induced in dark period after addition of 1% sucrose. This indicated that both genes did not obey to an internal circadian clock (figure 2A; *in* Results chapter), confirming that the *LjAMT1.1* and *1.2* transporters react as their homologues *AtAMT1.1*, *1.2* and *1.3* to the carbohydrates sources, being probably strongly regulated by photosynthates such as glucose. The effect of sucrose on the profile of *LjAMT1* expression is in agreement with most of the data reported in literature on the photosynthetic dependent regulation of channels and transporters in roots (Kerr *et al.,* 1985; Ruffy *et al.,* 1989; Riens *et al.,* 1994; Mito *et al.,* 1996, Lejay et *al.,* 2003) and the network derivative model from large screening of C/N metabolism (Price *et al.,* 2004, Guttierez *et al.,* 2007).

Noteworthy, our data indicate an inhibitory effect of sucrose on the peak of *LjAMT1.* and *1.2* expression observed during the light period at 13 p.m. (figure 2A; *in* Results chapter). Moreover, this inhibition seems to be specific to the ammonium transporters since the addition of sucrose continuously increases the expression of the *LjGLN1* gene (figure 2A; *in* Results chapter), in agreement with the studies of Wang *et al.,* (2003) and Price *et al.,* (2004). This could be a consequence of the specificity of the gene promoter regions that could interact with different factors for the integration of both C and N signaling.

Once again, the detailed set up of our experimental designs reveal the importance of each of the tested abiotic factors and how for example, the addition of synthetic sucrose into the medium could affect the normal photosynthesis-dependent regulation of some genes involved in the N/C metabolism,

by imposing a possible negative feedback on their expression. Thus, some of the analysis of the global profile of expression reported in literature could be biased by the experimental conditions used (Price *et al.*, 2004).
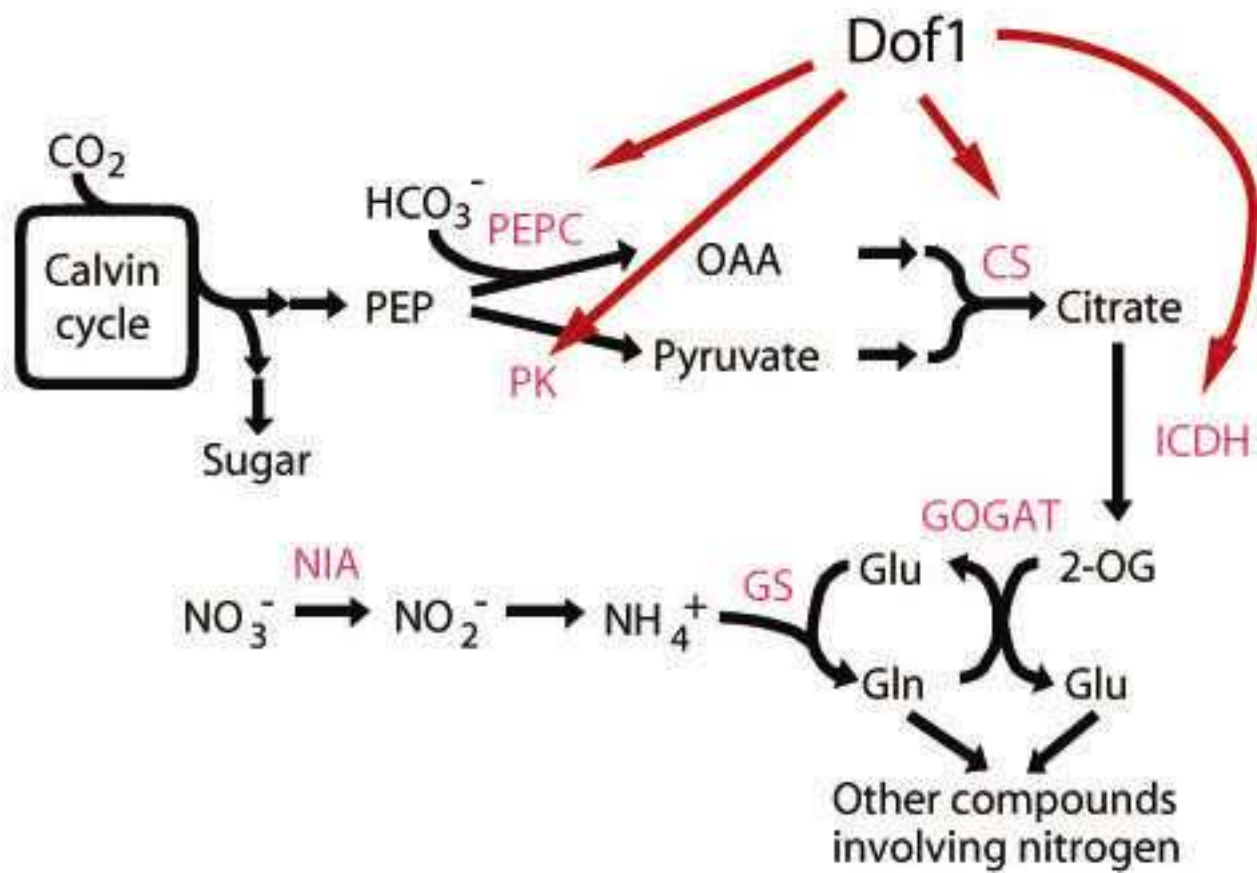

Figure 1. Scheme of the role played by the Dof transcritption factor in the control of the expression of key enzymes (PEP carboxylase and ICDH) whose action is crucial for linking carbon with nitrogen metabolism.

The results shown in figure 1 and 2 (*in* Results chapter) pushed us to make an *in silico* analysis of both *LjAMT1.1* and *LjAMT1.2* promoter regions to screen (softberry software) for the presence of specific regulatory elements (figure 3A, B *in* Results chapter). The most relevant point of this analysis was the finding of a higher density of motifs on the 5' regulatory *LjAMT1.2* region than that of *LjAMT1.1*. In particular, it is intriguing the presence of three specific regulatory sequences that could bind the GT transcription factors, known to belong to a multigenic family of master regulators (light responsiveness Transcription Factors) controlling the expression of genes involved in photosynthesis (Kuhlemeier *et al.,* 1988; Gilmartin *et al*., 1992; Dehesh *et al*., 1989; Ayadi *et al*., 2004). Interestingly, these regulatory sequences could be also found in the promoters of some light-independent genes. The pathogen defense-related tobacco PR-1a gene, contains GT elements in the promoter region (Buchel *et al.,* 1999) while the GT protein themselves are encoded by pathogen related genes (Rong Wanga *et al*., 2004) sharing common defense regulatory elements in their promoter sequences (Eulgem *et al*., 1999; Rushton *et al*., 2002). By contrast even though the *LjAMT1.1* promoter region does not present specific GT binding boxes, it contains other binding motifs such as the ones for the DET1 transcriptional factor that is thought to be a signal transduction component linking the perception of light to a switch in developmental programs (Bridey *et al.,* 2003); regulatory motifs found in the promoter regions of photosynthetic genes (rbcS3C; rbcS1); the DOF1 binding box that is tightly related to the nitrogen assimilation in plants under N deficiency (Yanagisawa *et al*., 2004). Presumably, this latter transcription factor is one of the fundamental regulators of the C/N metabolic imbalance in plants as it acts on key enzymes present in the bottleneck separating both C and N pathways (mentioned in the Introduction chapter; figure 1). Finally, other regulatory sequences found in the 5' *LjAMT1.2* promoter region belong to Tfs binding domains, mainly involved in drought resistance, salt tolerance and protein storage (Alfin, SEF) as well as plant development (RE in Agamous gene).

Because most of the *in silico* regulatory motifs that we found contained mismatches with the consensus sequence (in general not more than 2), and in order to experimentally evaluate the physiological roles of such motifs, we decided to take advantage of two *Lotus japonicus* transformed lines, carrying two different constructs, sharing contrasted length of the *LjAMT1.1* promoter region fused to the *gus*A reporter gene. The preliminary results demonstrated the importance of the region upstream of a 250 bp fragment (counting from the (+1) ATG codon triplet) for enhancing the GUS activity (figure. 3C, D *in* Results chapter). Interestingly, the 250

bp region contains only two *in silico* revealed motifs; the GARE 1 that binds an unknown TF and the CAB that binds the DET1 TF. Since the experiment were performed with the *Lotus* transgenic lines grown in the presence of 10mM NH_4NO_3 as sole N source and the plants were analysed at 13 pm (at the pick of expression of the *AMT1.1* gene) it is possible that these two regulatory elements bind TF(s) that is sufficient to ensure the basal transcription level of *LjAMT1.1* and probably the upstream sequence binds other TFs involved in enhancing the expression of this gene in response to different abiotic factors.

B.2. Unraveling the quick variations in expression and magnifying the small ones

As previously discussed, the steady state experiments (above) did not represent "a finality" *per se* and the objective of this first characterization was more specific. Indeed the steady state allowed us to draw the right conditions to design the "shifting conditions experiment" and even more, the subsequent experimental scheme serving as platform for the evaluation of genes involved in the N signaling pathways that are propedeutic to the occurring of the nodulation organogenesis in *Lotus japonicus.* Thus, the precise determination of the timing where the expression of the *LjAMT1* genes was knocked down or, respectively, up-regulated defined the ideal moment for shifting the plantlets from 10mM NH_4NO_3 to 10 µM NH_4NO_3 for a global transcriptomic analysis of the profile of gene expression. As expected, the *LjAMT1.1* expression showed a 5 fold transient induction at 48h post shift with a rapid decrease after 72 hours (figure 4 ; *in* Results chapter; D'Apuzzo *et al.,* 2004). This data is in agreement with data previously reported for *AtAMT1.1* showing a 5 fold induction, 72h post shift in N starvation (Gazzarini *et al.,* 1999), as well as for *LeAMT1.1* that showed a strong but not transient induction 2 days post shift (dps). Again it is important herein to briefly stress out the differences between our experimental design and the one described in those publications. Indeed, in our case we used 10 mM NH_4NO_3 concentration (instead of 1mM) with an incubation time of 4 weeks instead of 5 weeks (*L esculentum*) or 2 weeks (*A.thaliana*) and finally we transferred the plantlets in 10µM (instead of N-free medium). The duration of the pre-incubation treatment and the concentrations of NH_4NO_3 are crucial in determining the quickness of the plant response after shift in N starvation conditions probably because the tissues have different level of saturation at different NH_4^+ concentrations, with a consequent different rate of N depletion after reaching a physiological equilibrium in regard to the presence of NH_4^+ in the external medium. This latter point is just another example of how complicated can be the analysis of expression of metabolic

genes involved in the N/C metabolism. As already previously stressed out, the experimental conditions must be fixed in a way that the possible overlapping between different regulatory signals (diurnal cycle, N and photosyntate availability, presence of external source of sucrose, length of the treatment) can be evaluated. For example, the interpretation of some results shown in different papers are biased by the lack of information about the diurnal timing of the time course experiments analysing either RNA expression or NH_4^+ influx (Gazzarini *et al.,* 1999; Von Wiren *et al.,* 2000, Loqué and Von Wiren, 2004). An exception is represented by the analysis reported by Guttierez *et al.,* (2007) where the authors discriminated the effects of the different signals. The microarray analysis we performed by comparing the expression profile at the T0 and T48 of the experiment shown in figure 4 revealed a poor number of significantly regulated TCs (87 TCs) at FDR 5% (figure 5; in Results chapter) compared to the number obtained in Guttierez *et al.* This is a kind of expected result since the data delivered in that publication (5314 mRNA out of 14462 spotted *A. thaliana* affymetrix chips) concerned an analysis of variance (AOV) analysis that integrates different combinations of three C independent, N independent, C **x** N interaction conditions (additive or exclusive). This number of mRNA has been obtained in that work after normalizing all the ratios C/N that the author tested (different sucrose and nitrate combinations) against ratio C=0/N=0 and then integrating them in the AOV (below) to find out the valid significance:

$$Y = \mu + \alpha_{\text{sucrose}} + \alpha_{\text{nitrate}} + \alpha_{\text{sucrose X nitrate}} + \varepsilon$$

Where Y is the response (expression of the gene represented by its normalized signal), μ is the global mean and α coefficient corresponds to the effect between the different treatments is the qualitative variable explaining the different factors while ε is the residual variance. These entire variables follow a Normal distribution.

In our case this formula could be reduced to a single factor AOV

$$Y = \mu + \alpha_{\text{nitrate(NH4NO3)}} + \varepsilon$$

And hence for us $\alpha_{\text{nitrate (NH4NO3)}}$ represented by 2 N-contrasted (10mM NH_4NO_3 at T0 and 10µM NH_4NO_3 at T48 dps) conditions are reflected by the following ratio:

$$\frac{\text{T48h dps}=(C=0/N=10\mu M)}{\text{T0h}=(C=0/N=10 \text{ mM})}$$

We demonstrated that if we use a T-test where we compare the ratio of all the TCs to ratio 1, which means no variation in expression between T48 and T0 (in this case we consider that the distribution of the ratios is following a Normal distribution around 1), and we select all the
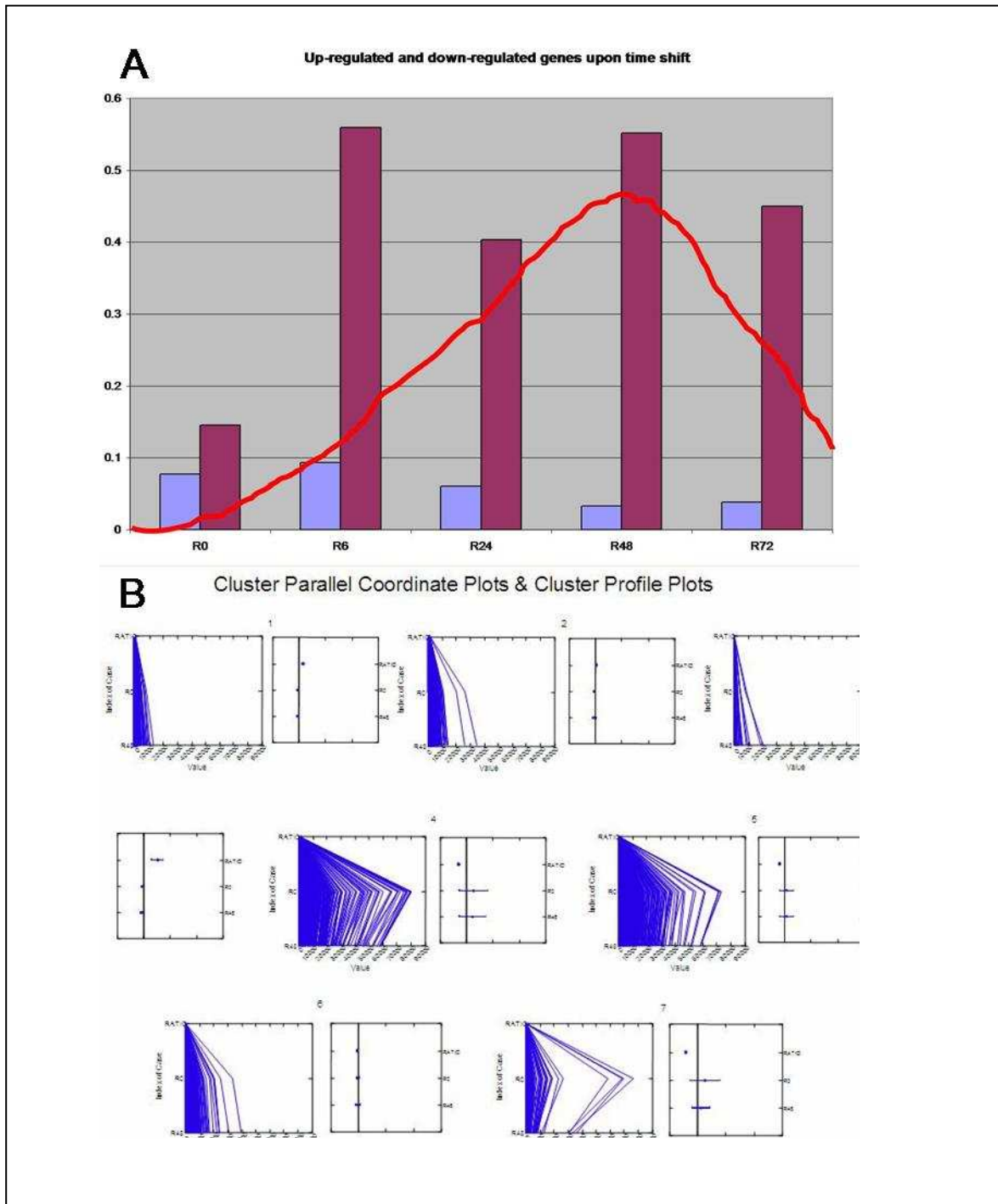
Figure 2 Observed tendencies. A. Time course (shift from 10mM NH_4NO_3 to 10μM NH_4NO_3) of the pattern of expression of two genes: the P450 cytochrome monooxygenase (red bars) and a putative deoxycyclate deaminase (blue bars) that are respectively up (3 folds) and down regulated (0.5 fold). The drawn red curve indicates the tendency followed by a marker gene such as AMT after the shift.
B. Cluster Parallel Coordinates Plots (right squares under the assigned group numbers) indicating for each of the 7 groups/clusters (see results) that the ratio T48/T0 is not informative for the small variations in expression. The plotting of the ratio against the absolute values of each TC at T0 and respectively T48, allows discriminating in each group, which TC is significantly moving. Cluster Profile Plots indicate the total variation in each of the 7 groups. Groups 4 and 7 are showing the highest absolute variation respectively in T0 and T48 but only the group 7 shows the highest variation in ratio.

highly significant data at the value of P (0.01) = 3.29, we could integrate more data (6501 up regulated and 2187 down regulated genes out of 12469; figure 6; *in* Results chapter). Consequently, we reached more or less the data obtained of Guttierez *et al.,* by testing the shift effect, looking only to 1 factor (NH_4NO_3 variation). In other words, the metabolism of C/N could be investigated without implementing artificial addition of sucrose or by the use of huge experimental combination of C/N to represent the total C and N-dependent variation in the profile of gene expression. It is very likely that plants adapt their metabolism as quick as the rapid fluctuations in the environment appear, by minimizing the disturbance at the genetic levels, where different rates of regulation can be observed for different genes (figure 2A). Therefore, the genetic background probably defines a reduced battery of key genes that are in charge to maintain a normal physiological status, while most of the genes are reacting with small variation in expression. Since the combimatrix technique is not a quantitative tool, we chose the statistical methodology described above (see also § B1.3. in Result chapter) to magnify these small differences in expression (figure 2B). A preliminary analysis of the results obtained in the *Lotus* background permitted the identification, among the significantly regulated Tcs, of some putative nodulin genes (**TC8247; TC16612; TC12598)** that should not exist in the non leguminous plant backgrounds (or at least having other functions).

B.3. Linking the plant N adaptation to the symbiosis: A leguminous paradigm

In order to <u>link</u> genes, appearing to be regulated by the shift condition to the nodulation pathway, we undertook the same kind of shift experiment to follow the nodulation phenotype. The set up of the experimental design (figure 8; *in* Results chapter) is peculiar and to date it was not described in literature this kind of interplay between bacterial infection, antibiotic use for the avoidance of "n" rounds of infection on the root infection zones and the successful emergence of root nodules after the rhizobia first infections (figure 7A and B; *in* Result chapter). In this regards, the methodology allowed us to define a strict discrimination of the nodulation phenotype between plantlets incubated in 10mM NH_4NO_3 (Pool P1) compared to the plantlets that were always maintained in 10µM NH_4NO_3 (Pool P2). Thus, we demonstrated that the pre-incubation in 10mM lowered the potentiality of *Lotus japonicus* seedlings to produce nodules of nearly a half fold while the pattern of nodulation of these plantlets were rescued only 9 dps (figure 10; *in* Results chapter). In this way, we were able to determine the fraction of time (between 6dps and 9 dps) that allowed this kind of inversion and hence the moment where plants
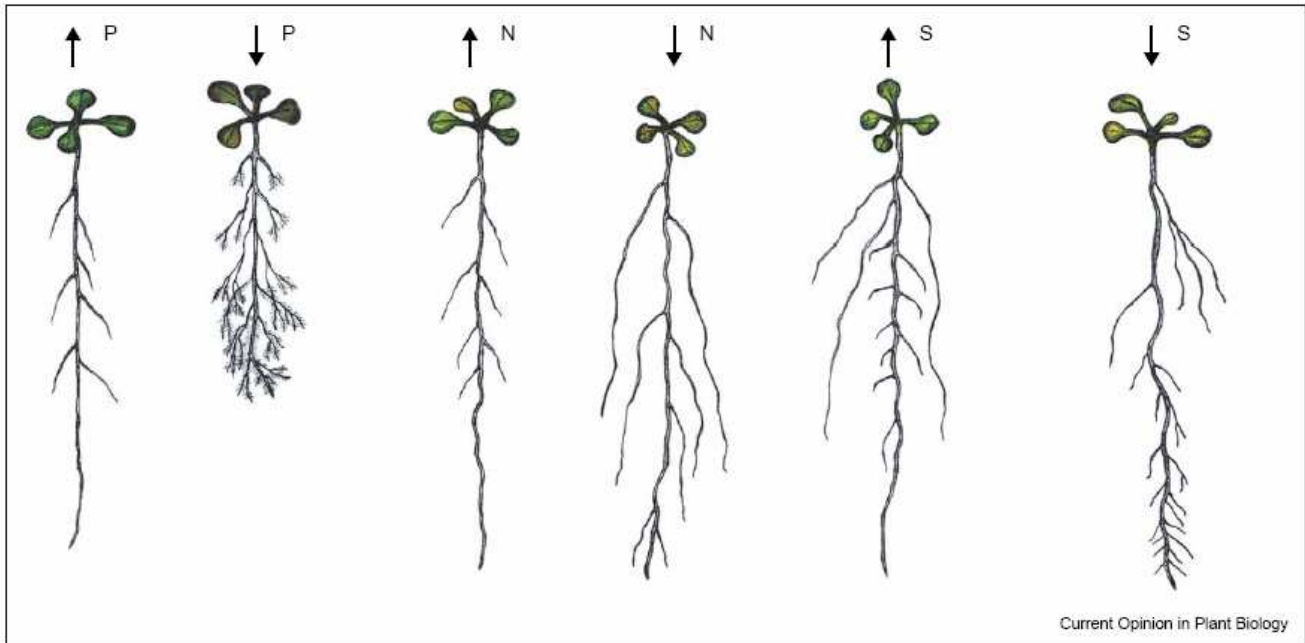
Current Opinion in Plant Biology

Figure 3. Responses of the *Arabidopsis* root systems to different nutrient supplies. The root systems were grown in nutrient-rich media with or without a high concentration of P, N and S.
 P and S deficiency can dramatically alter primary and lateral root growth, modifying the overall root architecture. Contrasting N availability may alter lateral root elongation

show a rescue of their nodulation potentialities after the pre-incubation in the inhibitory conditions represented by 10mM NH_4NO_3 concentration. During the phenotyping we followed also other parameters such as the shoot and root length and biomass as well as some traits that are key indicators of the physiological adaptation of the plantlets to their direct environment (figure 9 B, C, D; *in* Results chapter). In particular, at 34 days post inoculation, the fresh shoot biomass was increased in both P1 and P2 plantlets (figure 9 D, panel 1; *in* Results chapter) probably as consequence of the N fixation that supports the plant growth and makes this independent by the external N sources. By contrast, in roots, the growth patterns are not conserved (figure 9D; in Results panel 2) and this is probably due to the typical plant response observed in N stress conditions, when plants allocate most of the energetic sources to the roots to increase their subsoil surface, looking for additional N sources. The discrepancy observed between P1 and P2 shoot and roots phenotypes would suggest that the latter is related to a N-dependent effect that acts locally on the roots and it is not mediated by the nutritional status of the plant.

In general, the P1 plantlets are slightly heavier than their corresponding controls in P2 pools. This fact could represent a consequence of the pre-incubation on 10 mM NH_4NO_3. The latter result could be important for application in sustainable agriculture because plant legumes would maintain the same nodulation capacity and hence their bio-fertilizing actions by increasing at the same time their biomass.

Optical microscopy observations of the P1 and P2 pools showed that the plantlets of the P1 pool showed a marked phenotype in the root apparatus at 34 dpi with a patch of root hairs re-growth near the root tips and an increase in the secondary root formation while the P2 pool showed a marked chlorosis symptoms and an anthocyanin production in the shoot part (figure 10A and B; *in* Results chapter). These latter results are consistent with what is reported in literature, since in *Arabidopsis* it was demonstrated that high nitrate (> 10 mM) reduces lateral root elongation throughout the root system whereas, exposure to local patches of the primary root to high nitrate induces a local stimulation of lateral root elongation (Zhang and Ford, 1998). However, in the corresponding literature, the patch of root hairs re-growth was mainly attributed to a depletion of phosphorous and not to the progressive depletion of NH_4NO_3 or other minerals such as iron (Muller and Schmidt, 2004; Bucio *et al.,* 2003, see figure 3).

In order to assess a complete panel of the N inhibitory effect on the pathway of nodulation we decided to look also at early events of the root hair infection (between 0 dpi and 7 dpi). For this purpose we used two strains that gave us two complementary results. On one hand, the infection of the T0- P1 plants, with *M. loti lacZ* strain showed, at 6dpi, the uniform spreading of the bacteria on the surface of the roots and the root hairs indicating an anarchical bacteria cell division (figure 11 *in*

Result chapter). On the contrary, this phenotype is not maintained for the T0-P2 plantlets that clearly showed the initiation of the nodule primordia exactly at the level of infection drop spotted at 50 mm from the root tip (figure 11; *in* Results chapter). The RFP fluorescent rhizobia strain gave even a more precise picture of what could occurs at the level of the inoculation spotted point in the root symbiotic competent region (figure 12; *in* Results chapter). In this case the T0-P1 plantlets scored at 4 dpi showed bacteria overgrowth on both root hairs and root surface without any detection of initial infection signs (figure 12 *in* Results chapter), while the T0-P2 plantlets, in the same conditions, showed active root hair deformations and curling structure with bacteria entrapment pockets (figure 12C *in* Results chapter). These results are consistent with the known pleiotropic effects of the high concentration of NH_4^+ on the rhizobia behavior (Patriarca *et al.,* 2002), confirming that the successful infections could occur only in N starvation conditions. However, it's the first time that this N inhibitory effect is qualitatively and subsequently quantitatively (nodule phenotyping at 7dpi) assessed in *Lotus japonicus*.

Once we had the confirmation of the reproducibility of our nodulation phenotyping experiments (the shift/cef nodulation phenotyping experiment was repeated for 3 times), the development of a new array that assessed the most contrasted time points, was necessary for more than one reason. Firstly, the array based shift experiment design (figure 6 *in* Results chapter) was not supported by such an analysis that directly links nodule formation to the progressive suppression of the N inhibitory condition. Secondly the previous array has the objective to assess the genetic background of *Lotus japonicus* in a physiological situation (48h after shift) that could mimic the one that renders the plant competent to initiate the symbiotic dialogue with the bacterial host. As it is shown in figure 9A (*in* Result chapter), till 6 days post shift, the P1 plantlets nodulate one fold less than the P2 plants. Besides, looking with more attention to the graphs of the figure 10A, we could see that the slope of the nodulation curves at early time (between 0 dpi and the moment of the first screening at 7 dpi; figure 10A; *in* Results chapter) becomes more vertical for the 4 panels 0 dps till 13 dps, especially for the P1 pool. Hence these phenotyping issues argued in favor of a possible dual effect due to the timing of incubation and to the features of the growth media, on the nodulation kinetic. Finally, the plant growth conditions are quite different since in the shift/cef experiment we were obliged to infect plant grown on solid B5 media and therefore we do not expect necessarily, similar induction pattern of the AMT genes as in the shift experiment performed with hydroponic cultures.

B.4. Two independent chip experiments for assessing the nodulation competence

The results of the combimatrix gene chip aiming to assess the re-acquisition of the nodulation capacity by suppression of the N inhibition, reveal the genetic tendencies of the P1 pools for the T0, T6, T9 and T13 time points (figure 12; *in* Results chapter). Both fixed FDR 5% and FDR 10% determined cluster of genes that are progressively, or by contrast rapidly, up or down regulated while others showed very weak fluctuation, or ambiguous pattern of regulation. Even though the classification of the TCs inside of each of these clusters is under progress, the most relevant point lies in the qualitative confirmation that this second array gave in relation to the shift combimatrix array and especially to the third array that we decided to develop.

Indeed, this third combimatrix gene array concerning the evaluation of the phenotypic discrepancies in nodule number observed between P1 and P2 was made only at the T0 plants. Surprisingly, the results of this array, not only represent a good tool for the confirmation of the genetic tendencies of most of the clusters, but it definitively shed the light on genes that are of a high importance in the symbiotic pathway and hence could explain our phenotypic variability between P1 and P2. The first gene that is salient in this picture is termed Nod factor binding lectin-nucleotide phosphohydrolase TC8310 that was down regulated in P1 plants (0.23 at FDR 6%). Among the TCs identifying nodulins, that were found up or down regulated, only this one shared a complete matching between its sequence and the TIGR database sequence. Interestingly, this TC was described as having a dual role in binding Nod factors of *Bradirhizobia* hosted by the lupinus *D. biflorus* specie expressing the homologous lectin (Db-LNP), and having a N-dependent induced expression when the growth media was depleted from nitrate and ammonium (Eltzer *et al.,* 1999, Kalsi and Eltzer, 2000). Besides, in those papers an increased catalytic activity in hydrolyzing phosphoanhydride bounds of nucleoside of di- and tri-phosphate in the presence of carbohydrates was shown. We also identified a CPDK-related protein (Calcium/calmodulin-dependent protein kinase CaMK3 (TC16117) among the down regulated TCs. CCaMK is required very early during the symbiosis for deciphering the information that is encoded in the calcium spiking (Oldroyd and Downie, 2006). It has been recently reported that a small deletion in the auto-inhibitory domain of the CCaMK protein, generates a constitutively active form of this calcium-activated kinase, resulting in spontaneous nodule morphogenesis and induction of ENOD genes, in the absence of Nod factor or *M. loti* (Tirichine *et al.,* 2006, Gleason *et al.,* 2006).

A Consistent support to this combination of independent combimatrix experiments and consequent overlapping results was given by the split experiment where we reproduced for split plantlets the T0 condition (figure 13 *in* Results chapter). We showed that in different N combined sources (NH_4NO_3, KNO_3 and Ammonium Succinate) the number of nodules scored at 15 dpi and shared by the infected roots was significantly higher in the split plants where both infected and non infected roots were

incubated on a 10 µM concentration of NH$_4$NO$_3$, or KNO$_3$ or AS, while this number was quite reduced on the infected roots of the split plants where the non infected root was maintained on high concentration (10mM) of a N combined source (figure 13A; *in* Results chapter). Besides, we showed that the strongest reduction (total inhibition) of nodule formation was observed in the presence of AS followed by NH$_4$NO$_3$ and KNO$_3$ that is consistent with the data recently published by our team (Barbulova *et al.* 2007) showing the more severe steady state inhibitory effect of the NH$_4^+$ on the Nod factors-dependent nodulation pathway compared with the NO$_3^-$ effect (figure 13A *in* Results chapter). Unfortunately, we did not test yet at the time of writing the manuscript, the local or systemic effect of these combined N sources, on the nodulation phenotype by infecting the shifted split root sides at later time point as we performed for the shift/cef experiment (e.g infection after 1dps,…, 6 dps, 9 dps,, 13 dps).
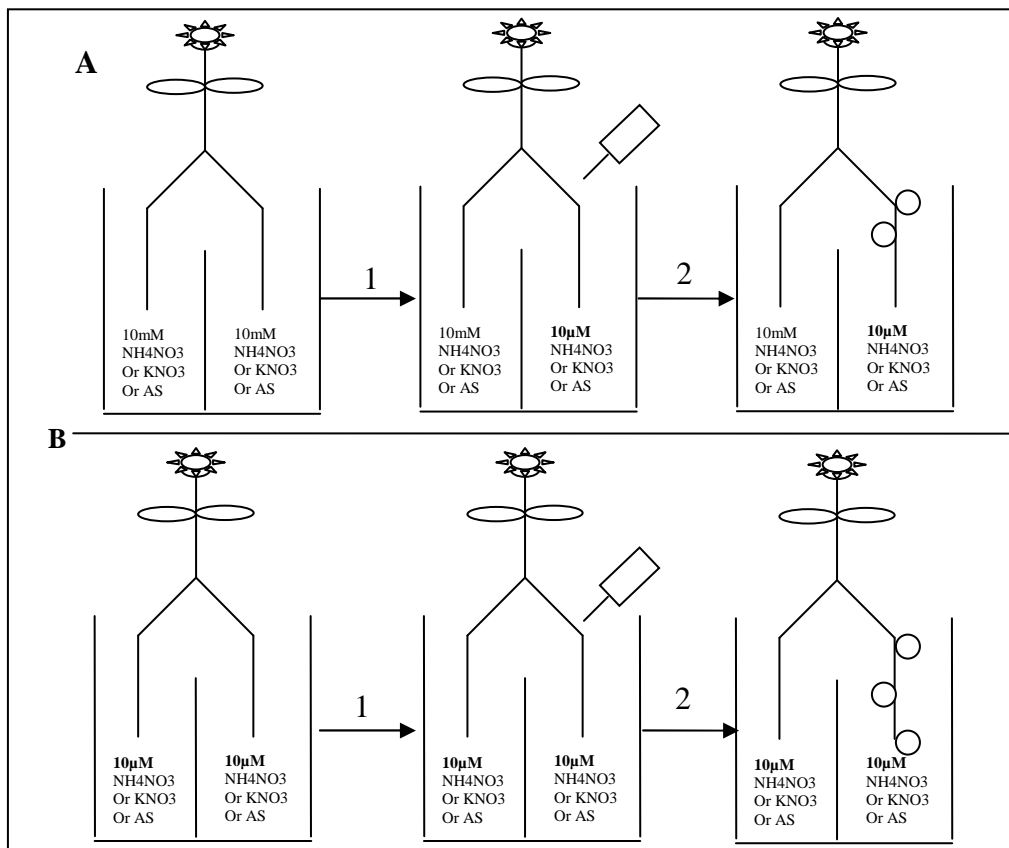

Figure 4. **Split root diagrams. A.** Split shifted plantlets; both split roots are incubated during 7 days in 10mM then only one root side is transferred on 10µM and infected at the same moment (1) the nodule number is assessed on the infected root at 15dpi (2). **B.** Split transferred plantlets. The procedure is identical to A except that both root sides are pre-incubated on 10µM during 7 days.

However, additional outputs can be obtained by the experiment shown in figure 4. The shoot length reduction was gradually marked from 10µM KNO$_3$, then 10µM AS till 10µM NH$_4$NO$_3$ (figure 13B; *in* Results chapter), consistently with data reporting that in the presence of low, identical concentration of nitrate and ammonium, the latter is the preferential nutrient form

because it can be immediately assimilated (Gazzarini *et al.,* 1999).The root hairs patch re-growth was observed in 10mM rather than in10µM NH_4NO_3 condition (figure 13D, E; *in* Results chapter) and this was in discordance with what we observed on the root surface of seedlings monitored in the shift/cef experiment (figure 10; *in* Results chapter) arguing in favor of a probable specific role of the NH_4^+ depletion that could monitor from the 10µM NH_4NO_3 side the root hair patch formation in 10mM NH_4NO_3. Nevertheless, an independent NH_4^+ depletion (or other nutrients such as Phosphorous or Iron) in the 10mM inducing the patch formation could not be excluded.

In all the cases, the experiments that we drawn out demonstrated that the N/excess inhibitory condition could have different targets on 1) rhizobia infections behavior, 2) root hair cell signaling eliciting the expression of the lectin Nod factor binding, 3) lectin transfer to the root hair surface.

C. Epilogue

In conclusion, we propose a model that integrates (figure 5) the one published by Barbulova *et al.,* 2007. In that paper ammonium and nitrate effects on the Nod factors-dependent transduction pathway were discriminated and positioned in different point of the cascade of events induced early during symbiotic interaction (see introduction). In particular, high ammonium concentration was demonstrated to act earlier and to inhibit root hair deformation. The root hair deformation can be uncoupled by the other early events induced by Nod factors, because concentration of these eliciting factors needed to induce this event, is much higher than the one necessary for initiating calcium influx and calcium spiking. Downie and Oldroyd (2005) proposed that a local accumulation of rhizobia is needed for synthesizing the amount of Nod factors necessary for inducing root hair deformation and that this is specifically correlated with the rhizobia infection process and the infection thread formation. Our array data suggest a possible molecular mechanism supporting this hypothesis. The Nod factors binding lectin could have a role for the accumulation of the Nod factors. At high concentration of ammonium the down regulation of the NFB lectin would avoid this action inhibiting root hair deformation and the infection event (figure 5). The lectin could bind Nod factor independently by the NFR1 and NFR5 receptors recently identified (Radutoiu *et al.,* 2005). We also suppose a role for the AMT proteins as sentries in regulating the process (*in* figure 5). They could directly sense the N/C ratio, controlling the signaling pathway leading to the down-regulation of the NFB lectin or, their action could be dependent by a master regulator having the sensing role.
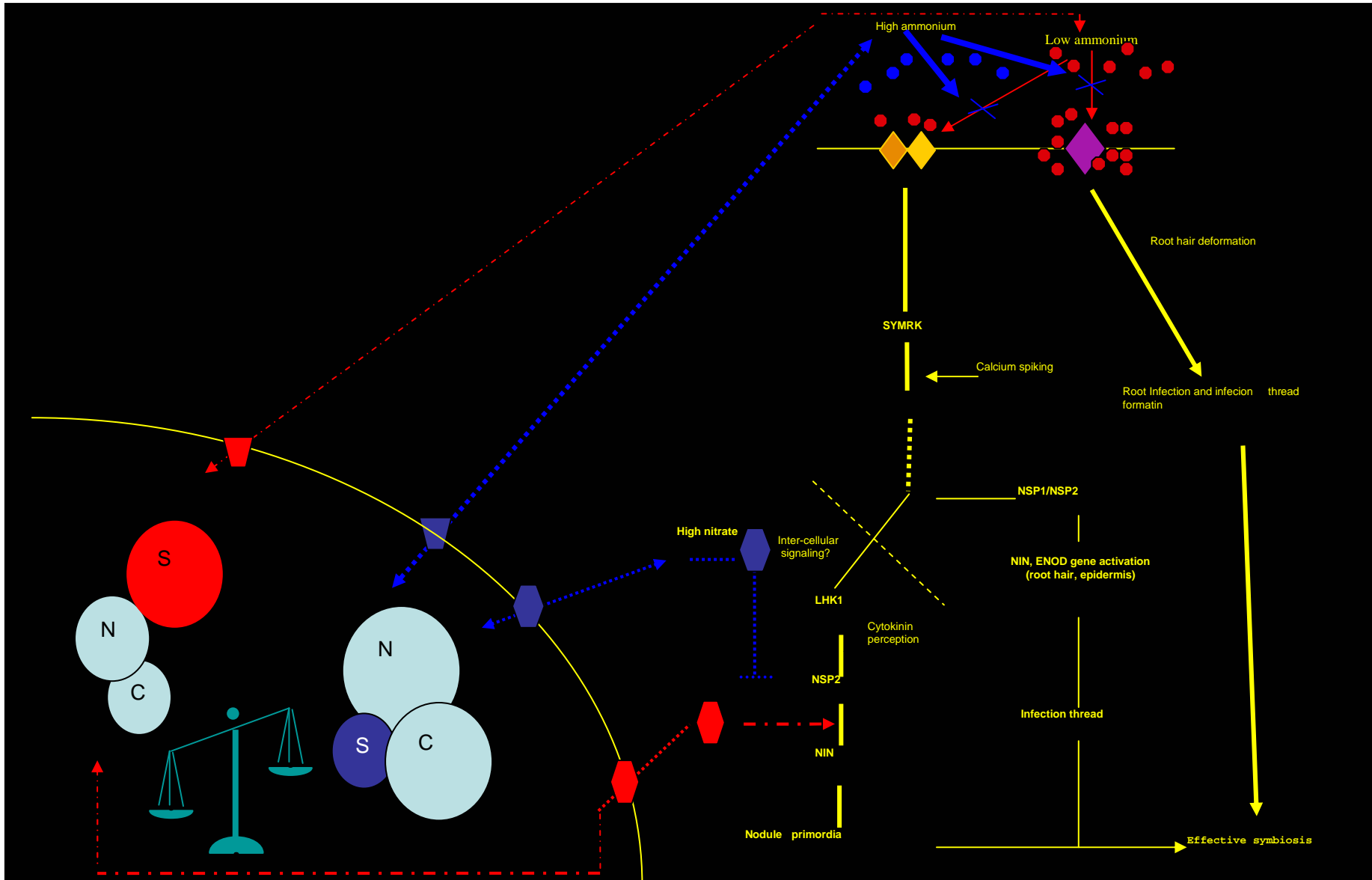
Figure 5. A Model for the N dependency of the Nod factor symbiotic signaling. This derives from the one described by Barbulova *et al.,* (2007). The Nod Factor Binding lectin (violet rhombus) expression is inhibited by high ammonium concentration. In the presented model NFBL acts independently by NFR1 and NFR5 Nod factor receptors orange rhomboids). The extra and/or intracellular concentrations of ammonium could precisely drive the inhibitory pathway (blue color). We also represented the possible imbalance of the C/N ratio in low combined N sources that leads to the reduction of the C metabolic demand with a possible feed back on the N metabolism till reaching the homeostasis C=N. And hence in the case of the leguminous plants, in condition of N increasing, where the N/C pool is enhanced, is induced a change in the plant nutritional status that is sensed by a master regulator (MR) and transduced to the symbiotic machinery. In this model we represent the transporters as key sentries in this physiological mechanism (hexagons = NO_3 transporters; semi hexagons = NH_4^+ transporters) that could work under N deficiency (red color, permissive pathway) or N excess (blue color, inhibitory pathway). S circle = symbiotic fraction of the genetic background. N and C circles Nitrogen and

IV. Materials and Methods

A. Common protocols and tools
A.1. Seeds sterilization and germination

Before germination *Lotus japonicus* seeds were sterilized with 2.5% Sodium hypochlorite supplemented with 0.05% Triton-X100. Seeds were gently shacked into this solution for 20 min. Then they were washed with sterile H_2O under laminar horizontal flow and stored up side down at 4C in sterile water in dark for 24H. Thereafter, they were transferred on plant agar (1%) Petri dishes and put again at 4C in dark for 24C. The day after the Petri dishes were transferred in growth chamber at 23 C for one more 24H covered with aluminum paper to maintain dark, necessary for germination. Finally roots of germinated seedlings were adjusted and the Petri were positioned vertically in growth chambers at 23 C under 16 h photoperiod and light intensity of 246 $\mu E\ s^{-1}\ m^{-2}$.

A.2. RNA extraction

The *Lotus japonicus* RNA extraction was carried out using a home made protocol (Modified Kistner and Matamoros (2005) protocol). Twenty to 30 mg of plant tissue were separated into two parts (shoot from root) in different 2mL eppendorfs and maintained briefly in liquid/solid nitrogen. Then, samples has been either stored at -80C or immediately squeezed by tissuelyzer (5-8 min at 30 Htz) into 550 µL of pre-warmed (65 C) RNA extraction buffer (CTAB 2%; PVP 2% (MW 360,000); Tris-HCl 100 mM; EDTA 25 mM ; NaCl 2M; to be autoclaved) supplemented with DEPC 0,01% and β-Mercaptoethanol 2%. After a quick spin into micro-centrifuge, 550µL of Phenol-chloroform-isoamyl-alcohol were added. The samples were vortexed and centrifuged (13,000 rpm) in cold room during 10min. The supernatant was carefully recovered and the last operation was repeated a second time. The second supernatant was recovered and transferred into new eppendorfs containing *v/v* (~ 450 µL) isopropanol. After a very brief vortexing, gentle mixing of the RNA extract was performed at room temperature time to time during 10 min. A final centrifugation in cold room is performed (13000 rpm) to precipitate the RNA. The pellet was, subsequently, washed with 100-200 µL Ethanol 15% without breaking it and re-centrifuged 5 min at max speed. The samples were dried by vacuum manifold or safely under office light for 15 min. Pellets are dissolved in
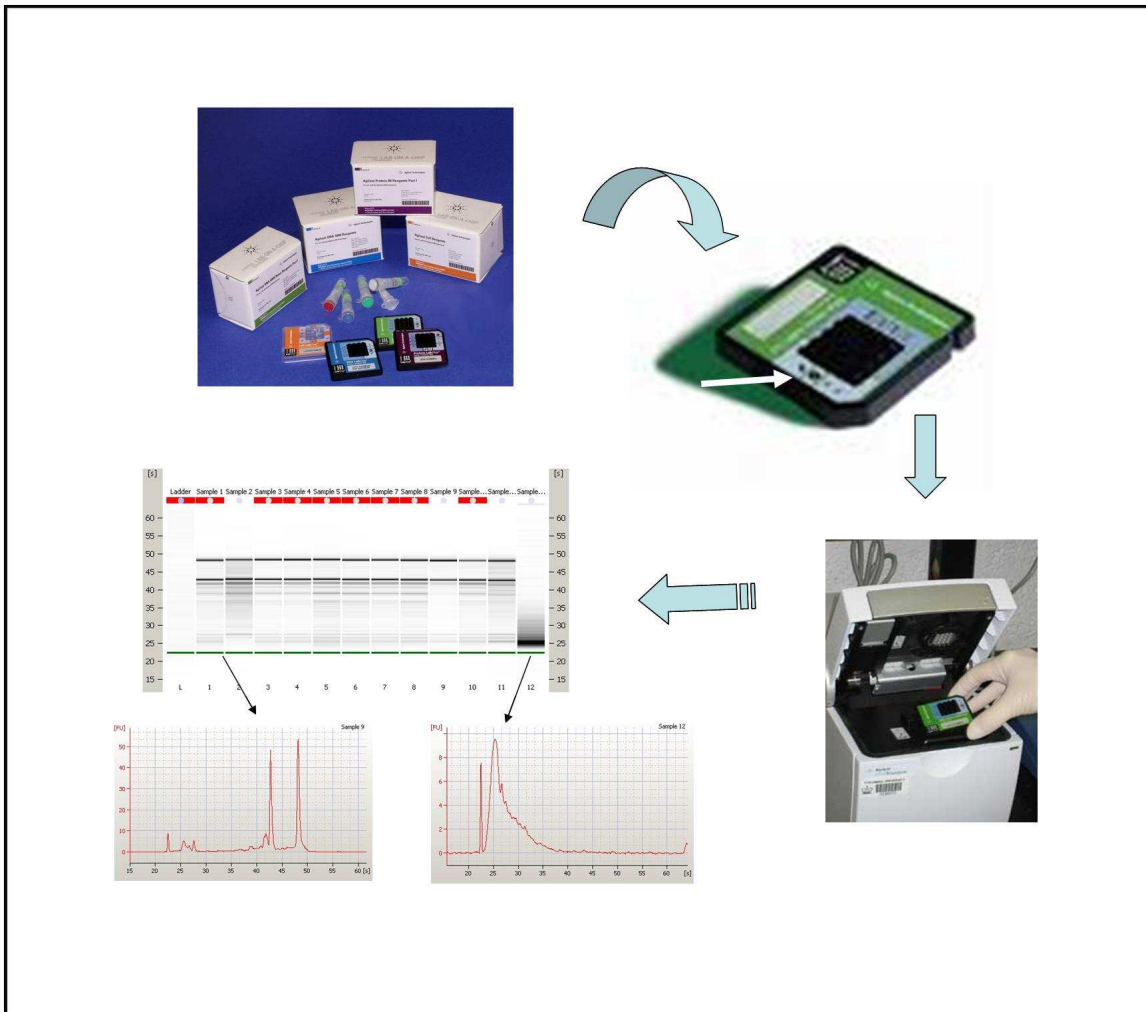
Figure 1. RNA quality checking by Bioanalyzer. All the reagent are provided in Lab on chip by the Agilent Tech. company. Arrow indicates the wells hosting the sample. Then the chip is inserted into the bioanalyzer compartment. The software (Agilent 2100) provided a picture of the RNAs sample gel running as well as the fluorescent spectral profile and so giving visual indication on their respective qualities. On the right of the gel a degraded sample showing bad fluorescent spectral profile while, on the left, the ideal spectral profile showing a major pick for the 28S (second pick starting form the left side of the picture) band compared to the 18S ribosomal RNA form. All the RNA forms revealed in the gel are aligned against an RNA progressive degradation spectrum database (Eucaryotic or Procaryotic RNA database) that allows comparing the samples and evaluating the level of degradation.

Rnase free water (could be DEPC water) in a volume that allows its total dissolution. Samples are stored for a short period in -20 C or at -80 C for long period.

A.3. RNA quantification and integrity checking

The RNA was quantified by NanoDrop spectrophotometer (ND-1000). Just a single drop of 1.5 µL taken directly from the samples was loaded on the receptacle laser cell to provide an information on the concentration (ηg/µL) as well as the absorbance ratio 260/230 and 280/260 that must be around 2.0. In the array experiment (see in result chapter-§A.1.6.) the absorbance was also checked at 650 ηm to verify the correct incorporation of the labeling (Cy5 fluorophores). For the array experiments quantification was checked by a bench spectrophotometer (quartz cuvettes) diluting 35 times the sample into TrisHcl-EDTA (1X, pH 8).

The RNA integrity check was performed by an electrophoresis running of 300 ηg RNA sample on agarose 2% Ethidium bromide pre-stained gel. Only the RNA samples used for the combimatrix array gene chip experiments were subjected to an integrity check by bioanalyzer as follow (figure 1):

- Fill the compartments of the gel chip with sterile water (300 µl) and then clean them by vortexing the chip during 10 s;

- Inject 9 µl of the pre-stained gel (bioanalyzer) into the G (black circle) well using the specific syringe;

- Inject in the two G wells 9 µl each as well as the Ladder in its designed well;

- Load the marker into the same well in which you load just before your RNA samples (12 sample wells/chip). This marker is necessary to align your RNA bands with the ladder;

- Vortex 1 min and analyze (software) the chip (30 min run);

- The bioanalyzer software produces different files: /.Jpeg (bitmap) files in which it reports the picture of the gel, the RNA picks and /.xls (figure) that is the numerical decoding of the bitmap pick files (figure 1) and in which it especially identify the integrity number of your RNA samples according to the chosen integrity number of database. This database is a collection of RNA samples from different organisms (Eucryotes, prokaryotes…) that a differentially and progressively degraded by Rnase treatments. A coefficient of 7 is given for the ideal RNA profile.

A.4. cDNA synthesis

In the semi quantitative and/or Real time experiment, cDNAs were synthesized by the support of the QuantiTect Reverse Transcription (Quiagen Kit). One-0.5µg of RNA was generally used/sample extracted. In this case the *Dnase* treatment is included at the beginning of the cDNA synthesis procedure while only for the array experiments the RNA samples were treated with *Dnase* (ambion kit) before to initiate the cDNA synthesis (see § A.1.6).

A.5. Semi-quantitative & Real time PCR transcript analysis

RNA was extracted quality checked and quantified as described previously. Semi quantitative PCRs is performed taking as internal standard the *Ljubiquitin* gene (housekeeping gene). Gene amplifications were carried in 25 µl final volume of 0,25 mM dNTP, 2,5 mM MgCl2 (Euroclone), Buffer 1x (Euroclone), Taq 0,2 U (Euroclone).

The PCR program used for the amplification was the following: 94° C for 4 min. 25 cycles of 94°C/45 sec., 57°C (for LjAMT1;1, 1;2, 1;3 and LjGS1) or 61° C (for Ljubiquitin), 72° C/40 sec.

The set of primers used for each gene are:

LjUBI F-1 5' TTCACCTTGTGGCTCCGTCTTC 3'

LjUBI R-1 5' AACAACAGCACACACAGACAATCC 3'

LjAMT1;1 F 5' AGCG CCTATGATTCAGGCAAC3'

LjAMT1;1 R5' TACTCCTCCTTGGCGAATAGC 3'

LjAMT1;2 F 5' AAAGCCTACGGTAACAACGGC3'

LjAMT1;2 R5'ATTAACAACCCGTACGGCCTC 3'

LjGS1 F 5'TGC CAAGGTTTTCGACCATC 3'

LjGS1 R5'CCTACTGAAGGGCCACTTG 3'

Notice: ***Primer pairs for the P450 cytochrome as well as for the putative Deoxycyclate desaminase are not shown (Confidential)***

All the PCR products were run on 1.5% agarose gel electrophoresis and Typhoon scanning gels was performed.

Once the semi quantitative PCR gave us the expected result for our RNA biological replicas and their respective cDNA, a Real Time qPCR was performed on the samples to have a statistical reproducibility of the technical procedure of our cDNA amplification. The real time allows 3 technical amplification of the same cDNA sample. Besides, the Real time provides a more accurate assessment of the real quantities of your transcript than that given by a typhoon gel scanning of the incorporated fluorescent molecules of Ethidum bromide in the transcript band.

The Real time transcript quantification is based on the following tools and components:

- Use sets of primers that amplify only short products 50-100 bp (see Primers sets for real time) generally the

- The Real Time PCR is performed in Engine Opticon 2 (MJ Research, Boston).

- The Real time reaction is performed the Syber green dye to quantify the fluorescence and the internal housekeeping 18S Ribosomal RNA Primer-Competimer with ratio 1:9.

- The reaction program used is 13 min at 95 C denaturation, 35 cycle X [95 C/20 min ; Tm 60 C/15 min; 72 C 15]

Thus, the real time procedure provides from each single template a clean amplicon. The reaction follows an exponential increment of the amplicon that incorporates during each amplification cycle a fluorophore. The fluorescence is immediately quantified by a laser cell whilst the software Opticon Monitor Analysis version 2.01 (MJ Resaerch) gives for each cycle the curve of its respective amplicon. A melting curve could be determined indicating the absolute expression of your transcript before the saturation (melting of all the curves). The amplification reaction is achieved once the sigmoid shape of the curves is lost indicating the depleting of the template (saturation point). The numerical quantification is determined by the calculation of the CT value of your gene which is the absolute value reached at the cycle having the highest increment of amplification before saturation. The expression of your amplicon is determined relatively to the expression of the control amplicon (housekeeping gene).

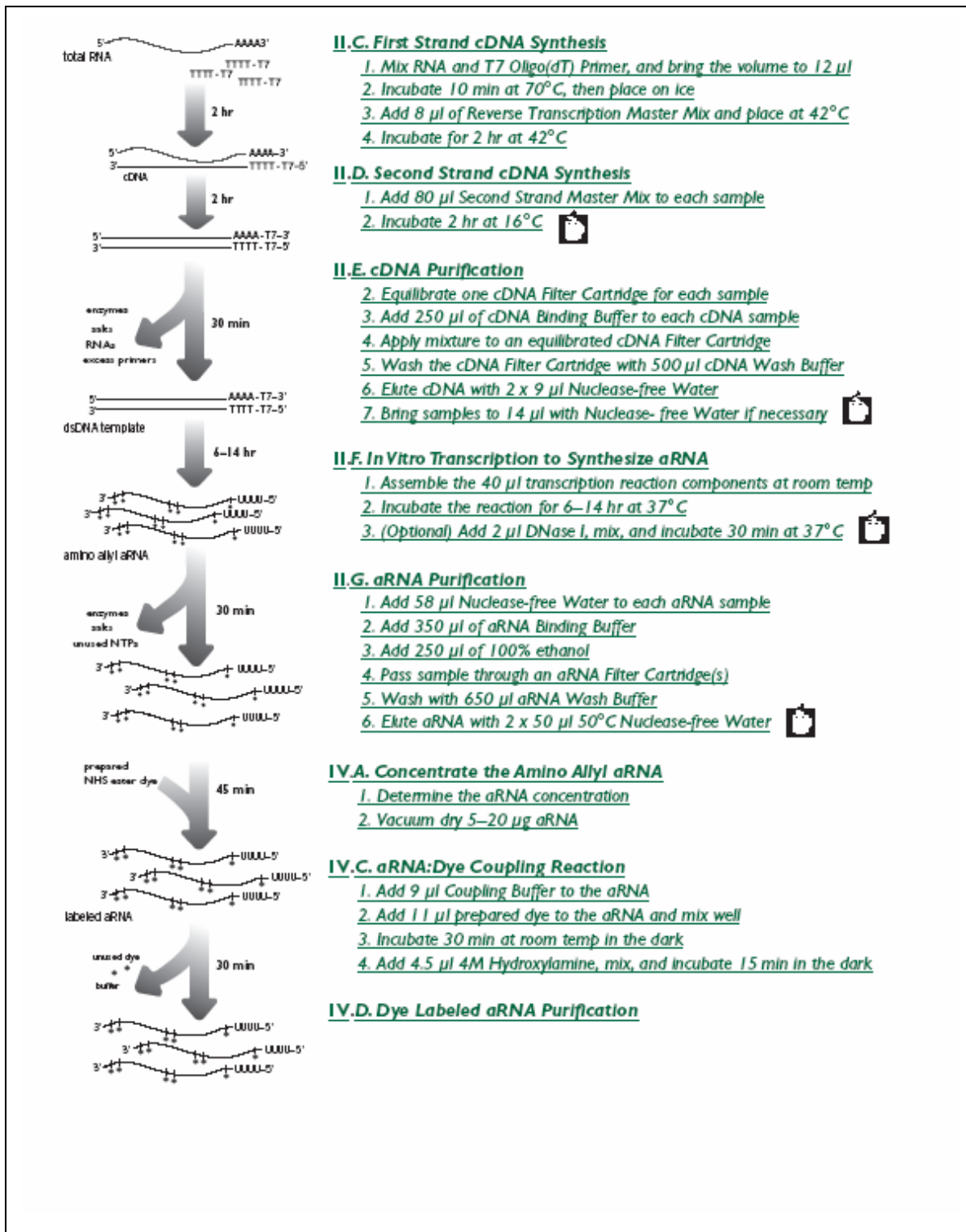*The calculation is: $2^{-\Delta CT}$, with $\Delta CT = C_{t\,gene} - C_{t\,housekeeping}$.*

II.C. First Strand cDNA Synthesis
  1. Mix RNA and T7 Oligo(dT) Primer, and bring the volume to 12 µl
  2. Incubate 10 min at 70°C, then place on ice
  3. Add 8 µl of Reverse Transcription Master Mix and place at 42°C
  4. Incubate for 2 hr at 42°C

II.D. Second Strand cDNA Synthesis
  1. Add 80 µl Second Strand Master Mix to each sample
  2. Incubate 2 hr at 16°C

II.E. cDNA Purification
  2. Equilibrate one cDNA Filter Cartridge for each sample
  3. Add 250 µl of cDNA Binding Buffer to each cDNA sample
  4. Apply mixture to an equilibrated cDNA Filter Cartridge
  5. Wash the cDNA Filter Cartridge with 500 µl cDNA Wash Buffer
  6. Elute cDNA with 2 x 9 µl Nuclease-free Water
  7. Bring samples to 14 µl with Nuclease- free Water if necessary

II.F. In Vitro Transcription to Synthesize aRNA
  1. Assemble the 40 µl transcription reaction components at room temp
  2. Incubate the reaction for 6–14 hr at 37°C
  3. (Optional) Add 2 µl DNase I, mix, and incubate 30 min at 37°C

II.G. aRNA Purification
  1. Add 58 µl Nuclease-free Water to each aRNA sample
  2. Add 350 µl of aRNA Binding Buffer
  3. Add 250 µl of 100% ethanol
  4. Pass sample through an aRNA Filter Cartridge(s)
  5. Wash with 650 µl aRNA Wash Buffer
  6. Elute aRNA with 2 x 50 µl 50°C Nuclease-free Water

IV.A. Concentrate the Amino Allyl aRNA
  1. Determine the aRNA concentration
  2. Vacuum dry 5–20 µg aRNA

IV.C. aRNA:Dye Coupling Reaction
  1. Add 9 µl Coupling Buffer to the aRNA
  2. Add 11 µl prepared dye to the aRNA and mix well
  3. Incubate 30 min at room temp in the dark
  4. Add 4.5 µl 4M Hydroxylamine, mix, and incubate 15 min in the dark

IV.D. Dye Labeled aRNA Purification

Figure 2. Flow chart of the CDNA synthesis procedure for the Combimatrix technology

A.6. Amplification of the RNA samples for the Combimatrix

1 µg of a quality checked RNA sample was amplified as follow (*in* figure 2):

1. *First strand cDNA synthesis* is primed with the T7 Oligo(dT) Primer to synthesize cDNA with a T7 promoter sequence by reverse transcription.

2. *Second strand cDNA synthesis* converts the single-stranded cDNA with the T7 promoter primer into double-stranded DNA (dsDNA) template for transcription.

3. *cDNA purification* removes RNA, primers, enzymes, and salts from the dsDNA that inhibit in vitro transcription.

4. *In vitro transcription* with aaUTP generates multiple copies of amino allyl modified aRNA from the double-stranded cDNA templates; it is the amplification step.

5. *aRNA purification* removes unincorporated NTPs, salts, enzymes, and inorganic phosphate to improve the stability of the aRNA and facilitate NHS ester coupling or subsequent enzymatic manipulations.

6. *Dye coupling reaction* takes place between the amino allyl modified UTP residues on the aRNA and amine reactive dyes.

7. *Labeled aRNA purification* removes free dye and exchanges the buffer with Nuclease-free Water.

A

Semiconductor → Addressable microelectrodes → Porous Reaction Layer → 12469 TCs

B

Hybridization and Imaging of CustomArray™ 90K Workflow

Target Preparation: **RNA** or **DNA** (user chooses kit): **Biotin** or **Fluorochrome** Labeling	1-3 days
Pre-hybridization / **RNA** Fragmentation (**RNA** targets only)	40 min (10-15 min hands on)
Hybridization	4 – 16 hours (10 min hands on)
Hybridization Washing	30 min
Biotin-labeled Targets: Post-hybridization Blocking, Labeling, and Washing — 60 min (20 min hands on) — **Fluorochrome**-labeled Targets	
Final Washing	15 min
Imaging	10 min

Figure 3. A. TC synthesis. 12469 available TCs (Tentative consensus sequences) were retrieved form the *Lotus japonicus* Tiger database (free web access). The TCs sequences are synthesized on a semiconductor chips that addresses through its electrodes the nucleotides in the desirable TC sequence order. The firsts nucleotides are attached on a Porous Reaction Layer (PRL) and then the synthesis continue forming a virtual flask. **B.** Flowchart of the combimatrix procedure (consider that we do not use the Biotin labeling for our samples). The used Dye was the Cy5. The hybridization are performed on the chip that is enclosed into the hybridization cap (small picture)

A.7. Combimatrix chip for transcript analysis:

The purified labeled aRNA is quantified by spectrophotometer (RNA is quantified at λ_{260nm} while the incorporated Cy5 is quantified at λ_{650nm}). Usually, 1-5 µg labeled RNA are used per hybridization. In our case we used 4µg. The hybridization procedure consists of putting the hybridization mix (see reagent solution) containing your labeled RNA sample in contact to the semi conductor on which the TCs were synthesized (figure 3A).

Different steps are necessary to achieve the protocol (in figure 3 B):

- **Start the pre-hybridization procedure:**

During this step the surface of the semi conductor hybridization CustomArray™ 90K chamber was filled with a pre-hybridization solution (see reagent for array hybridization). Then put in a preheated (65 C) incubator on an adapted rotisserie support rotating at 3 rpm during 30 min. This pre-hybridization is recommended to block non-specific binding of target on the TCs.

- **RNA fragmentation procedure:**

During the pre-hybridization, the labeled RNA samples are fragment using an RNA fragmentation solution. Generally 2-8 µg RNA (4 µg labeled RNA in this experiment) could be mixed to this solution that is incubated at 95 C for 20 min then placed on ice. The fragmentation solution produces 50 to 200-base fragments. this works best to maximize binding specificity and detection sensitivity.

- **Hybridization:**

All the fragmentation solution containing the different RNA labeled fragments is mixed to the hybridization solution and denatured at 95 C during 3 min. Then, the mix is filled into the hybridization chamber at the place of the pre-hybridization solution. The CustomArray™ 90K is then put at the desired hybridization temperature (see table) rotating (3rpm) during 16h.

- **Hybridization washing:**

This step is very important to eliminate the excess of fluorescence and the hybridization mix that could interfere with the real hybridization signal during the scanning.

Different washing steps are required from the most stringent washing to the less stringent one (as described in table below):

first a washing step with the 6X SSPET wash solution preheated at 50 C and let rotate in the rotisserie 65 C for 5 min. Then 6 washing (with one 1 min gapes between washings; put the CustomArray™ 90K in dark) using the 3X SSPET, followed with 3 washing with 0.5X SSPET and finally a washing with 1X PBST solution and let stay the CustomArray™ 90K in PBS (1X) in dark before the chip imaging. Otherwise it can be stored in PBS (1X) if desired for up to 1 month.

Step	Solution	For 10 ml
6X SSPET Wash	6X SSPE, 0.05% Tween-20	3 ml 20X SSPE 50 µl 10% Tween-20 6.95 ml Nuclease-free water
3X SSPET Wash	3X SSPE, 0.05% Tween-20	1.5 ml 20X SSPE 50 µl 10% Tween-20, 8.45 ml Nuclease-free water
0.5X SSPET Wash	0.5X SSPE, 0.05% Tween-20	250 µl 20X SSPE 50 µl 10% Tween-20 9.7 ml Nuclease-free water
PBST Wash	2X PBS, 0.1% Tween-20	2 ml 10X PBS, 100 µl 10% Tween-20, 7.9 ml Nuclease-free water
PBS Wash	2X PBS	2 ml 10X PBS, 8 ml Nuclease-free water

- **Imaging of CustomArray™ 90K:**

At the end of the washing The CustomArray™ 90K must be scanned wet using the Imaging Solution supplied. First the PBS wash solution must be emptied from the hybridization chamber and then the clip and the cap must be carefully removed from the CustomArray™ 90K. The imaging solution has to cover all the surface $1cm^2$ of the semiconductor and covered (without bubbles) with an appropriate coverslip. The coverslips provided with the CustomArray™ have been specifically designed to retain the Imaging Solution without contacting the microarray surface. Do not use a standard coverslip with CustomArray™ 90K.

The customarray is inserted into the scanner (scannarray 4000 XL) and scanning is set up with scanarray express software for imaging with a PMT (photo-multiplier tube) value around 60-65 as well as the laser intensity (633). This was made to have, more or less, the same intensity on all the scanned CustomArray™ 90K gene chips.

Note the chip could be used for no more of 3 times after stripping the first hybridization

(Stripping protocol not shown in this manuscript).

A.8. Strains

A.8.1. Bacteria

DHα5: cells for heat shock either electro-competent transformation

F' Φ80*lac*ZΔM15 Δ(*lac*ZYA-argF)U169 deoR recA1 endA1 hsdR17 (rK-mK+) phoa supE44 λ- thi-1

Top 10 F': cells for heat shock either electro-competent transformation has this genotype: F'[lacI^q Tn*10*(Tet^R)] *mcr*A Δ(*mrr-hsd*RMS-*mcr*BC) Φ80*lac*ZΔM15 Δ*lac*X74 *rec*A1 *ara*D139 Δ(ara-leu)7697 *gal*U *gal*K *rps*L (Str^R) *end*A1 *nup*G.

Bl21 (DE3): IPTG inducible cells for in vitro Recombinant protein production has this genotype: F-ompT hsdSB (rB- mB-) gal dcm (DE3)

Rhizobia W-type strain: The symbiosis island of M. Loti strain R7A is a field reisolate of strain ICMP3153 also known as NZP2238 and culture collection of these strains may differ by the presence or absence of a plasmid. Strain R7A lacks plasmids (Jarvis *et al.,* 1982, Sullivan *et al.,* 1995). The R7A strain is rifampicin resistant an display a Nod(+/-) Fix- phenotype in the infected roots.

Rhizobia Lac Z strain: another derivative of the M. Loti wild type strain. It is known as NZP2235. It carries a hemA::LacZ reporter gene allowing the visualization of the infection thread formation during the root hairs rhizobium process.

Rhizobia GFP and CFP strains: Modified R7A strains expressing enhanced green as well as red (cyanine) fluorescence. The plasmids carrying the GFP and CFP cassettes are respectively the pMP2464 and pMP4516. These strains were used to detect the root/root hair rhizobia colonization and the IT formations by confocal microscopy (Zeis and Leica instruments). These strains are described in Struuman *et al.,* (2000). Both plasmids carry the Rifampicin and gentamicin resistance.

A.8.2. Yeast

The yeast strain cdc25-2 used for the Reverse Ras Recruitment system is able to grow at the permissive temperature of 24 C but unable to grow at 36 C because of mutation in the monomeric G protein: Ras guanyl nucleotide exchange factor. A schematic diagram describing the bases of the method is shown in figure reported in § B.2.3.

The cdc25-2 genotype is mating type "a": ura3 trp1 leu2 ade2 his3 ras1::URA3

The yeast strain ΔMep1, 2, 3 (31019b) is unable to grow on media with less than 5mM ammonium source (generally NH4SO4 is used) because of a triple mutation in the membrane permease ammonium transporter genes Mep1, 2 and 3 aborting the uptake of the NH4+. This strain is used to evaluate the functionality of the construct carrying the full length ammonium transporters sequence of Lotus japonicus. This ultimate complementation allows the growth of the yeast strain in limiting NH4+ media.

The ΔMep1, 2, 3 genotype is mating type "a": ura3, Mep1Δ Mep2Δ leu2 Mep3Δ::KanMx2

The control strain to verify the succeeding of the complementation is the wild-type Σ1278 mating type "α".

A.9. Vectors

A.9.1. Gateway

pCR 2.1 vector from TA cloning kit (Invitrogen) is used for most of the cloning programs needing a the sequence checking of the insert before to be sub-cloned into the vector of interest. This vector contains: (1) Lac promoter allowing bacterial expression of the LacZα fragment for α complementation (blue white screening) (2) lacZα fragment encoding the first 146 amino acids of β-galactosidase. Complementation in *Trans* with Ω fragments active galactosidase for blue-white screening. (3) Double resistance: kanamycin and ampicilin. (4) pUC origin allowing replication, maintenance and high copy number. (5) T7 promoter and priming site allowing *in vivo* and *in vitro* transcription of antisens RNA and sequencing of the insert. (6) M13 Forward (-20) and M13 Reverse priming sites allowing the amplification of the insert for the sequencing. (7) f1 origin Allowing rescue of sense strand for mutagenesis and single strand sequencing.

A.9.2. Plant transformation constructs

Promoter AM1.1::GUS fusion was made using two different lengths of the promoter region inserted into pB101.1 sharing the Kanamycin Resistance as well as the Hygromicin cassette and the *A tumefaciens* ORF contruct :

- A 1198 bp (from the ATG) fused to the GUSa cassette
- A 250 bp (from the ATG) with the same GUSa fusion.

A.9.3. Protein-protein interaction vectors

Two kinds of constructs depending on the nature of the experiment

a/ *in vitro* experiments : Ni+ column-pull down

The pET-22b(+) construct carrying the c-terminal tail of the LjAMTs genes this construct shares an N terminal *pelB* signal sequence for potential periplasmic localization, plus optional C-terminus His-tag sequence immediately right after the polylinker site. The vector carries the ampicilin resistance cassette. A high-level expression of the DNA pieces of interest inserted into the polylinker cloning site is produced by the T7/*lac* promoter. Thus, the T7/*lac* promoter contains a *lac* operator sequence immediately downstream of the strong T7 promoter for additional regulation of basal expression.

b/ _in vivo_ experiments : Y-2-Hybrid-_RRRsystem_

The used bait vector was the p450-Met25::ΔBamHI (Figure) carrying the Met mutation promoter for the induced expression of the insert in medium lacking methionin, the Leucine selective amino acid marker for the yeast growth, a bacterial origin of replication and bacterial resistance cassette to the ampicilin and the polylinker site.

The pUra-Ras plasmid under the control of the yeast Gal1 inducible promoter under + Galactose condition and repressed under + glucose growth condition is used for the prey inserts. The plasmid carries the mutated RAS gene (600 bp) right next the polylinker site. It shares the Ampicilin resistance cassette and a bacterial origin of replication.

A.10. Transformation procedure

A.10.1. Bacterial transformation procedure

a/ Heat shock transformation:

Centrifuge the vials containing your mix DNA reaction (Ligase, plasmids…) meantime the -80 C frozen competent cells were thawed on ice for 15 min. The ligase or the construct of interest was added to the competent cells and let other 15 min on ice. The transformation mix was then transferred for 42 s into a preheated water bath at 42 C. The transformation mix was then immediately thawed on ice and 1mL of TY, LB or Soc without antibiotic. The mix was then transferred for 1 hour in a water bath preheated at 37C. Finally cells were plated on the appropriate medium supplemented with the appropriate antibiotic.

b/ Electro-transformation:

The vials containing the DNA reaction was briefly centrifuged (an unsalted DNA or a limited volume~ 1µl). The electro-competent cells (Top 10 F') were thawed in ice during 15 min and the transformation cuvettes were also cooled down on ice. The Cells supplemented with the clean DNA were added to the cuvette under vertical laminar flow. Immediately after electroporation the SOC was added to the electroporated cells.

A.10.2. Plant transformation procedure

The flowchart is undertaken as follow:

1. Pre-culture: the roots must be enough long but still young in terms of tissue quality. A pre culture after germination of the seedlings during 10 days is necessary then transfer them for 5 more days after

separating them from the shoot medium on CIM medium to bring them enough thick. The CIM, callus induction medium induce callogenesis;

2. Infection: cut the roots in small pieces (0.5 cm) and let them 10 min into the *A. tumefaciens* liquid of growth and squeeze them from time to time using forceps;

3. Co-culture: transfer the explants on fresh CIM medium supplemented with 200 mg/L Cefotaxim and 15 mg/L hygromicin and 3% sucrose for 48 hours;

4. Wash the explants with sterile water and dry them on paper filter before to transfer them on selective CIM medium supplemented with 200 mg/L Cefotaxim and 15 mg/L hygromicin and 3% sucrose;

5. Incubation: Incubate the plants in growth chamber (16H photoperiod; 23 C) 3 to 4 week until green callus are formed. Generally the green callus is formed on the surface of the explants;

6. Transfer on SIM (shoot induction medium supplemented with 200mg/L Cefotaxim, 15mg/L Hygromicin, 0.5 mg/L TDZ (Thidiazuron phyto-hormon) and 3% sucrosee) only the green calli that indicates the potential success of the transformation procedure since they are resistant to the Hygromicin by contrast to the rest of the white-necrotic untransformed tissues. This step requires 15 days before the rising of the shoot primordial. Then transfer the shoot on SIM medium containing 200 mg/L cefotaxim, 10 times less TDZ (0.05 mg/L) and 3% sucrose;

7. Transfer the shoot primordia on SEM supplemented with 200 mg/L cefotaxim and 1% sucrose by dissecting them carefully from he rest of the tissue. This step requires 15 days to obtain sufficient shoot lengths allowing their easy separation form the rest of the callus;

8. Shoots are transferred on RIM (Root induction medium). This consents the root organogenesis in the basal cut part of the shoot. 10 days are required to obtain roots;

9. The small regenerated potential transformants are transferred on REM (root elongation medium) for one more week before to be transferred in ground.

From the roots to the new transformant 3 months are needed and other 4 are usually necessary before the flowering and the first mature pods (containing T1 seeds) harvestings.

A.10.3. Yeast transformation procedure

This protocol was either used for the ΔMep1, 2, 3 strain complementation or for the cdc25-2 single and double plasmid transformation. Only the selective media as well as the cell optical density and the growth temperature could be changed from an experiment to another (see specific protocols in §.B.):

1 A single colony is grown over night in 2 to 4 mL YPD medium (temperature depend on yeast strain);

2 The $OD_{\lambda 600 \eta m}$ is read and dilution is made for a subsequent re-growth ensuring 4 cell division cycles. (e.g. dilute to $OD_{\lambda 600 \eta m} = 0.15$ (10^6 Cs/mL) and rich $OD_{\lambda 600 \eta m} = 0.6$ (6×10^6 Cs/mL) or dilute to $OD_{\lambda 600 \eta m} = 0.5$ (5×10^6 Cs/mL) and rich $OD_{\lambda 600 \eta m} = 2$ (2×10^7 Cs/mL)

3 After re-growth plate and/or dots 100 µL onto Two YPD medium (This to check the number revertants in case of cdc25-2 strain (number has to be < 10 colonies)), otherwise proceed immediately to the pelting of the cells as follow:

- Centrifuge 5 min at 2500 rpm take out the supernatant and re-suspend the cells in sterile water (half initial growth volume) or in 1/10 initial volume of LiSorb (100mM LiAc, 1M Sorbitol in 10mM Tris-HCL, 1mM EDTA pH 8) and re-centrifuge again (same initial settings);

- Take out the supernatant and re-suspend the cells in 1/10 initial volume of TE/LiAc (freshly prepared) or 1/10 initial volume of LiSorb and centrifuge (same initial settings);

- Take out the supernatant and re-suspend the cells in 50µL TE/LiAc (or 100 µL LiSorb) x number of transformations; Let rotating if using LiSorb (3rpm; 30min) ;

- Prepare extemporarily for each transformation 2mL eppendorfs containing 1 µg of the plasmid carrying the specific construct, 50 µg Salmon sperm DNA (denaturized at 95 C during 10 min), 33% PEG/TE/LiAC (in final mix) and finally add the cell volume to this mix. In the case of the cells re-suspended in LiSorb add 100µg Salmon sperm (denaturized at 95 C during 10 min), 33% LiPEG.

- Let the tube shaking at 220 rpm (or rotating) at the permissive temperature of growth during 30 min.

- Start immediately to the heat shock reaction 42 C during 10-15 min (depends on the strain if TS strain reduces the time to 10 min). In the case of the cells re-suspended in LiSorb and LiPEG add 100 µl DMSO before the heat shock.

• Put the samples quickly in Ice and start washing procedure the aliquots re-suspendend in LiAC and LiPEG centrifuge while for that of the resuspend in 100 µl 1M sorbitol before plating an aliquote or the total volume on the appropriate medium of growth/selection

• Washing steps if requested:

      - Add 1.5 mL sterile water and centrifuge 5 s;

      - Resuspend in 2mL sterile water and centrifuge 6 s;

      - Repeat the washing with 2mL sterile water and then re-suspend in a final volume of 1mL and plate an aliquot of 100-50µl

Note that the protocol using the sorbitol, LiSORB and the LiPEG was preferred to the LiAC and LiACPEG when cdc strain was used. This, indeed, allows a highest efficiency of success in terms of colony growth.

The efficiency of transformation =number of colonies (transformants)/1µg construct/10^8 cells

A.11. Rhizobium infection

The chosen Rhizobia strain is inoculated from the -80 C stock into 5 mL TYR (CaCl2) supplemented with the appropriate antibiotic (Rifampicin for wild type strains) and let grow for 2 days (rotation) at 30C. Cells were harvested at 4000 rpm, 4 C during 10 min and washed with PBS (1X) before to be centrifuged again (same settings). The optical density was checked at 600 ηm and 10^7cells/20µL are loaded at the level of the root susceptible infection zone

A.12. Gus staining revelation

The protocol was used to unravel the activity of the *gusA* cassette that provides a tissue localization and if desired a quantification of the promoter part activity of the gene of interest. Entire seedlings or organ parts (shoots/roots parts) or even pieces of leaves coming from the transgenic plants expressing the GUS cassette were used. Those plant materials were placed into 2mL eppendorfs containing the GUS staining solution Mix : Buffer Phosphate 100mM (NaPO4) , pH 8.0, X-Glucorinidase 1mM (dissolved in dimethylformamid) and 0.01% Triton-100X. The eppendorfs were placed under vaccum for 10 min then the sample are incubated in dark over night at 37C. The day after the sample could be either taken to be analyzed under microscopy or let one more day in dark at 37 C. To reveal weak coloration in shoot part, a post treatment of the sample with Ethanol 100% is necessary to eliminate the green color chlorophyll.

A.13. Lac Z staining revelation

To obtain the blue stained tissue allowing the clearly discrimination of the infection threads, the procedure was performed as follow:

- The infected roots are washed in 2mL eppendorfs containing sterile water and slowly rotating for 30 min;
- A second brief Washing of the infected roots is made with buffer Phosphate 50mM; pH 7.2;
- Before the revelation Fix the tissue proteins with a fix solution 1% (v/v) para-formaldehyde, 0.3 M Mannitol dissolved in Buffer phosphate 50 mM; pH 7.2) for 1 h;
- Wash again the roots with phosphate 50 mM; pH 7.2;

Proceed to the staining by immerging the roots into the staining solution (Buffer phosphate 10 mM; pH 7.2; 150 mM NaCl, 1mM MgCl2, 5 mM potassium $Fe^{3+}CN$ (K3), 5mM $Fe^{2+}CN$ de potassium (K4), 1% triton-100X) and put them into a vaccum manifold during 5 min

- Incubate the root tissue in dark at 37C for 5 min;
- Add 40 µg X-Galactosidase to start the revelation of the staining and re-incubate at 37 C in dark for 1 to 24 h depending on the staining revelation;
- Wash the root tissue with phosphate 50 mM; pH 7.2 to take out the excess of staining if necessary;
- Fix again with the fix solution for 1 h to obtain the final fixed staining;
- The infected root hairs and the ITs could be immediately observed by microscopy and may be conserved at 4 C.

A.14. Bacterial medium composition

A.14.1. *E. coli*

TY (1 L): 5 g Yeast extract (DIFCO); 8 g NaCl; 10 g BactoTryptone (Difco)

For solid TY add 1.5% Bacto-agar (4.5 g in 300 mL).**:**

TYR (1 L): 3 g Yeast extract (Difco); 5 gr BactoTrypton (Difco); 6 mM CaCl$_2$

A.14.2. Yeast medium composition

YPD (1L): 1% yeast extract; 2% Bactopepton; 3% Glucose

Ynb minimal Glucose medium (1L): 1.7 g Yeast nitrogen base (W/O amino acids and NH_4SO_4/ Difco 0335-15-9); 5 g NH_4SO_4 ; 20 gr Glucose; 35 g Bactoagar (Difco 0140-07-4).

Ynb minimal Galactose medium (1L) : Instead of Galactose add: 30 g Galactose (Sigma G-0750 or Serva 22020); 20 gr Rafinose (Sigma R-0250); 20 gr Glycerol

Notice: to the minimal media add the following 1:100 of 5 mg/mL stock exclude the ones that are encoded by the plasmid you transfect when you are using the RRRS screening.

Leucine (Sigma L-8125), uracyl (Sigma, U-0750), tryptophan (Sigma T-0271), methionine (Sigma, M-2893), Lysine (Sigma, L-5626), adenine (Sigma, A-3159), histidine (Sigma, H-9511). For media which includes methionine intend to suppress expression from Met425 promoter, a 4X methionine concentration (1:100 20 mg/mL methionine stock) was used.

A.15. Plant medium composition
A.15.1. Murashige and Skoog medium (MS): This medium is the bases for the SIM, the SEM medium

Micro-elements	concentration (mM)	Final Concentration (µM)
$CoCl_2 \cdot 6H_2O$	0.025	0.11
$CuSO_4 \cdot {}_5H_2O$	0.025	0.10
NaFeEDTA	36.70	0.10
H_3BO_3	6.20	0.10
KI	0.83	5.00
$MnSO_4 \cdot H_2O$	16.90	0.10
$Na_2MoO_4 \cdot 2H_2O$	0.25	1.30
$ZnSO_4 \cdot 7H_2O$	8.60	29.91

Macro-elements	Concentration (mM)	Final concentration (mM)
$CaCl_2$	332.02	2.99
KH_2PO_4	170.00	1.25
KNO_3	1900.00	18.79
$MgSO_4$	180.54	1.50
NH_4NO_3	1650.00	20.61

Vitamins	Concentration (mM)	Final concentration (μM)
Acido niconitico	1.00	8.12
Piridoxina- HCl	1.00	4.86
Tiamina HCL	10.00	29.65

A.15.2. Gamborg's B5 medium (B5)

Micro-elementi	Concentration (mM)	Final concentration (μM)
$CoCl_2 \cdot 6H_2O$	0.025	0.11
$CuSO_4 \cdot 5H_2O$	0.025	0.10
NaFeEDTA	36.70	0.10
H_3BO_3	3.00	48.52
KI	0.75	4.52
$MnSO_4 \cdot H_2O$	10.00	56.16
$Na_2MoO_4 \cdot 2H_2O$	0.25	1.30
$ZnSO_4 \cdot 7H_2O$	2.00	6.96

Macro-elements	Concentration (mM)	Final concentration (mM)
$CaCl_2$	113.23	1.02
KH_2PO_4	2500.00	24.73
KNO_3	1900.00	18.79
$MgSO_4$	121.56	1.01
NH_4NO_3	130.44	1.09
$(NH_4)_2SO_4$	134.00	1.01

Vitamine	Concentration (mM)	Final concentration
Myo-inositolo	100.00	0.56 mM
Acido niconitico	1.00	8.12 μM
Piridoxina- HCl	1.00	4.86 μM
Tiamina HCL	10.00	29.65 μM

A.15.3. Transformation media

a/ CIM (callus induction medium)

B5+ Phytohormon cocktail (3 mg/L IAA (indol acetic acid); 0.15 mg/L 2,4-D (2,4-dichloro-phenoxyacetic acid); 0.6 mg/L BA (N-benziladenine) and 0.3 mg/L IPA (N-isopentenyladenosine)) + 3% sucrose; pH 5.7

b/ SIM (Shoot induction medium)

 MS+ 0.5 mg/L TDZ (thidiazuron)+ 3% sucrose

 MS+ 0.05 mg/L TDZ + 3% sucrose

c/ SEM (Shoot induction medium)

MS+ 1% sucrose

d/ RIM (Root induction medium)

B5/2 + 0.1 mg/mL NAA (1-naphtalenic acid)+ 1% sucrose

e/ REM (Root elongation medium)

B5/2+ 1% sucrose

A.16. Analysis & Statistics

A.16.1. Phenotyping

The different measures taken to quantify the nodule number, the fresh biomasses or the length of different organs were applied on each single seedling/plantlets and then averaged according to the total number of seedlings per set of growth condition. For each single condition of growth 1 to 2 independent replicas were set up. The minimum number forming a set of seedling/plantlets per condition of growth is 8 while the maximum is 10. For all the experiments 1 to 2 extemporary replicas were performed. A final averaging upon the different replicas is performed if necessary.

A.16.2. Array

The TIF images file linked to the .txt file and released by the scanner (4100 XL) were exported to the Microarray Imager 5.8 (Combimatrix) for the densitometric analysis of the spots. A 90 K net aligned on all the spots of the chip and adjusted to tightly fit them. The densitometric analysis gave, in an Excel file, the value of the fluorescence for each single spot linked it to its own probe annotation (TC). To take out the fluorescent noise (background) the median value of the fluorescence was calculated for every chip by R program () and a box plot representation allowed the visualization of the fluorescence repartition (figure). The median was then adjusted for all the fluorescent to substract equally the noise (in figure). The fluorescence of each single probe value was extracted from the median box plots and the respective value was normalized by the centering of the data (Microarray Bioinformatics" Dov Stekel"/.pdf version web available). A SAM analysis was implemented on the centered data (type Two Clas Unpaired") for the case of the T0 vs C0 experiment and a Multiclass analysis for the tendency pattern of the time points T0 vs T6, T9 and T13 dps http://www-stat.stanford.edu/~tibs/SAM/pnassam.pdf) with a selected FDR varying between 5% and 10% depending on the analysis.

B. Specific protocols and experimental design

B.1. Plant experimental design

All the experiments were carried out with W-type *Lotus japonicus* (Regel) K.Larsen B129 F9 GIFU ecotype plants. Seeds were surface sterilized and germinated as described in § A.1. After one week, seedlings were transferred in on the different medium (Gamborg, 1970) that contain B5 basal salts (Duchefa 2007 catalogue), B5 vitamins (Duchefa catalogue 2007), pH 5.7 supplemented if necessary with Cefotaxim (200 mg/l). When seedliings were grown in solid media, 1% plant agar (Sigma, cat. #A-7921) was added to the B5 liquid media. Sucrose 1% (29mM) and Cefotaxim (200 mg/mL) antibiotic was added depending to the followed experimental design.

Important notice: All the Plant experiment designs are intentionally mentioned (or integrated) as preamble into their respective result part (See Section Results) for reader commodity and comprehension

A T7 promoter | Lac Z | cterm AMT1.1 | His Tag | Amp^R

B T7 promoter | Lac Z | His Tag | cterm AMT1.1 | Amp^R

C

```
5'CATAG (NdeI)
  /
 ATG CAT CAC CAT CAC CAT CAC  TTC ATT CTG AAT AAG ATG AA

  M   H   H   H   H   H   H
                              TTC  ATT  CTG  AAT  AAG  ATG AAG TTG CTT CGG ATC
                               F    I    L    N    K    M   K   L   L   R   I

 TCA ACG GAG GAT GAA CTT GCG GGT ATG GAT CTG ACC CGA CAT GGT GGG TTT GCG TAT GCC
  S   T   E   D   E   L   A   G   M   D   L   T   R   H   G   G   F   A   Y   A

 TAT GAG GAT GAT GAA TCG CAC AAG CCA GGG ATT CAG CTA CGG AAG ATT GAA CCT AAC TCT
  Y   E   D   D   E   S   H   K   P   G   I   Q   L   R   K   I   E   P   N   S

 TCT TCC ACT CCT AGT GCT GAG TCA TGA
  S   S   T   P   S   A   E   S   Z        GGATCC (BamHI )
```

Figure4. A. The first conformation of the Recombinant carboxylic AMT 1.1 tail using the native His tag motives present in the pET22(b+)

B. The second conformation of the recombinant carboxylic AMT1.1 tail where a His Tag motive is synthesized right after the Methionin of the recombinant protein. This conformation could be considered as the most similar to the native one since the carboxylic part of the construct is free and not bound to the Nickel as is the case of the c-Term inside of the plant cytoplasm.

C. The mutation in the DNA sequence that did not affect the amino acidic sequence.

A for G and A for concerving the Alanin aa.

B.2. Protein-Protein interaction

B.2.1. Over expression of bait protein and purification

The C-terminus of AMT1.1, AMT1.2 and AMT1.3 were cloned in pET-22b(+) vector (Invitrogen), clonings were designed to place at C-terminus of the proteins the 6xHis tag domain. Upon the three constructs only the c-terminus part of the carboxylic AMT1.1 tail in the *in vivo* conformation that liberates the N-term of the RP from the His tag (figure 4). In order to create this new RP, I was obliged to re-design the insert due to the incompatibility of the pET22 b (+) cloning sites with restriction sites present inside of the insert. Thus, I have introduced two point mutations that did not affect the amino acidic sequence of our native carboxylic tail (figure) by changing the recognition sequence of the restriction enzyme (NdeI, CATATG) used for the subcloning into the pET plasmid.

Over expression of the recombinant proteins was made in *E. coli* BL21(DE3), a typical IPTG inducible strain. After 3 hours of induction cells were harvested by centrifugation in Sorvall centrifuge (30 min; 7,000xg at 4 °C) and washed with PBS (1X). Purification was made for AMT1.1-His tag; cells were briefly resuspended in 40 mM sodium phosphate buffer pH 7.5 containing 10 mM imidazole, 1 % Triton X-100, 0.5 mM EDTA, 0.1 M benzamidine and 0.1 M PMSF. Disruption was achieved with a French Press apparatus (IBP facility), and cellular debris were removed by centrifugation (20 min; 30,000xg at 4 °C). Before loading the sample onto the Column, Ni-NTA resin (Qiagen) was added with imidazole at the final concentration of 10 mM. The column was equilibrated with 40 mM sodium phosphate buffer pH 7.5 containing 10 mM imidazole. The recombinant AMT1.1-His tag protein was purified using successive steps of washing with 10 and 30 mM imidazole, and elution was obtained between 50 and 100 mM imidazole. Protein purity was evaluated by SDS-PAGE. Only the ctem AMT1.1 tail cloned in the native conformation was further purified through FPLC to ensure the elimination of contaminants.
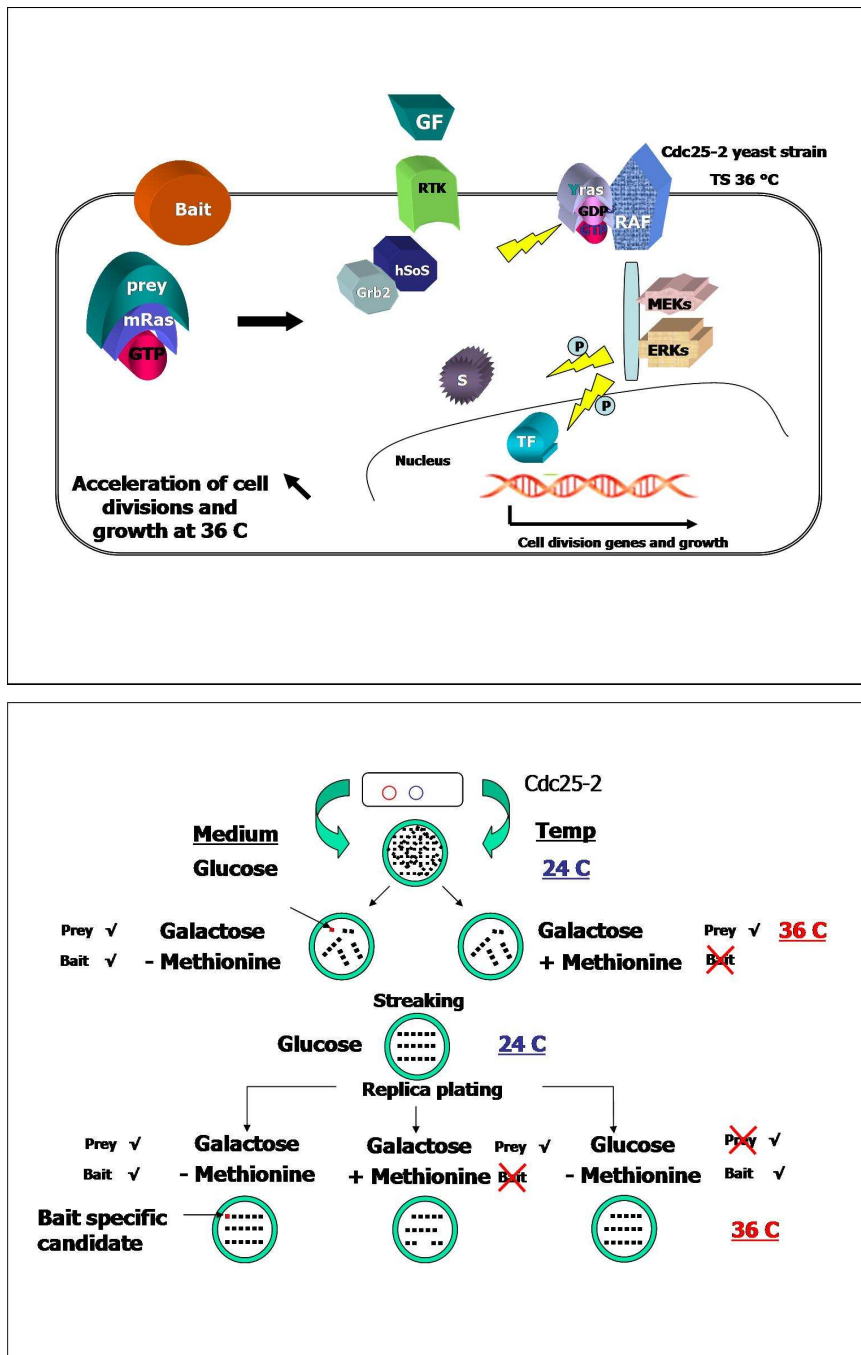
Figure 5 A. This membrane-associated two-hybrid **system** makes use of the **Ras** pathway in **yeast** (Aronheim, 1997). When localized at the plasma

membrane, the **yeast Ras** guanyl nucleotide exchange factor (RGEF) cdc25 stimulates GDP/GTP exchange on **Ras** and promotes downstream signalling events that ultimately lead to the **cell** growth. A mutant **yeast** strain harbouring the temperature sensitive cdc25-2 allele is still able to grow at 25°C but fails to grow at 36°C. However, the human RGEF (hSOS) when targeted to the plasma membrane efficiently complements the mutation, leading to **cell** growth at 36°C. In the SRS the translocation of hSOS is dependent on a protein-protein interaction:

the bait X (LjAMT1.1 in our case) is fused to C-terminally truncated hSOS, which is active but unable to target to the plasma membrane. The bait is co-expressed with a prey Y (RPS6; see results), which can either be an integral membrane protein or a soluble protein that is anchored to the membrane by means of a myristoylation signal

B. Cdc25-2 strain flowchart transformation

B.2.2 Plant extract and interaction with bait protein

Total crude extract from mature tissues of *L. japonicum*, shoot and root separately, were obtained by grounding them in liquid nitrogen. The recovered ground tissues were mixed 1 h at 4 °C in 40 mM sodium phosphate buffer pH 7.5, containing 1 % Triton X-100, 0.5 mM EDTA, 0.1 M benzamidine and 0.1 M PMSF. Crude extract was supplied with imidazole at final concentration of 10 mM and loaded onto Ni-NTA resin (Qiagen), at which previously we bind the bait protein. After washing with imidazole at 10 and 30 mM, elution of AMT1.1-His tag with putative ligand was performed at 50 and 100 mM of imidazole. As control crude extract was loaded onto Ni-NTA resin without AMT1.1-His tag bounded, and the same procedure of washing and elution were followed.

In two independent experiments we loaded crude extract from shoot and root, and we used the same steps of washing and elution. AMT1.1-His tag and ligand were revealed by SDS-PAGE and silver stain. The Bands of interest were digested with trypsin and analyzed by SELDI-TOF (IBP facility). To identify the ligand Mass Blast of the digest fragments were run on the Prosite Mass blast data base.

B.2.3. Reverse Ras Recruitment system (RRRs) screening

This protocol was initially established to screen interaction between bait membrane recruited proteins and protein produced from a cDNA library. In our case in absence of a library to screen, we used the RRRs screening to ensure that the putative interactions obtained with the *in vitro* system are confirmed *in vivo* (here *in heterologous* system; See Figure 5A).

In this experiment the protein bait protein was the LjAMT1.1 while the prey was none of the interactants fished with the in vitro procedure subcloned into the pRAS vector (EcoRI-XhoI).

The screening of interaction between known proteins is performed as reported in this flowchart (Figure 5B) :

- Following co-transformation the yeast is plated on a fresh growing amplification medium supplemented with glucose and let it grown 6-7 days at 24 C.

- With velvet replicas of the colonies was made onto two different plates, one containing Galactose without Methionine and the other containing Galactose supplemented with methionin. The plates were placed at 36 C for additional 5-7 days.

- The pattern of growth was compared between both plates and the colonies exhibiting preferential growth on the Galactose plate lacking methionine as compared to galactose plate containing methionie were picked up and plated on glucose plate –ura-leu and grown at 24 C for additional 2 days.

- A replica plating into 4 plates :

  - (1) galactose –leu-ura-met

  - (2) galactose –leu-ura

  - (3) glucose-leu-ura-met

  - (4) YPD

The colonies that grew at 36 C on plate 1 but not on plate 2, 3 and 4 could be considered as positive interactants and should be further analyzed.

The screening for co-transformed CDC25-2 colonies growing at the restrictive temperature (36° C) will be followed as described by A. Aronheim 1997.

Annex

Motifs	*LjAMT*1.1	Motifs	*LjAMT*1.2
RE: 132. AC: RSP00132//OS: Phaseolus vulgaris /GENE: beta-phaseolin, or phas/RE: vicilin box /BF: ROM1, ROM2	Motifs on "+" Strand: Mean Exp. Number 0.01572 Up.Conf.Int. 1 Found 1 536 GCCACCTC 543 (Mism.= 0)	RE: 135. AC: RSP00135//OS: tobacco,Nicotiana plumbaginifolia /GENE: cab-E/RE: AT-1 (4) /BF:unknown	Motifs on "+" Strand: Mean Exp. Number 0.02204 Up.Conf.Int. 1 Found 1 57 AAcATTTTTAcC 68 (Mism.= 2)
RE: 234. AC: RSP00234//OS: Arabidopsis thaliana /GENE: AGAMAOUS (AG)/RE: CArG Box 2 /BF: unknown	Motifs on "+" Strand: Mean Exp. Number 0.02948 Up.Conf.Int. 1 Found 1 460 GCTTGTAAAG 469 (Mism.= 2)	RE: 206. AC: RSP00206//OS: pea, Pisum sativum /GENE: rbcS-3A/RE: BOX II* /BF: GT-1	Motifs on "+" Strand: Mean Exp. Number 0.03099 Up.Conf.Int. 1 Found 1 248 GTGAGGTcATcT 259 (Mism.= 2)
RE: 285. AC: RSP00285//OS: parsley (Petroselinum crispum) /GENE: PAL-1/RE: Box P /BF:unknown	Motifs on "+" Strand: Mean Exp. Number 0.03438 Up.Conf.Int. 1 Found 1 129 CTCCAACAAACCt 141 (Mism.= 1)	RE: 231. AC: RSP00231//OS: Arabidopsis thaliana /GENE: AGAMAOUS (AG)/RE: CCAAT box 1 /BF: unknown	Motifs on "-" Strand: Mean Exp. Number 0.02833 Up.Conf.Int. 1 Found 1 12 CCAATCA 6 (Mism.= 0)
RE: 355. AC: RSP00355//OS: Oryza sativa /GENE: Rep-1/RE: GARE2 /BF:unknown	Motifs on "+" Strand: Mean Exp. Number 0.04257 Up.Conf.Int. 1 Found 1 961 TAACAGAA 968 (Mism.= 0)	RE: 235. AC: RSP00235//OS: Arabidopsis thaliana /GENE: AGAMAOUS (AG)/RE: LBS/WBS1 /BF: LFU; WUS	Motifs on "-" Strand: Mean Exp. Number 0.01925 Up.Conf.Int. 1 Found 2 78 cTAATtCAATGG 67 (Mism.= 2) 49 TTAAaCaAATGG 38 (Mism.= 2)
RE: 434. AC: RSP00434//OS: Arabidopsis /GENE: eEF-1beta/RE: TFIIIA-box /BF: TFIIIA	Motifs on "-" Strand: Mean Exp. Number 0.02224 Up.Conf.Int. 1 Found 1 774 CTaaATTGAAGAA 762 (Mism.= 2)	RE: 434. AC: RSP00434//OS: Arabidopsis /GENE: eEF-1beta/RE: TFIIIA-box /BF: TFIIIA	Motifs on "-" Strand: Mean Exp. Number 0.01014 Up.Conf.Int. 1 Found 1 520 gTGGATTGAAGgA 508 (Mism.= 2)
RE: 442. AC: RSP00442//OS: maize /GENE: cyPPDK1/RE: box b /BF: DOF1	Motifs on "-" Strand: Mean Exp. Number 0.03120 Up.Conf.Int. 1 Found 1 242 cAACTTTGCA 233 (Mism.= 1) TTTGAAACGT	RE: 471. AC: RSP00471//OS: alfalfa, Medicago sativa /GENE: MSPRP2/RE: Alfin1 BS1 /BF: Alfin1	Motifs on "-" Strand: Mean Exp. Number 0.01083 Up.Conf.Int. 1 Found 1 196 GTGTGtGGCaC 186 (Mism.= 2)
RE: 557. AC: RSP00557//OS: tomato, Lycopersicon esculentum /GENE: rbcS3C/RE: UN U2 /BF:unknown	Motifs on "-" Strand: Mean Exp. Number 0.01723 Up.Conf.Int. 1 Found 1 923 TTTTGtTTTTTTtTaTC 908 (Mism.= 3)	RE: 472. AC: RSP00472//OS: alfalfa, Medicago sativa /GENE: MSPRP2/RE: Alfin1 BS2 /BF: Alfin1	Motifs on "+" Strand: Mean Exp. Number 0.00507 Up.Conf.Int. 1 Found 1 245 AAAGTGaGGtCA 256 (Mism.= 2)
RE: 607. AC: RSP00607//OS: tomato, Lycopersicon esculentum /GENE: rbcS1/RE: AT-rich F /BF:unknown	Motifs on "-" Strand: Mean Exp. Number 0.03525 Up.Conf.Int. 1 Found 1 732 TTgGATTTgGTGATTT 717 (Mism.= 2)	RE: 474. AC: RSP00474//OS: alfalfa, Medicago sativa /GENE: MSPRP2/RE: Alfin1 BS4 /BF: Alfin1	Motifs on "+" Strand: Mean Exp. Number 0.00512 Up.Conf.Int. 1 Found 1 430 CAAGTGGTcCTt 441 (Mism.= 2)
RE: 735. AC: RSP00734//OS: Arabidopsis thaliana /GENE: CAB2/RE: CDA-1 BS /BF: DET1; CDA-1	Motifs on "+" Strand: Mean Exp. Number 0.03061 Up.Conf.Int. 1 Found 1 1105 CAAAACGC 1112 (Mism.= 0)	RE: 503. AC: RSP00503//OS: Tobacco, Nicotiana tabacum /GENE: Ntltp1/RE: D1 box /BF: Different bZIP factors, including RITA-1	Motifs on "+" Strand: Mean Exp. Number 0.00698 Up.Conf.Int. 1 Found 1 447 CTAGCTAG 454 (Mism.= 0) Motifs on "-" Strand: Mean Exp. Number 0.00698 Up.Conf.Int. 1 Found 1 454 CTAGCTAG 447

			(Mism.= 0)
		RE: 508. AC: RSP00508//OS: soybean, Glycine max /GENE: beta-conglicinin alfa'/RE: SEF4 BS /BF: SEF4	tifs on "+" Strand: Mean Exp. mber 0.02216 Up.Conf.Int. Found 1 58 aCATTTTTAcCA 69 ism.= 2) otifs on "-" Strand: Mean Exp. mber 0.02486 Up.Conf.Int. Found 1 474 cCATTTTTATaA 463 ism.= 2)
		: 522. AC: P00522//OS: carrot, ucus carota /GENE: 3/RE: E2-core /BF: DPBF- DPBF-2;	tifs on "-" Strand: Mean Exp. mber 0.02010 Up.Conf.Int. Found 1 436 CCACTTG 430 (Mism.=
		: 600. AC: P00600//OS: tomato, copersicon esculentum ENE: rbcS1/RE: TSS N F:unknown	tifs on "-" Strand: Mean Exp. mber 0.02517 Up.Conf.Int. Found 1 202 ATcCCAgTGTGT 191 ism.= 2)
		: 744. AC: P00743//OS: Nicotiana umbaginifolia /GENE: b-E/RE: box 3 /BF: GT-1	tifs on "+" Strand: Mean Exp. mber 0.02356 Up.Conf.Int. Found 1 238 GAGTaGTAAAgT 249 ism.= 2)
		: 749. AC: P00748//OS: Arabidopsis aliana /GENE: Pc/RE: box1 /BF: GT-1	: 749. AC: RSP00748//OS: abidopsis thaliana /GENE: Pc/RE: box1 /BF: GT-1 otifs on "-" Strand: Mean Exp. mber 0.03026 Up.Conf.Int. Found 1 72 cAATGGTAAaAA 61 ism.= 2)

Literature cited:

A

"Ané JM Personal communication in MPMI Iternational congress (July 2007) held in Sorrento, Italy"

"Akiyama K, Matsuzaki K, Hayashi H. 2005: Plant sesquiterpenes induce hyphal branching in arbuscular mycorrhizal fungi. Nature, 435:824-827."

"Amor BB, Shaw SL, Oldroyd GE, Maillet F, Penmetsa RV, Cook D, Long SR, Denarie J, Gough C 2003. The NFP locus of Medicago truncatula controls an early step of nod factor signal transduction upstream of a rapid calcium flux and root hair deformation. Plant J , 34:495-506."

"Andrade, S.L., Dickmanns, A., Ficner, R. and Einsle, O. 2005 Crystal structure of the archaeal ammonium transporter Amt-1 from Archaeoglobus fulgidus. Proc. Natl. Acad. Sci. USA 102, 14994–14999"

"Ané JM, Kiss GB, Riely BK, Penmetsa RV, Oldroyd GE, Ayax C, Lévy J, Debellé, Baek JM, Kalo P, Rosenberg C, Roe BA, Long SR, Dénarié J, Cook DR. 2004. Medicago truncatula DMI1 required for bacterial and fungal symbioses in legumes. Science. 303(5662): 1364-7"

"Arambarri A. (1999) Illustrated catalogue of Lotus L. Seeds (Fabaceae) In: Trefoil: The science and technology of Lotus. Beuselinck P., Ed.). American Societey of Agronomy, pp. 21-24"

Arnozis PA and Findeenegg GR (1986) Electrical charge balance in the xylem sap of beet and sorghum plants and grown with either NO3-NH4+ nitrogen. J plant physiol125: 441-449

"Aronheim (1997) Improved efficiency sos recruitment system: expression of the mammalian GAP reduces isolation of Ras GTPase false positives. Nucleic acid Res., 25(16):3373-3374"

"Asamizu E; Nakamura Y, Sato S. Taba S. (2000) Generation of 7137 non redundant expressed sequencing tags from a legume, Lotus japonicus. DNA Research 7, 127-130. "

"Asuaga (1994) Lotus subbiflorus cv el Rincon a new alternative of extensive improvement of natural pastures. Proceedings of the first international Lotus symposium (Boselink and Roberts, eds) pp 147-149"

B

"Banba M., Siddique A.B., Kouchi H., Izui K., Hata S., 2001. Lotus japonicus forms early senescent root nodules with Rhizobium etl. MPMI Vol 14. Pp173-180"

"Barbulova A., Rogato A, D'Apuzzo E., Omrane S., Chiurazzi M. 2007: Differential Effects of Combined N Sources on Early Steps of the Nod Factor-Dependent Transduction Pathway in Lotus japonicus. MPMI 20(8):994-1003.

"Bhuvaneswari TV, Bhagwat AA, Bauer WD (1981) Transient susceptibilityof root cells in four common legumes to nodulation by rhizobia. Plant Physiol 68: 1144–1149"

BOLLARD EG 1957 Translocation of organic nitrogen in the xylem. Aust J BiolSci 10: 292-301ol Biochem5: 109–119
"Bonfante P. (1984) Anatomy and Morphology of VA mycorrhizae. In C.L. Powell and DJ Bayaraj, pp5-33"

"Boogerd FC, van Rossum D (1997) Nodulation of groundnut by Bradyrhizobium: a simple infection process by crack entry. FEMS Microbiol Rev 21: 5-27"

"Bridey B. Maxwell2, Carol R. Andersson3, Daniel S. Poole, Steve A. Kay, and Joanne Chory* 2003 HY5, Circadian Clock-Associated 1, and a cis-Element, DET1 Dark Response Element, Mediate DET1 Regulation of Chlorophyll a/b-Binding Protein 2 Expression Plant Physiology, December, Vol. 133, pp. 1565-1577,"

"Buchel, A.S., Brederode, F.T., Bol, J.F., Linthorst, H.J., (1999). Mutation of GT-1 binding sites in the Pr-1A promoter influences the level of induciblegene expression in vivo. Plant Mol. Biol. 40, 387-396."

C

"Catoira R, Galera C, Billy F, Penmetsa RV, Journet E, Maillet F, Rosenberg C, Cook D, Gough C, Denarie J (2000). Four genes of Medicago truncatula controlling components of a nod factor transduction pathway. Plant Cell, 12:1647-1665."

"Charpentier M, personal communication in UE- INTEGRAL meeting May 2007 held in Sevilla, Spain"

"Colebatch G Debraosses G, Ott J , Krussel L., Montanari O., Kloska S., Kopka J., Udvardi MK., (2004) Global changes in transcription orchestrate metabolic differentiation during symbiotic nitrogen fixation. The Plant Journal. Vol 39. Pp 487- 512"

"Colebatch G., Kloska S., Trevarski B., Freund S, Altmann J, Udvardi MK. (2002). Novel aspects of symbiotic nitrogen fixation uncovred by transcript profiling with cDNA arrays. Molecular Plant-Microbe Iteraction. Vol15. Pp 411-420"

"Conroy, M.J., Durand, A., Lupo, D., Li-X-D., Bullough, P.A., Winkler, F.K. and Merrick, M. (2007). The crystal structure of the Escherichia coli AmtB-GlnK complex reveals how GlnK regulates the ammonia channel. Proc. Natl. Acad. Sci. USA. 104, 1213-1218"

"Coutts G., Thomas G., Blakey D., Merrik M. (2002). Membrane sequestration of the signal transduction protein GlnK by the ammonium transporter AmtB. EMBO J. 15;21(4):536-45"

"Crawford NM, Glass ADM. 1998. Molecular and physiological aspects of nitrate uptake in plants. Trends in Plant Sciences 3, 389-395."

D

"D'Apuzzo E, Rogato A, Simon-Rosin U, El Alaoui H, Barbulova A, Betti M, Dimou M, Katinakis P, Marquez A, Marini AM, Udvardi MK, Chiurazzi M., 2004. Characterization of three functional high-affinity ammonium transporters in Lotus japonicus with differential transcriptional regulation and spatial expression. Plant Physiol. 134(4):1763-74."

"Debrosses G.G., Kopka J, Udvardi M., (2005) Lotus japonicus Metabolic profiling. Development of Gas Chromatography-Mass Spectrometry Resources for the study of plant-Microbe interactions Plant Physiol., 137(4): 1302-1318. "

"Denarié J, Debellé F., and Promé J-C (1996) Rhizobium lipochitooligosaccharide nodulation fcators: signaling molecules mediating recognition and morphogenesi. Annu. Rev. Biochem, 65, 503-535. "

"D'Haeze and Holsters (2002) Nod factor structures, responses, and perception during ininitiationof nodule development. Mini Review. Glycobiology vol.12 (6) 79-105"

"Diaz P., Borsani O. and Monza J., (2005) Lotus-related species and their agronnomic importance 25-37 in Lotus japonicus Handbook AJMarquez (ed.) Springerverlag"

Doerner P (2007) Plant Meristems: Cytokinins-The Alpha and Omega of the Meristem. (in press)

"Downie JA: Functions of rhizobial nodulation genes. In The Rhizobiaceae. Edited by Spaink HP, Kondorosi A, Hooykaas PJJ. Kluwer Academic Publishers; 1998:387–402."

E, G

"Eulgem, T., Rushton, P.J., Schmelzer, E., Hahlbrock, K., Somssich, I.E.,1999. Early nuclear events in plant defence signalling: rapid gene activation by WRKY transcription factors. EMBO J. 18, 4689– 4699."

"Gazzarrini S., Leijay L., Gojon A., Ninnemann O., Frommer W.B., von Wiren N., (1999). Three functional transporters for constitutive, diurnally regulated, and starvation-induced uptake of ammonium into Arabidopsis roots. Plant Cell 11: 937-948."

"Gepts P., William D., Beavies D., Brummer C., Shoemaker R.C., Stalker H.T., Weeden N.F., and Young N.D. (2005): Legumes as a Model plant Family. Genomics for Food and feed Report of the cross-Legume Advances through Genomics conference. Plant physiology. Vol 137, pp. 1228-1235."

" Geurts R., Bisseling T., Long SR (2002): Rhizobium symbiosis: Nod factors in perspective. Plant Cell, 8:1885-1898"

"Giles ED Oldroyd and J Allan Downie 2006 Nuclear calcium changes at the core of symbiosis signaling Current Opinion in Plant Biology, 9:1-7"

"Gilmartin & Chua. 1990. Spacing between GT-1 binding sites within a light responsive element is critical for transcriptional activity. The Plant Cell. Vol2; 447-455"

"Glass D.M., Dev T. Britto, Brent N. Kaiser, James R. Kinghorn, Herbert J. Kronzucker , Anshuman Kumar, Mamoru Okamoto, Suman Rawat, M.Y. Siddiqi, Shiela E. Unkles and Joseph J. Vidmar. 2002. The regulation of nitrate and ammonium transport systems in plants. Journal of Experimental Botany, Vol. 53, No. 370, Inorganic Nitrogen Assimilation Special Issue, pp. 855–864"

"Gleason C, Chaudhuri S, Yang T, Munoz-Gutierrez A, Poovaiah BW, Oldroyd GED: 2006 Legume nodulation independent of rhizobia is induced by a modified calcium activated kinase lacking autoinhibition. Nature. in press"

"Gonzales M.D., Archuleta E., Farmer A, Gajendran K., Grant D., Shoemaker R, Beavies W.D., Waugh M.E. (2005) The Legume Information System (LIS): an integrated information resource for comparative legume biology. Nucleic Acid Research. Vol 33 (1 database issue), pp, 660-665."

"Gordon A.J. Lea P.J:, Rosenberg C. Trinchant J.C. 20011 Nodule formation and function. In Lea PJ Morot Gaudry J-F, eds. Plant nitrogen Berlin: Springer Verlag, 101-146"

"Goyal SS, Lorenz OA, Huffaker RC (1982) Inhibitory effects of ammoniacal nitrogen on growth of radish plants. I. Characterization of toxic effects of NH4+ on growth and its alleviation by NO3-. J Am Soc Hortic Sci 107:125-129"

"Guinel FC, Geil RD (2002) A model for the development of the rhizobial and arbuscular mycorrhizal symbioses in legumes and its use to understand the roles of ethylene in the establishment of these two symbioses. Can J Bot 80: 695–720"

"Gutièrrez RA, Lejay LV, Dean A, Chlaromonte F, Sasha DE, Coruzzi GM (2007) Qualitative network models and genome-wide expression data define carbon/ nitrogen responsive molecular machine in Arabidopsisenome Biol. 8(1):R7"

"Handberg, K, and Stougaard J. (1992). Lotus japonicus , an autogamous, diploid legume species for classical and molecular genetic. Plant Journal. Vol 2. Pp 487-496."

"Haris JM, Wais R. and Long S.R. (2003) Rhizobium-induced calcium spiking in Lotus japonicus.MPMI 16:335-341"

"Heckmann, A. B., Lombardo, F., Miwa, H., et al. 2006, Lotus japonicus nodulation required two GRAS domain regulators, one of which is functionally conserved in a nonlegume, Plant Physiol., 142, 1739–1750."

"Heller R,. Esnault, R. Lance, C. 1996. Physiologie végétale. Tome 1 (Nutrition). 5 eme edition Masson: 130-161"

"Howitt SM, Udvardi MK. 2000. Structure, function and regulation of ammonium transporters in plants. Biochim Biophys Acta. 1;1465(1-2):152-70"

"Hsieh MH, LamHM, Van de Loo FJ, Coruzzi G (1998) A PII like protein in Arabidopsis: putative role in nitrogen sensing PNAS 10; 95(23): 13965-70"

"Izawa S, Good NE (1972) Inhibition of photosynthetic electron transport and photophosphorylation . Methods Enzymol 24: 355-377"

"Jarvis, B.D.W., Pankhurst, C.E. & Patel , J.J. (1982) Int. J. Syst. Bacteriol. 32, 378-380."

Javelle A. Morel M., Rodriguez-Pastrana B.R., André B., Marini A.M., Brun A and CHalot M. 2003 : Molecular characterization, function and regulation of ammonium transporters (Amt) and Ammonium, metabolizing enzymes (GS, NADPH-GDH) in the ectomycorrhizal fungus Hebeloma cylindrosporum. Molecular Microbiology. 47(2), 411-430.

"Javelle A, Severi E, Thornton J, Merrick M., 2004. Ammonium sensing in Escherichia coli. Role of the ammonium transporter AmtB and AmtB-GlnK complex formation. J Biol Chem. 5;279(10):8530-8."

"Kaiser, B.N., Rawat, S.R., Siddiqi, M.Y., Masle, J. and Glass, A.D. (2002) Functional analysis of an Arabidopsis T-DNA knockout'' of the high-affinity NH+4 transporter AtAMT1;1. Plant Physiol. 130, 1263–1275."

"Kalo P, Gleason C, Edwards A, Marsh J, Mitra RM, Hirsch S, Jakab J, Sims S, Long SR, Rogers J et al. 2005. Nodulation signaling in legumes requires NSP2, a member of the GRAS family of transcriptional regulators. Science, 308:1786-1789."

"Kanamori N, Madsen LH, Radutoiu S, Frantescu M,Quistgaard EM, Miwa H, Downie JA, James EK, Felle HH, Haaning LL et al.: From the cover: a nucleoporin is required for induction of Ca2+ spiking in legume nodule development and essential for rhizobial and fungal symbiosis. Proc Natl Acad Sci USA 2006, 103:359-364."

"Kaneko T., Nakamura Y, Sato S., Aasmizu E., Kato T., Sasamoto S., Watanabe A., Idesawa K., Ishikawa A., Kawashima., Kimura T., Kishida, Y., Kiyokawa C., Kohara M., Matsumoto, M., Matsuno A., Mochizuki Y., Nakayama S., Nakazaki N., Shimpo S., Sugimoto M., Takeuchi C., Yamada M., and Tabata S. (2000) Complete genome structure of the nitrogen fixing symbiotic bacterium Mesorhizobium loti. DNA Research Vol7. Pp 331-338."

"Kawagushi M., 2000. Lotus Japonicus ""Miyakojima"" MG-20: an early flowering acession suitable for indoor handeling. Journalof plant research 113, 507-509 "
"Kerr, P.S., Rufty, T.W.,Jr., and Huber S.C.(1985) Changes in non structural carbohydrates in different parts of soybean (Glycine max [L.]Merr.) plants during a light/dark cycle and in extendend darkness. Plant physiol. 78, 576-581."

"Khademi, S., O'Connell 3rd, J., Remis, J., Robles-Colmenares, Y., Miercke, L.J. and Stroud, R.M. (2004) Mechanism of ammonia transport by Amt/MEP/Rh: structure of AmtB at 1.35A ? Science 305, 1587-1594"

"Kistner and Matamoros, 2005"

"Kistner C, Winzer T, Pitzschke A, Mulder L, Sato S, Kaneko T, Tabata S, Sandal N, Stougaard J, Webb KJ et al. 2005: Seven Lotus japonicus genes required for transcriptional reprogramming of the root during fungal and bacterial symbiosis. Plant Cell, 17:2217-2229."

"Krussel L., Madsen L. H., Sato S., Aubert G., Genua A., Szczyglowski K., Duc G., Keneko T., Tabata S., De Broijn F., Pajuelo E., Sandal N., Stougaard J. (2002).Shoot control of root development and nodulation is mediated by a receptor like kinase. Nature: 1-5."

"Kuhlemeler C, Strittmatter G., Ward K., Chua N.H. 1989. The Pea rbcS-3A promoter Mediates light responsiveness,but not organ specificity. The Plant Cell. Vol 1; 471-478."

Kumar *et al.* 2003
Kumar A, Silim SN, Okamoto M, Siddiqi MY, Glass AD. 2003:Differential expression of three members of the AMT1 gene family encoding putative high-affinity NH4+ transporters in roots of Oryza sativa subspecies indica. Plant Cell Environ. 26(6):907-914.

L

"Lejay L., Gansel X., Cerezo M., Tillard P., Muller C., Krapp A., von Wiren N., Daniel-Vedel F. and Gojon A. 2003. Regulation of root ion transporters by photosynthesis: Functional importance and relation with hexokinase. The plant Cell, Vol 15, 2218-2232"

"Lejay L., Gansel X., Cerezo M., Tillard P., Muller C., Krapp A., von Wiren N., Daniel-Vedel F. and Gojon A. 2003. Regulation of root ion transporters by photosynthesis: Functional importance and relation with hexokinase. The plant Cell, Vol 15, 2218-2232. "

"Levy J, Bres C, Geurts R, Chalhoub B, Kulikova O, Duc G, Journet EP, Ane JM, Lauber E, Bisseling T et al 2004. A putative Ca2+ and calmodulin-dependent protein kinase required for bacterial and fungal symbioses. Science, 303:1361-1364."

"Lewis O.A.M., Leidi EO, Lips SH (1989) Effect of nitrogen source on growth response to salininty stress in maize and wheat11/29/2007ew Phytol 111:155-160"
"Lhuissier FGP, De Ruijter NCA, Sieberer BJ, Esseling JJ, Emons AM (2001) Time course of cell biological events evoked in legume root hairs by Rhizobium nod factors: state of the art. Ann Bot (Lond) 87: 289-302"

"Lindt T and Feller U (1987) Effect of nitrate and ammonium on long distance transport in cucumber plant. Bot Helv 97: 45-52"

"Little DY, Rao H, Oliva S, Daniel-Vedele F, Krapp A, Malamy JE (2005) The putative high-affinity nitrate transporter NTR2.1 represses lateral root initiation in response to nutritional cues. Proc. Natl. Acad. Sci. 102: 13693-13698"

"Lo´ pez-Bucio Jose´, Alfredo Cruz-Ramirez and Luis Herrera-Estrella 2003The role of nutrient availability in regulating root architecture Current Opinion in Plant Biology, 6:280–287"

"Lombari P, Ercolano E, El Alaoui, H. and Chiurazzi M. (2003) A new transformation-regeneratio procedure in the model legume Lotus japonicus. Root explants as a source of large number of cells susceptible to Agrobacterium mediated transformation. Plant Cell Report 21: 771-777."

"Loqué D. and von Wirèn N. 2004. Regulatory level for the transport of ammonium in plant roots. Journal of experimental botany. Vol 55, No 401: 1293-1305. "

"Loquè D., Yuan L., Kojima S., Gojon A., Wirth J., Gazzarrini S., Ishiyama K., Takahashi H., von Wirèn N. (2006). Additive contribution of AMT1;1 and AMT1;3 to high-affinity ammonium uptake across the plasma membrane of nitrogen deficient Arabidopsis root. The Plant Journal 48: 522-534."

"Loque, D., Lalonde, S., Looger, L.L., von Wiren, N. and Frommer, W.B. (2007) A cytosolic trans-activation domain essential for ammonium uptake. Nature 446, 195–198"

"Loque´, D., Ludewig, U., Yuan, L. and von Wiren, N. (2005) Tonoplast aquaporins AtTIP2;1 and AtTIP2;3 facilitate NH3 transport into the vacuole. Plant Physiol. 137, 671–680"

Lorenz M.C. and Heitman J., 1998: The MEP2 ammonium permease regulates pseudohyphal differentiation in S. cerevisiae. EMBO Journal 17 1236-1247.

"Ludewig U, Benjamin Neuha¨user, Marek Dynowski (2007) Minireview Molecular mechanisms of ammonium transport and accumulationin plants. FEBS Letters (in press)"

"Ludewig U., Stephanie Wilken, Binghua Wu, Wolfgang Jost, Petr Obrdlik, Mohamed El Bakkoury, Anne-Marie Marini, Bruno Andre, Tanja Hamacher, Eckhard Boles, Nicolaus von Wiren, and Wolf B. Frommer (2003). Homo- and Hetero-oligomerization of Ammonium Transporter-1 NH4 Uniporters. The Journal of Biological Chemistry 278: 45603- 45610"

"Ludewig, U. et al. (2003) Homo- and hetero-oligomerization of ammonium transporter-1 NHþ4 uniporters. J. Biol. Chem. 278, 45603–45610"

"Ludewig, U., von Wire´n, N. and Frommer, W.B. (2002) Uniport of NHþ4 by the root hair plasma membrane ammonium transporter LeAMT1;1. J. Biol. Chem. 277, 13548-13555."

"Madsen EB, Madsen LH, Radutoiu S, Olbryt M, Rakwalska M,Szczyglowski K, Sato S, Kaneko T, Tabata S, Sandal N et al 2003.: A receptor kinase gene of the LysM type is involved in legume perception of rhizobial signals. Nature, 425:637-640."

"Margarete Mu¨ller and Wolfgang Schmidt* Environmentally Induced Plasticity of Root Hair Development in ArabidopsisPlant Physiology, January 2004, Vol. 134, pp. 409–419,"

"Mayer, M. and Ludewig, U. (2006) Role of AMT1;1 in NH4+- acquisition in Arabidopsis thaliana. Plant Biol. (Stuttg) 8, 522–528."

"Mayer, M., Dynowski, M. and Ludewig, U. (2006) Ammonium ion transport by the AMT/Rh homolog LeAMT1;1. Biochem. J. 396, 431–437."

"Mehrer I and Mohr H (1989) Ammonium toxicity: description of the syndrome in Sinapis alba and the search for its causation. Physiol Plant 77: 545-554"

"Miercke, L.J. and Stroud, R.M. (2004) Mechanism ofammonia transport by Amt/MEP/Rh: structure of AmtB at 1.35 A ?. Science 305, 1587–1594."

"Mito N, Wimmers, L.E., and Bennett, A.B. (1996) Sugar regulates mRNA abundance of H+ATPase gene family members in tomato Plant Physiol, 112, 1229-1236"

"Mitra RM, Gleason CA, Edwards A, Hadfield J, Downie JA, Oldroyd GE, Long SR: A Ca2+/calmodulin-dependent protein kinase required for symbiotic nodule development: gene identification by transcript-based cloning. Proc Natl Acad Sci USA 2004, 101:4701-4705."

"Margarete Mü ller and Wolfgang Schmidt 2004: Environmentally Induced Plasticity of Root Hair Development in Arabidopsis. *Plant Physiology*, Vol. 134, pp. 409–419"

"Murray J. et al., Science 16 November 2006 (10.1126/science.1132514)."

"Neuha¨user, B., Dynowski, M., Mayer, M. and Ludewig, U. (2007) Regulation of NH4 transport by essential cross-talk between AMT monomers trough the carboxyl-tails. Plant Physiol. 143,1651–1659."

"Nielsen, K.H. and Schjoerring, J.K. (1998) Regulation of apoplastic NH+4 concentration in leaves of oilseed rape. Plant Physiol. 118, 1361–1368"

"Nishimura R, Hayashi M, Wu G, Kouchi H, Imaizumi-Anraku H, Murakami Y, Kawasaki S, Akao S, Ohmori M, Nagasawa M et al. (2002) HAR1 mediates systemic regulation of symbiotic organ development. Nature 420: 426–429"

"Nishimura R., Hayashi M., Wu Gj., Kouchi H., Imaizumi-Anraku H., Murakami Y, Kawasaki S., Akao S.? Ohomori M, Nagasawa M., Harada K., Kawaguchi M. (2002) HAR1 mediates systemic regulation of symbiotic organ development. Nature Vol 420 (6914), pp 426-429."

"Niwa S, Kawagushi M, Imaizumi-AnrakuH., Chechetka SA, Ishizaka M., Ikuta A. and Kuchi H., (2001) Responses of a model legume Lotus japonicus to lipochitin oligosaccharide nodulation factors purified from Mesorhizobium loti JRL501. MPMI 14, 848-856"

"Nutman PS (1952) Studies on the physiology of nodule formation. III. Experiments on the excision of root tip and nodules. Ann Bot 16: 81–102"

"Palenchar PM., Kouranov A., Lejay L.V., Coruzzi GM. 2004. Genome wide patterns of carbon and nitrogen regulation of gene expression validate the combined carbon and nitrogen (CN)_signaling hypothesis in plants. Genome Biology 5, R91 "

"Papadopoulos Y and Kelman W (1999) Traditional breeding of Lotus species IN: Trefoil : The science and technology of Lotus (Beuselinck P,Ed.) American Society of Agronomy pp. 187-198"

"Patejs 1973. Uptake, assimilation and transport of nitrogen compounds by plants. Soil Biochem 5:109-119"

Patriarca E.J.,Taté R and Iaccarino M., 2002: Key role of Bacterial NH4+ Metabolism in rhizobium-Plant Symbiosis. Microbiology and molecular Reviews 66(2):203-222.

"Penmesta R.V. and Cook DR. (1997). A legume ethylen-insensitive mutant hyperinfected by its rhizobial symbiont. Science 27, 527-530"

"Perry JA., Wang T.L, Welham T.J., Gardner S.,, Pike JM., , Yoshida S., and Parninske M., (2003). Tilling Reverse Genetics tool and web-accessible collectionof mutantsof the legume Lotus japonicus. Plant Physiology. 131, Pp 866-871. "

"Peter R. McClure AND Daniel W. ISRAEL Transport of Nitrogen in the Xylem of Soybean Plants'Plant Physiol. (1979) 64, 411-416"

"Price John ,a Ashverya Laxmi,a Steven K. St. Martin,a and Jyan-Chyun Janga 2004,Global Transcription Profiling Reveals Multiple Sugar SignalTransduction Mechanisms in Arabidopsis. The Plant Cell, Vol. 16, 2128-2150, August "

"Radutoiu S, Madsen LH, Madsen EB, Jurkiewicz A, Fukai E, Quistgaard EM, Albreksten A.S., James E.K., Thirup S., Stougaard J. (2007) LysM domains mediate lipochitin oligosaccharide recognition and Nfr genes extend the symbiotic host range. EMBO J 26(17): 3923-35"

"Radutoiu S,Madsen LH, Madsen EB, Felle HH, Umehara Y, Gronlund M, Sato S, Nakamura Y, Tabata S, Sandal N, et al (2003) Plant recognition of symbiotic bacteria requires two LysM receptor-like kinases. Nature 425: 585-592"

"Rawat, S.R., Silim, S.N., Kronzucker, H.J., Siddiqi, M.Y. and Glass, A.D. (1999) AtAMT1 gene expression and NH4+ uptake in roots of Arabidopsis thaliana: evidence for regulation by root glutamine levels. Plant J. 19, 143-152."
"REINBOTHE H, K MOTHES 1962 Urea, ureides and guanidines in plants. Annu Rev Plant Physol 13: 129-150"

"Remans T., Nacry P., Pervent M., Girin T., Tillard P., Lepetit M., Gojon A., (2006) A central role for the nitrate transporter NRT2.1 in the integrated morphological and physiological responses of the root system to nitrogen limitation in Arabidopsis. Plant Physiology. 140: 909-921"

"Riens, B, Lohaus, G., Winter, H. and Heldt, H.W. (1994). Production and diurnal utilization of assimilates in leaves of spinach (Spinacia oleracea L.) and barley (Hordeum vulgare L.). Planta 192, 497-501"

"Rong Wanga,b, Guofan Honga,b, Bin Han (2004) Transcript abundance of rml1, encoding a putative GT1-like factor in rice,is up-regulated by Magnaporthe grisea and down-regulated by light Gene 324 105- 115"

"Ruffy, TW, Jr., MacKnown, C.T., and Volk R.J. (1989) Effects of altered carbohydrates avalability on whole plant assimilation of 15 NO3-. Plant Physiol. 89, 457-463"
"Rushton, P.J., Reinstadler, A., Lipka, V., Lippok, B., Somssich, I.E., 2002. Synthetic plant promoters containing defined regulatory elements provide novel insights into pathogen- and wound-induced signaling. Plant Cell 14, 749-762."

"Sandal, N., Petersen, T. R., Murray, J., et al. 2006, Genetics of symbiosis in Lotus japonicus: recombinant inbred lines, comparative genetic maps, and map position of 35 symbiotic loci, Mol. Plant-Microbe Interact., 19, 80-92."

"Sato S. and Tabata S., (2006) Lotus japonicusas a plateform for legume research. Current opinion in Plant Biology. Vol 9 (2), pp. 95-98"

"Schauser L., Roussis A., Stiller J., Stougaard J. (1999) A plant regulator controlling development of symbiotic root nodules. Nature 402: 191-195."

"Schauser L., Roussis A., Stiller J., Stougaard J. (1999) A plant regulator controlling development of symbiotic root nodules. Nature 402: 191-195."

"Shelden, M.C., Dong, B., de Bruxelles, G.L., Trevaskis, B., Whelan, J., Ryan, P.R., Howitt, S.M. and Udvardi, M.K. (2001) Arabidopsis ammonium transporters, AtAMT1;1 and AtAMT1;2, have different biochemical properties and functional roles. Plant Soil 321, 151-160"

"Shussler A., Shwarzott D. and Walker, C 2001. A new fungal phylum, the Glomeromycota: phylogeny and evolution, Myco. Res 105(12): 1413-1421"

"Siciliano V, Genre A, Balestrini R, Cappellazzo G, deWit PJ, Bonfante P (2007) Transcriptome analysis of arbuscular mycorrhizal roots during development of the prepenetration apparatus. Plant Physiol. 144(3):1455-66"

"Smit P, Raedts J, Portyanko V, Debelle F, Gough C, Bisseling T, Geurts R 2005. NSP1 of the GRAS protein family is essential for rhizobial nod factor-induced transcription. Science, 308:1789-1791."

"Sonoda Y , Ikeda A, Saiki S, Von Wiren N, Hayakawa T., Yamaya T, Yamagushi J, (2003) Distinct expression and function of three ammonium transporters genes (OsAMT1.1-3). Plant cell physiol 44: 726-734"

"Stracke, S., Kistner, C., et al. 2002. A plant receptor-like kinase required for both bacterial and fungal symbiosis. Nature 417:959."

"Struuman N, Bras C.P., Schlaman H.R.M., Wijfjes A.H.M., Blomberg G and Spaink H.P. (2000) Use of green fluorescent protein color variants expressed on stable broad-host-range vectors to visualize rhizobia interacting with plant. MPMI Vol 13 N°11 pp 1163-1169. "

"Sullivan J. T.,Patrick H.N., Lowther W. L., Scott D.B., Ronson C.W. (1995),Nodulating strain of Rhizobium loti arise through chromosomal symbiotic gene transfer in the environment. PNAS Vol 92, pp. 8985-8989"

"Szczyglowski K, Amyot L (2003) Symbiosis. Inventiveness by recruitment? Plant Physiol 131: 935-940"
"Tate, R., Riccio, A., Merrick, M. and Patriarca, E.J. (1998) The Rhizobium etli amtB gene coding for an NHþ4 transporter is down-regulated early during bacteroid differentiation. Mol. Plant Microbe Interact. 11, 188-198"

"Thomas G.H., Mullins J.G., Merrick M. (2000). Membrane topology of the Mep/Amt family of ammonium transporters Mol Microbiologo 37 (2): 331-344."

"Tirichine L, Imaizumi-Anraku H, Yoshida S, Murakami Y, Madsen LH, Miwa H, Nakagawa T, Sandal N, Albrektsen AS, Kawaguchi M et al.: 2006 Deregulation of a Ca2+/calmodulin dependent kinase leads to spontaneous nodule development. Nature. Vol 441"

Triplett E.W. 2000 Procaryotic nitrogen fixation. Wymondham: Horizon Scientific Press.

"Tritichine L., Sandal N., Madsen L.H., Radutoiu S., Albrektsen A.S., Sato S., asamizu E., Tabata S., Stougaard J. (2006). A Gain-of-Function Mutation in a Cytokinin Receptor Triggers Spontaneous Root Nodule Organogenesis. 16 November 2006 Pp 1-4"

"Udvardi M.K., Tabat S., Parninske M. and Stougaard J. (2005) Lotus japonicus :legumeresearch in the fast lane. Trends in plant science. Vol10 (5) Pp 222-228."

"Udvardi MK, Day DA (1995) Metabolite transport across symbiotic membranes of legume nodules. Annu Rev Plant Physiol Plant Mol Biol 48: 493-523"

"van Brussel AAN, Bakhuizen R, van Spronsen PC, Spaink HP, Tak T, Lugtenberg BJJ, Kijne JW(1992) Induction of pre-infection thread structures in the leguminous host plant by mitogenic lipo-oligosaccharides of Rhizobium. Science 257: 70-72"

"van Brussel AAN, Tak T, Boot KJM, Kijne JW (2002) Autoregulation of root nodule formation: signals of both symbiotic partners studied in a split-root system of Vicia sativa subsp. Nigra. Mol Plant-Microbe Interact 15: 341-349"

"Van Spronsen PC, Gronlund M., Pacios Bras C., Spaink H.P., Kijne J.W. (2001) Cell biological changes of outer cortical root cells in early determinate nodulation. MPMI 14(7):839-47."

"VandenBosh K.A., and Stacey G. (2003), Summaries of legume Genomics Projects from around the globe, Community Resource for Crops and Models. Plant Physiology, Vol 131. pp 840-865."

W, Y, Z

"Wais RJ, Galera C, Oldroyd G, Catoira R, Penmetsa RV, Cook D, Gough C, Denarie J, Long SR: Genetic analysis of calcium spiking responses in nodulation mutants of Medicago truncatula. Proc Natl Acad Sci USA 2000, 97:13407-13412."

"Winkoop S. and Saalbach G. (2003) Proteome analysis: novel proteins indentified at the peribacteoid membrane from Lotus japonicus root nodules. Plant Physiology 131, 1080-1090"

"Woldendorp, J. W., and H. J. Laanbroek. 1989. Activity of nitrifiers in relation to nitrogen nutrition of plants in natural ecosystems. Plant Soil 115:217-228"

"Wood, C.C., Poree, F., Dreyer, I., Koehler, G.J. and Udvardi, M.K. (2006) Mechanisms of ammonium transport, accumulation, and retention in ooyctes and yeast cells expressing Arabidopsis AtAMT1;1. FEBS Lett. 580, 3931-3936."

"Wopereis J., Pajuelo E., Dazzo F.B., Jiang Q., Gresshoff P. M., de Bruijn F. J., Stougaard J. and Szczyglowski K. (2000).Short rot mutant of lotus japonicus with a dramatically altered symbiotic phenotype.The plant Journal, 23: 97-114"

Yakunin A.F. and Hallenbeck P.C. 2002: AmtB is necessary for NH4 induced Nitrogenase switch-Off and ADP-Ribosylation in *Rhodobacter capsulatus*. Journal of Bacteriology. Vol 184 (15) 4081-4088.

"Yanagisawa S, Akiyama A, Kisaka H, Uchimiya H and Miwa T 2004. Metabolic engineering with Dof1 transcription factor in plants: Improved nitrogen assimilation and growth under low nitrogen conditions, PNAS 101, 7833-7838"

"Yoshida S, Parniske M 2005. Regulation of plant symbiosis receptor kinase through serine and threonine phosphorylation. J Biol Chem, 280:9203-9209."

"Zhang H, Forde B 1998. An Arabidopsis MADS box gene that controls nutrient-induced changes in root architecture. Science, 279:407-409."

TABLE OF CONTENTS

I. INTRODUCTION

II. Results

III. Discussion

IV. Materials and Methods

Annex
Bibliography